PHARMACOLOGICAL CHARACTERIZATION OF THE PISCF-ALLATOSTATIN RECEPTOR IN *CARAUSIUS MOROSUS*

by

Ali İşbilir

B.S., Biochemistry, Ege University, 2012

Submitted to the Institute for Graduate Studies in
Science and Engineering in partial fulfillment of
the requirements for the degree of
Master of Science

Graduate Program in Molecular Biology and Genetics
Boğaziçi University

2016

ACKNOWLEDGEMENTS

I would like to sincerely thank my supervisor Assoc. Prof. Necla Birgül İyison, at first place, for that she has given me the opportunity to conduct this work under her supervision and guidance. She pursued every possible opportunity for me to carry out this project from the beginning until the very end. I am very grateful for of her endless support, trust and tremendous guidance. I am also thankful to my thesis committee members Assoc. Prof. İbrahim Yaman and Prof. Osman Uğur Sezerman for dedicating their valuable time to evaluate my thesis.

I am very grateful to Prof. Moritz Bünemann for allowing me to perform an important part of this work in his laboratory, and for critically evaluating a certain part of this work. His efforts and help have been a stepping-stone in this work and my career. Next to that, I am thankful to Dr. Cornelius Krasel and all other members of the group of Prof. Bünemann for their tremendous help in and outside of the laboratory.

What made this work done with a lot of encouragement is the bliss that I shared every day with the members of my laboratory. I am very thankful to İzzet Akiva, Tolga Aslan and Tuncay Şeker for being my teachers and mentors-at-instant, but more for their beautiful friendship that I hope to be long-standing. I would like to single out Burçin Duan Şahbaz, not only for her endless encouragement and support throughout this work, but also for being next to me anytime I needed. I would also like to express my very special thanks to Ruçhan Karaman, Ayşin Akpınar, Gizem Gül, Aida Shahraki and Kübra Zırhlıoğlu, Can Gürkaşlar, Beren Aylan and Sema Elif Eski for creating an enviable laboratory environment.

I am very grateful to Assoc. Prof. İbrahim Yaman for his intellectual help and enriching my ideas, and also to Assoc. Prof. Stefan Fuss for helping me to avoid going into wrong direction and stay on track at certain parts during this work.

I would specially like to thank to my friends in the department, namely Bahadır Çağrı Çevrim, Ferdi Rıdvan Kıral, Kaan Mika, Mustafa Yalçınkaya, Ahmet Buğra Tufan, Aybüke Alıcı Garipcan, Mehmet Can Demirler (master of confocal imaging), Metin Özdemir, Ulduz Sobhi Afshar, Fulya Akçimen and Seda Yaşa, who made the last two years of my life very enjoyable, and helped me several times on scientific matters.

I cannot thank my family enough. This work would not have been possible without the unqualified support and trust of my parents and my sister in every decision I have made. Also, I am indebted to my aunt and uncle, Çiçek Türker and İhsan Türker, my cousins Ersin Türker, Eray Türker, Dilek Sayıl, Fırat Sayıl, İdil Sayıl and Demet Türker for being a great family to me and always sharing all they have.

A very special thanks goes to Hamid Hamzeiy, who has been an excellent house-mate, more than a friend, and a great person with whom I could discuss a huge variety of silly and serious matters with lots of joy and delight.

This work was supported by GLISTEN (COST Action CM1207).

ABSTRACT

PHARMACOLOGICAL CHARACTERIZATION OF THE PISCF-ALLATOSTATIN RECEPTOR IN *CARAUSIUS MOROSUS*

Allatostatins (ASTs) are multifunctional insect neuropeptides that suppress juvenile hormone (JH) synthesis and feeding behavior. Three different classes of ASTs in insects are known as FGLa/ASTs (A-type), MIP/ASTs (B-type) and PISCF/ASTs (C-type). Each type of ASTs exert its activity through binding to its cognate G protein coupled receptor families, called as Allatostatin receptors (AstRs). Very little is known on how JH synthesis is regulated and how AST/AstR system regulates this process. AstRs are also potential targets for pesticide development, since their activation negatively modulates insect growth and feeding-related processes. A transcript from an invasive African pest, *Carausius morosus*, which shows high sequence similarity to other insect PISCF/AST receptors was previously identified by our group. In this study, we characterized the pharmacological properties and early signaling events of this PISCF/AST receptor (CamAstR-C) by means of FRET using a heterologous expression system. A dose-dependent activation of $G\alpha_{i1}$ and $G\alpha_{o}$ were detected upon stimulation of CamAstR-C. Receptor coupling with $G\beta\gamma$ subunits was observed only in the presence of $G\alpha_{i1}$ or $G\alpha_{o}$, but not other $G\alpha$ subunits. A partial inhibition of adenylyl cyclase 5-mediated cAMP production upon receptor activation with PISCF/AST and a dose-dependent interaction between β-arrestin2 and the receptor was detected. In summary, a PISCF/AST receptor from *Carausius morosus* has been functionally characterized, activated by *Drosophila* PISCF/AST, but not *Drosophila* FGLa/ASTs.

ÖZET

CARAUSIUS MOROSUS'TA PISCF-ALLATOSTATIN RESEPTÖRÜNÜN FARMAKOLOJİK OLARAK NİTELENMESİ

Allatostatinler (AST), böceklerde jüvenil (gençlik) hormonu (JH) üretimini ve beslenme davranışlarını baskılayan çok işlevli nöropeptidlerdir. Allatostatinler FGLa/AST (A-türü), MIP/ASTs (B-türü) ve PISCF/ASTs (C-türü) olmak üzere üç sınıfa ayrılır. Her bir Allatostatin türü, işlevini Allatostatin reseptörü (AstR) olarak adlandırılan, kendine özgü G protein kenetli reseptör sınıfından bir proteine bağlanarak gösterir. Böceklerde JH üretiminin nasıl düzenlendiği ve AST/AstR sisteminin bu süreçteki rolü hakkında çok az bilgi mevcuttur. Ayrıca, böcek gelişimi ve beslenmesi ile ilişkili süreçlerde AstR'lerin baskılayıcı rolü nedeniyle, bu reseptörler pestisit geliştirilmesinde potansiyel bir hedeftir. Daha önce, bizim grubumuz tarafından Afrika kökenli istilacı bir böcek olan *Carausius morosus*'tan diğer böcek PISCF/AST reseptörleri ile yüksek bir dizi benzerliği gösteren bir transcript belirlenmiştir. Bu çalışmada, FRET yöntemi ile heterolog bir gen ifade sisteminde, bahsedilen PISCF/AST reseptörünün farmakolojik özellikleri ve erken sinyal yolakları belirlenmiştir. Reseptörü ifade eden hücrelerin PISCF/AST muamelesi ile birlikte, $G\alpha_{i1}$ ve $G\alpha_o$ proteinlerinin doza bağımlı olarak etkin hale geldiği gözlenmiştir. Reseptörün $G\beta\gamma$ alt birimleri ile etkileşimi $G\alpha_{i1}$ ve $G\alpha_o$ proteinlerinin dışında hiç bir $G\alpha$ alt biriminin varlığında gözlenmemiştir. Adenilil siklaz 5 aracılı cAMP üretiminin ise PISCF/AST muamelesi ile kısmi olarak engellendiği, ve reseptörün β-arrestin2 ile doza bağımlı olarak etkileştiği belirlenmiştir. Kısaca, *Carausius morosus*'a ait bir PISCF/AST reseptörü işlevsel olarak nitelendirilmiş, ve *Drosophila* PISCF/AST peptidi ile fonksiyonel olarak etkin hale gelirken, *Drosophila* FGLa/AST peptidi ile etkin hale gelmediği gösterilmiştir.

TABLE OF CONTENTS

LIST OF FIGURES

LIST OF TABLES

LIST OF SYMBOLS

A	Alanine
Ala	Alanine
bp	Basepair
C	Cysteine
Cys	Cysteine
D	Aspartic Acid
E	Glutamic Acid
F	Phenylalanine
G	Glycine
gr	Gram
H	Histidine
I	Isoleucine
K	Lysine
kb	Kilobase
kDa	Kilodalton
L	Liter
M	Molar
mg	Milligram
min	Minute
ml	Milliliter
mm	Millimeter
mM	Millimolar
ms	Millisecond
mW	Milliwatt
N	Asparagine
ng	Nanogram
nm	Nanometer
nM	Nanomolar
P	Proline

pQ	Pyroglutamate
Q	Glutamine
^{o}C	Centigrade degree
rpm	Revolutions per minute
S	Serine
sec	Second
V	Volt
W	Tryptophan
X	Any Amino Acid
Y	Tyrosine
µg	Microgram
µM	Micromolar
µl	Microliter
α	Alpha
β	Beta
γ	Gamma
ε	Epsilon
κ	Kappa
Δ	Delta

LIST OF ACRONYMS / ABBREVIATIONS

AC	Adenylyl cyclase
AP-2	Adapter Protein 2
APS	Ammonium Persulfate
ASK	Apoptosis Signal-Regulating Kinase
AST	Allatostatin Peptide
AstR	Allatostatin Receptor
BSA	Bovine Serum Albumin
c-Raf	Raf Proto-Oncogene Serine/Threonine-Protein Kinase
CA	Corpora allata
Ca^{2+}	Calcium
cAMP	Cyclic adenosine monophosphate
CC	Corpora cardiaca
CCP	Clathrin-Coated Pit
cDNA	Complementary DNA
Cer	Cerulean Fluorescent Protein
CFP	Cyan Fluorescent Protein
Cl^-	Chlorine
CO_2	Carbondioxide
DAG	Diacyl Glycerol
DMEM	Dulbecco's Modified Eagle Medium
DMSO	Dimethyl Sulfoxide
DNA	Deoxyribonucleic Acid
dNTP	Deoxy ribonucleotide three phosphate
ECL	Extracellular Loop
EDTA	Ethylenediaminetetraacetic Acid
ERK	Extracellular-Signal-Regulated Kinase
FBS	Fetal Bovine Serum
FRET	Fluorescence (Förster) Resonance Energy Transfer
GAP	GTPase-Activating Protein

GDP	Guanosine Diphosphate
GIRK	G protein-Coupled Inwardly-Rectifying Potassium Channel
GPCR	G protein-Coupled Receptor
GTP	Guanosine Triphosphate
GTPase	Guanosine Triphosphate-Hydrolyzing Enzyme
GFP	Green Fluorescent Protein
H_2O	Water
HBSS	HEPES Balanced Salt Solution
HEK	Human Embryonic Kidney
ICL	Intracellular Loop
IgG	Immunoglobulin G
IP_3	Inositol 1, 4, 5-Triphosphate
JH	Juvenile Hormone
JNK3	c-Jun N-terminal Kinase 3
K^+	Potassium
LB	Luria-Bertani Broth
MAPK	Mitogen-Activated Protein Kinase
MKK4	Mitogen-Activated Protein Kinase 4
$MgCl_2$	Magnesium Chloride
MHC	Major Histocompatibility Complex
NaCl	Sodium Chloride
NAD	NACHT-associated Domain
Na^+	Sodium
NHE	Sodium-Hydrogen exchanger
OD	Optic Density
ORF	Open Reading Frame
PBS	Phosphate Buffered Saline
PCR	Polymerase Chain Reaction
Pen/Strep	Penicillin/Streptomycin
PI3K	Phosphoinositide-3 kinase
PIP_2	Phosphatidylinositol 4, 5 Bisphosphate
PKA	Protein Kinase A
PKC	Protein Kinase C

PLC	Phospholipase C
PLC-β	Phospholipase C-β
Rap1	Ras-Proximate-1
RapGAP	Ras-Proximate-1 GTPase-Activating Protein
SDS	Sodium Dodecyl Sulfate
SDS-PAGE	SDS-Polyacrylamide Gel Electrophoresis
TAE	Tris-Acetate-EDTA
TBS	Tris Buffered Saline
TBS-T	Tris Buffered Saline Tween
TEMED	N, N, N', N'-Tetramethylethane-1, 2-diamine
TGFα	Transforming Growth Factor α
TM	Transmembrane
Tween	Polysorbate
v	Volume
w	Weight
WB	Western Blot
YFP	Yellow Fluorescent Protein
WT	Wild-Type
ZO-1	Zona Occludens 1

1. INTRODUCTION

1.1. G Protein-Coupled Receptors

In order to function properly and continue essential biological processes within an organism, cells must be able to respond to the changes originated by its local and distant environment of the organisms, and also generate signals for other cells to receive. Luckily, cells are highly communicative and responsive units of life. They can sense specific changes in their environment, process them and generate responses by activating intracellular pathways, also called signal transduction cascades. These information-processing circuits are responsible at amplifying and integrating external stimuli. As a result, biological responses, such as changes in enzymatic activity, gene expression, or ion-channel activity, are generated.

How do cells receive signals present outside of their borders? Most of the molecules cells sense as signals do not penetrate through the cell membrane due to their size and high polarity. These signals are recognized by membrane-associated receptor proteins that bind to specific signaling molecules, undergo conformational changes, become activated and initiate specific biological responses.

Cell surface receptors are grouped into three families depending on the mechanisms they use for signal transduction. These families are channel-linked receptors, enzyme-linked receptors, G protein-coupled receptors and intracellular receptors (Purves *et al*., 2001). Among them, G protein-coupled receptors (GPCRs), also referred to as 7-transmembrane receptors (7-TMRs), constitute the fourth largest protein families in human genome, with more than 1000 genes identified so far (Takeda *et al*., 2002). GPCRs are able to respond to various inducers, also called ligands, such as biogenic amines, peptides, lipids, nucleotides, hormones, neurotransmitters, chemokines, ions, odorants and photons by binding them and transferring this information from extracellular to intracellular environment. As a consequence, GPCRs mediate a great variety of physiological processes,

including cellular growth, development, differentiation, neurotransmission, secretion, inflammation and infection. Due to their involvement in such critical and finely-tuned cellular events, abnormalities in the functions of GPCRs cause abnormal cellular function, eventually lead to several diseases and disorders. For that reason, GPCRs have been a major target for the development of numerous drugs that regulate GPCR function, thus treat various medical implications. Therefore, it is important to study the structure and function of GPCRs in order to understand the cellular mechanisms that underlie central physiological processes, and design new therapeutics that regulate the GPCR-dependent alterations. Nearly 50% of the prescribed drugs target members of this integral membrane protein superfamily (Salon *et al*., 2011).

1.2. Classification and Structural Features of GPCRs

GPCRs are integral membrane proteins that are composed of a single peptide chain. They span the cell membrane several times, creating intracellular and extracellular domains. Three main structural domains of GPCRs, as represented in Figure 1.1, can be listed as (1) the seven α-helical transmembrane (TM) domains of 25-35 residues, which are connected to each other through (2) extracellular (ECLs) and (3) intracellular loops (ICLs). While the N-terminal part of the receptor is located on the extracellular side, C-terminal counterpart is in the cytoplasm (Venkatakrishnan *et al*., 2013).

1.2.1. Different Classes of GPCRs

GPCRs are classified into five families based on the structural similarities of TM domains (Fredriksson *et al*., 2003). First one of those classes, Class A, or rhodopsin family, accounts for almost 80% of GPCRs. Ligands are mostly peptides, lipids or biogenic amines. Receptors in Class B, or secretin family, have an N-terminal domain of 100-160 residues, which is the main difference from Class A receptors. Their ligands are mostly neuropeptides and hormones. Class C family consists of the metabotropic glutamate-like receptors that have an important role in neurotransmission. Class C receptors also have

relatively larger N- (300-600 residues) and C-terminal regions. They also have their signature domain, the Venus Fly trap module that is connected via a cysteine (Cys)-rich domain to the TM domains of the receptor (Kunishima *et al*., 2000). Class D, or fungal mating pheromone receptors are divided into two subfamilies, Ste2 and Ste3. Receptors that fall in this group do not share most of the characteristic domains of Class A receptors. Cyclic AMP (cAMP) receptors constitute the Class E receptor family. Most of the receptors in this family are characterized in *Dictyostelium discoideum* as cAMP-sensing receptors. The last class of GPCRs is the Class F, which consists of 24 Frizzled and Smoothened receptors, operates Wnt-mediated pathways and Hedgehog signaling, respectively (Prabhu and Eichinger, 2006).

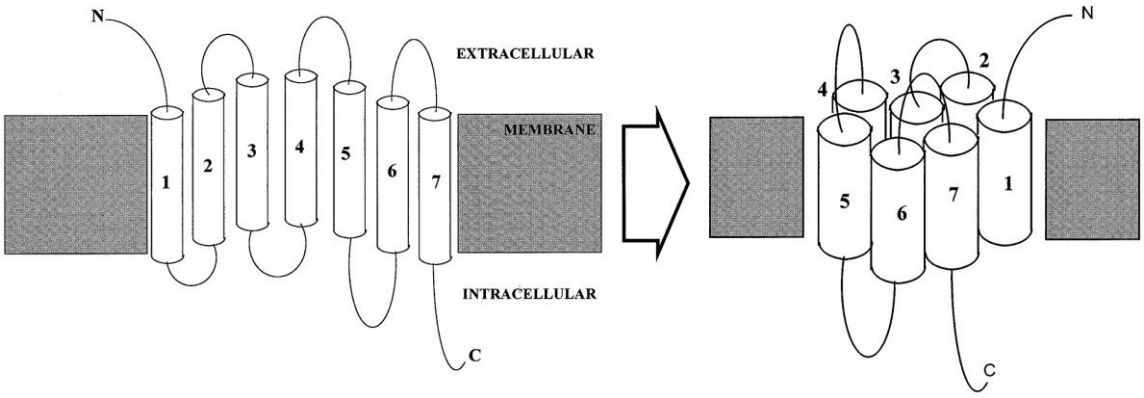

Figure 1.1. Schematic representation of the membrane topology and three dimensional packing of a GPCR. (Adapted from Flower, 1999).

1.2.2. Structural Features of Class A GPCRs

Because they comprise the largest family and are involved in many important physiological processes, rhodopsin-like receptors have been subjected to extensive structural studies. Within past decades, a tremendous progress has been achieved revealing detailed structural information on several Class A GPCRs (Stevens *et al*., 2013). The information obtained from crystal structures of GPCRs uncovered the structural patterns that are common for specific GPCR families.

When looking at the sequences of rhodopsin-like GPCRs, it can first be noticed that the major similarity is within the helices composed of hydrophobic residues. These domains are linked by alternating extra- and intracellular loops varying in different GPCRs. Mostly within these transmembrane domains and at their proximal regions, there is a series of conserved residues that are termed as fingerprint residues, as shown in Figure 1.2. These residues are important in regulating the transition of the receptor conformation from inactive to active state upon ligand binding.

One of the most highly conserved motifs is the D/ERY (Glu/Asp-Arg-Tyr) motif that is located at the third helix, close to its cytoplasmic end. This motif forms a salt bridge between its Arg residue and another conserved residue of the fourth helix, Glu or Asp. This salt bridge between two transmembrane helices act as an ionic lock that constrains receptors in the inactive conformation (Rovati *et al*., 2007). Several studies have shown that the mutations within this motif disrupts the ionic lock and causes constitutive activation (Alewijnse *et al*., 2000).

Another highly conserved motif in Class A GPCRs is the NPxxY motif, located close to the cytoplasmic end of the seventh helix. Residues in this motif mostly interacts with water molecules and form hydrogen bonds that affect G protein binding to the receptor (Fritze *et al*., 2003).

Two cysteine residues located at the extracellular end of the third transmembrane (3TM) domain and the second extracellular loop (ECL2) are also a common motif in many rhodopsin-like receptors. These residues form a disulfide bond that is responsible for correct folding and orientation of the receptor at the cell membrane (Karnik and Khorana, 1990), and maintaining the ligand binding site (Palczewski *et al*., 2000).

Apart from the above-mentioned conserved motifs, there are several other domains or residues that are found to have importance in the structural organization of GPCRs. For example, glycosylation of aspartic acid residues at the N-terminal domain is necessary for

correct folding and its stability (Wheatley and Hawtin, 1999). It was later found in a number of receptors that mutations in glycosylation sites of ECL2 caused decreased ligand binding, because the receptor was misfolded (Lanctot *et al*., 2005).

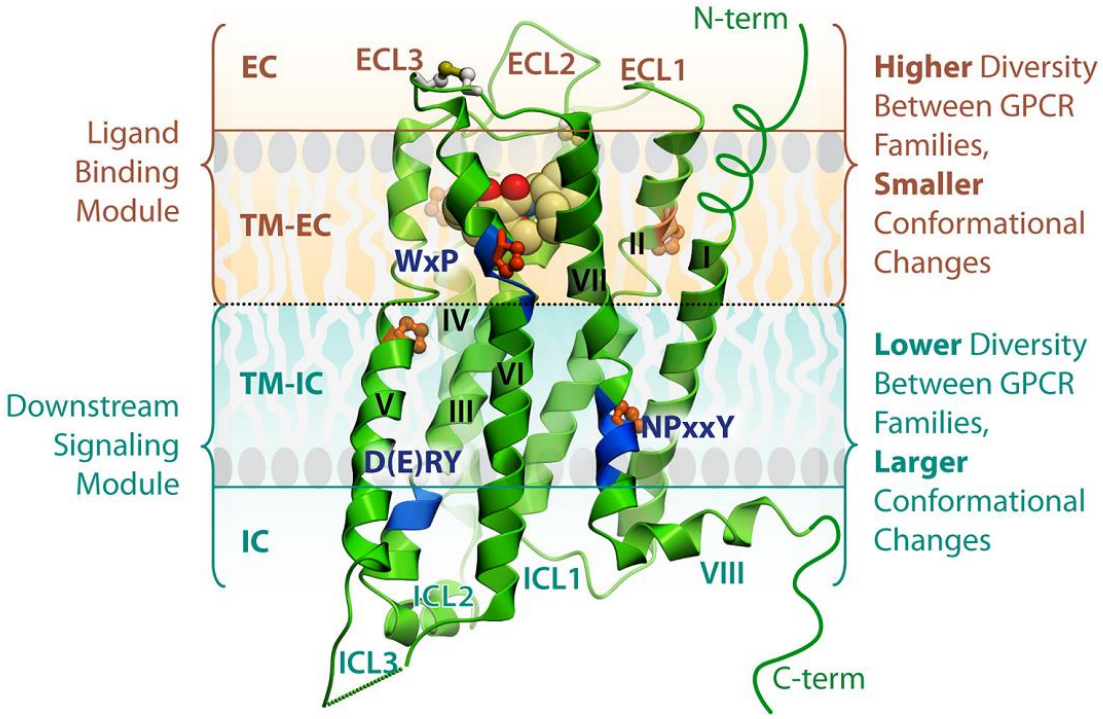

Figure 1.2. General architecture and main structural features of GPCRs. Extracellular domain elements, N-terminal domain and extracellular domains are involved in accommodating ligand binding to the receptor. Upon binding of the ligand, conformational changes occur within extracellular and intracellular parts of the TM domains. Following the structural changes, intracellular elements interact with downstream signaling proteins (Katritch *et al*., 2013).

Another highly conserved feature of GPCRs is the proline and tryptophan residues within the TM domains. These residues were found to play important roles in receptor expression, ligand affinity and activation of downstream pathways (Wess *et al*., 1993). C-terminal Ser and Thr residues are also well-conserved residues within GPCRs and these residues are crucial for receptor phosphorylation. Mutant GPCRs at this specific residues were not phosphorylated. Thus, β-arrestin-mediated signaling, desensitization

and internalization of mutant receptors are inhibited (Tobin, 2008). There are also few other conserved residues within ICLs that are important for receptor coupling with intracellular proteins (Venkatakrishnan *et al*., 2013).

1.2.3. Structure-Function Relationship of GPCRs

Structural studies of GPCRs have been contributing valuable information on the activation mechanisms of GPCRs. Elucidating the structures at both agonist and antagonist-bound states and their comparison with the unbound receptor give several opportunities to reveal the conformational changes that mediates activation (Lebon *et al*., 2011) or inactivation (Ijzerman *et al*., 2008). The general concept for GPCR activity is the activation of the receptor upon ligand binding. However, GPCRs are not fully-inactive when they are not bound to a ligand, but they are in a dynamic equilibrium between inactive and active states (Kobilka and Deupi, 2007). Upon binding to a ligand, these constraining interactions are disturbed and activation interactions between several domains and residues are formed (Bouvier, 2013). If an agonist binds to a receptor, the equilibrium is shifted towards the active state, while binding of an inverse agonist shifts this equilibrium towards the inactive state. Degree of shifting the active/inactive state equilibrium reflects the potency of that ligand. While full agonists stabilize the active state, partial agonists can shift the equilibrium towards active state only to a certain degree. On the other hand, inverse agonists inhibit the basal activity, while antagonists only block the binding site and have no effect on basal activity (Deupi and Kobilka, 2007).

Ligands of GPCRs bind to specific binding pockets that are finely-organized cavities by combination of residues within ECLs and TM domains. Binding of a ligand triggers large-scale conformational changes throughout the receptor. These conformational rearrangements accommodate a new structure that either inhibits basal activity completely, or mediates activation of receptor and facilitates binding of intracellular effectors to the receptor. The most striking conformational changes upon ligand binding mostly occur within TM domains. Movements and rearrangements of helices result in an upward

and outward swinging, kinking, bending and unwinding of helices that allows ligand settling in the binding pocket and opening of a cavity for G protein binding (Katritch *et al*., 2013). Overall, these conformational rearrangements facilitate activation of the receptor and trigger downstream signaling pathways, giving rise to biological responses.

1.3. G Protein-Coupled Receptor Signaling

Upon binding of a ligand, GPCRs become activated and interact with several effector proteins within the cytoplasm. This interaction activates the effector proteins and trigger effector-specific signaling pathways.

1.3.1. G Protein-Mediated Signaling

Upon activation by an agonist, a receptor couples with a heterotrimeric G protein complex and activates it. G proteins (Guanine nucleotide binding proteins) are members of a superfamily of GTPases. There are three different G protein subunits: Gα (~39-45 kDa), Gβ (~37 kDa) and Gγ (~8 kDa). The heterotrimeric G protein is formed by the assembly of one of the 20 Gα, 6 Gβ and 12 Gγ subunits in humans. In other organisms, there are several subtypes of G protein subunits that enable functional diversity and specificity (Hillenbrand *et al*., 2015). Among them, Gβ and Gγ are strongly associated to each other, so that they act as a single unit. In the heterotrimeric complex, while Gα interacts with Gβ, Gγ does not contribute to this interaction (Wall *et al*., 1995). The heteromeric complex is attached to the membrane through post-translational modifications, such as myristoylation or palmytoylation of Gα and prenylation of Gγ (Wedegaertner *et al*., 1995). Even though G proteins are attached, they can freely move along the membrane. Gα subunit bears two functional domains. One of them is the GTPase domain, which mediates hydrolysis of GTP, and the other is the helical domain that is responsible for interacting with the receptor. Gβ and Gγ subunits also have effector interaction domains (Blake *et al*., 2001).

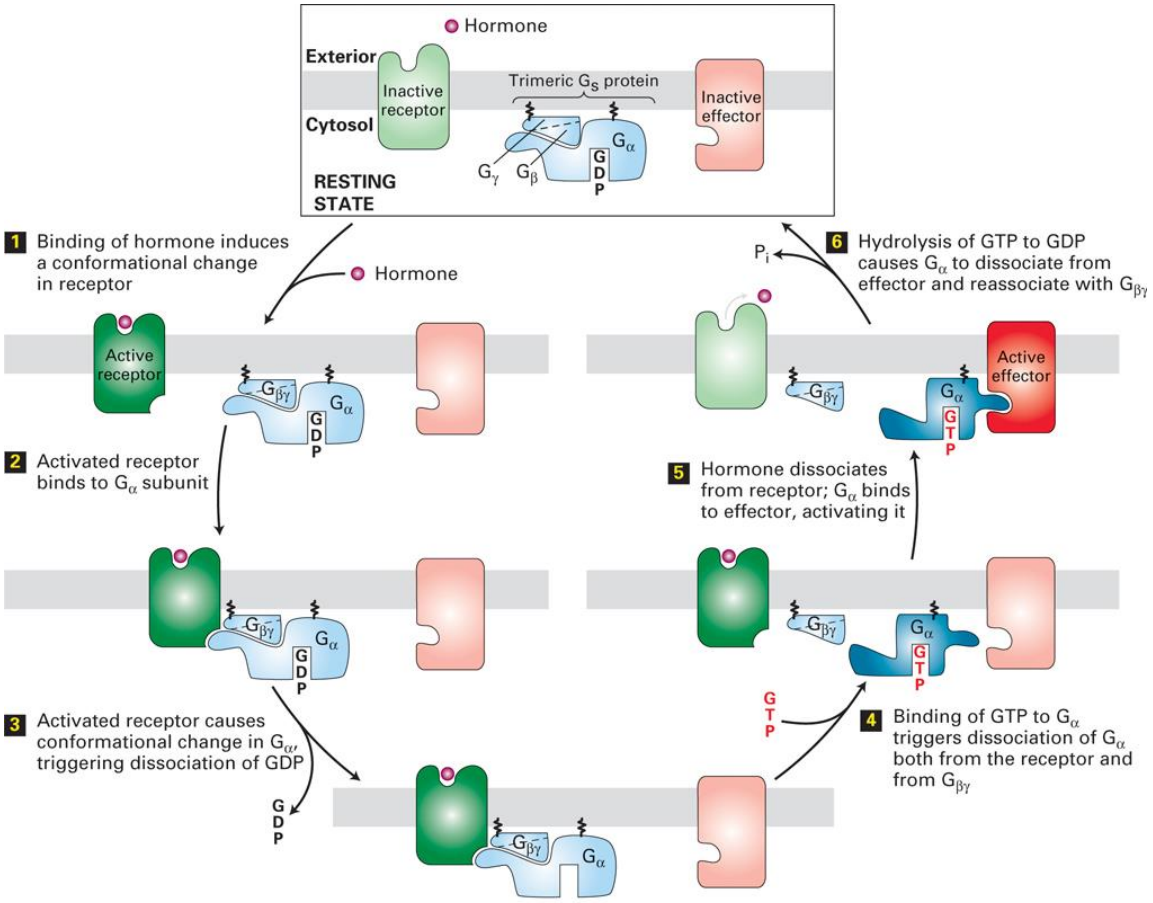

Figure 1.3. Schematic diagram of the heterotrimeric G protein activation cycle (Uzman *et al*., 2000).

When a heterotrimeric G protein is in inactive state, three G protein subunits are interacting, and a guanosine diphosphate (GDP) molecule is bound to Gα subunit. Once an agonist binds and activates its target receptor, conformational changes occur within the receptor and G protein binding cavity becomes accessible. Heterotrimeric G protein, then, interacts with a number of key residues at the ICL3, TM5 and TM6 of the activated receptor via the C-terminus of the Gα subunit. Upon this interaction, G protein undergoes a conformational switch that causes replacement of GDP with GTP. Binding of GTP causes another conformational change in Gα, and upon these changes GTP-bound Gα dissociates both from the receptor and Gβγ, which also becomes released from the receptor. Free GTP-Gα subunit, as well as Gβγ, interacts with its specific effector and triggers its activation. Signaling of GTP-bound Gα is terminated by hydrolysis of the gamma (γ) phosphate

of the GTP, which results in dissociation of the GDP-bound Gα from its effector, and association with Gβγ, and inactivates it as well (Sprang *et al*., 2007). This cycle is repeated upon activation of the same or another receptor, as schematized in Figure 1.3.

1.3.2. Different Classes of G Protein Subunits

Gα proteins are classified based on their sequence identity and the effectors they activate. To date, more than 20 different Gα subunits are identified in mammals and they are divided into four different subfamilies (Offermanns, 2003). Most ubiquitously expressed members of the Gα superfamily are within the $G\alpha_{i/o}$-subfamily. Members of this subfamily inhibit adenylyl cyclases (ACs), which catalyze the conversion of adenosine triphosphate (ATP) to 3', 5'-cyclic adenosine monophosphate (cAMP). $G\alpha_{i/o}$ can also activate G protein gated inwardly rectifying potassium channel (GIRK). An outstanding member of this family, $G\alpha_o$, does not inhibit ACs, but activates a GTPase-activating protein (GAP), namely RapGAP (Jordan *et al*., 1999). Contrary to the members of $G\alpha_{i/o}$, members of the $G\alpha_s$ family interact with and stimulate the activity of ACs and increase cAMP levels and eventually activate Protein Kinase A (PKA). Members of the $G\alpha_{q/11}$ family, namely $G\alpha_q$, $G\alpha_{11}$, $G\alpha_{15}$ and $G\alpha_{16}$ trigger phospholipase C-β (PLC-β) activation, which finally increase intracellular calcium (Ca^{2+}) and activate Protein Kinase C (PKC). The $G\alpha_{12/13}$ family is composed of $G\alpha_{12}$ and $G\alpha_{13}$. These subunits interact with several effectors, such as Rho guanine exchange factor (RhoGEF), RasGEF, cadherin and sodium-hydrogen exchanger (NHE).

There are several isoforms of Gβ and Gγ subunits identified in humans and other organisms. These different isoforms can form functional units of different combinations and interact with different Gα subunits. Assembly of different subtypes regulate activity of different effectors, such as GIRK channels, voltage-dependent Ca^{2+} channels, certain AC isoforms, PLC, phosphoinositide 3 kinase (PI3K) and mitogen-activated protein kinases (MAPKs) (Khan *et al*., 2013).

1.3.3. Canonical Downstream Effectors of G Proteins

Different subtypes of Gα and Gβγ subunits couple and regulate the activities of several effectors. Regulation of the effectors via activated G protein subunits trigger several cellular signaling cascades that eventually affect key cellular processes. Overview of the effectors that are activated by G proteins are summarized in Figure 1.4.

Cyclic AMP (cAMP) is a crucial secondary messenger produced by cells. It is produced via the catalysis of ATP by adenylyl cyclases (ACs), which are membrane bound enzymes. ACs are tightly regulated by the members of $G\alpha_{i/o}$ and $G\alpha_s$ classes. While the subtypes of $G\alpha_{i/o}$ inhibit the activity of ACs and decrease the intracellular cAMP level, $G\alpha_s$ subtypes activate them, thus increase cAMP level. In total, nine different isoforms of ACs were characterized in humans. While all of them are activated via $G\alpha_s$, AC2, AC4 and AC7 are not affected by $G\alpha_{i/o}$. On the other hand, AC2, AC4 and AC7 are activated by Gβγ unit, while AC1, AC5 and AC6 are negatively regulated. It is an interesting aspect that the AC isoforms that are not regulated by $G\alpha_{i/o}$ are positively regulated by Gβγ (Hanoune and Defer, 2001). Cyclic AMP can interact with several proteins, such as PKA, which then phosphorylates a number of proteins that are important in glucose metabolism, hormone and transmitter secretion and intracellular Ca^{2+} mobilization (Seino and Shibasaki, 2005). Exchange protein directly activated by cAMP (Epac), or cAMP-GEF is another intracellular protein that binds to cAMP and activates a small GTPase, namely Rap1, which triggers B-Rad and MAPK pathway that regulates cellular functions such as differentiation and proliferation (X. Cheng *et al*., 2008).

There are several G protein subunits that can activate phospholipases. While PLC-β isoform from 1 to 4 can be activated by all members of the $G\alpha_q$ family, PLC-ε is activated by $G\alpha_{12}$. A number of phospholipases are also activated by Gβγ, such as all isoforms of PLC-β and PLA2 (Runne and Chen, 2013). Activation of PLC leads to phosphatidylinositol 4, 5 bisphosphate (PIP_2) cleavage into diaglycerol (DAG) and inositol 1, 4, 5-triphosphate (IP_3). After DAG activates PKC, IP_3 translocates into endoplasmic reticulum and activates intracellular Ca^{2+} flux (Lanzafame *et al*., 2003).

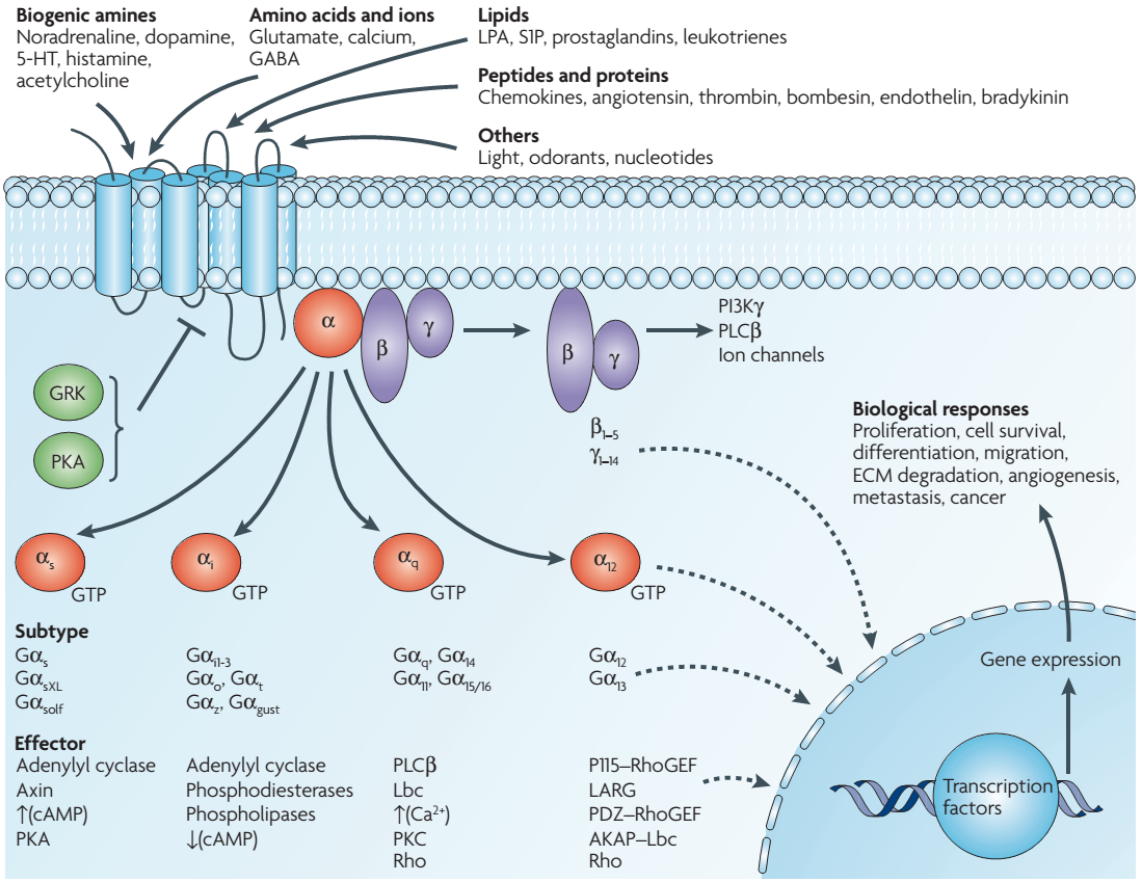

Figure 1.4. Signaling pathways activated by different G protein subunits. Different ligands activate their cognate receptors, which in turn activate a ligand-specific G protein subunit. Activated G protein subunit triggers a signaling cascade via a specific effector (Dorsam and Gutkind, 2007).

Ion channels are another diverse group of membrane proteins that are responsible of transfer of ions (Na^+, K^+, Ca^{2+} and Cl^-). Regulation of membrane potential, activation of certain signaling pathways, maintenance of cellular plasticity and operating molecular secretions are important functions of ion channel proteins (Grigoriadis *et al.*, 2009). A number of ion channels are regulated by G proteins. These "ligand gated" ion channels can be activated directly by G protein subunits, or their effectors. Direct activation of ion channels are operated through the binding of Gβγ (derived from $G\alpha_{i/o}$ or $G\alpha_{q/11}$ activation) to the receptor (Lanzafame *et al.*, 2003). Indirect activation of ion channels is mediated through the phosphorylation of the channel via an activated PKA by cAMP (Dascal, 2001).

G proteins can also directly activate small GTPases and regulate several downstream pathways including the MAPK pathway that regulates key cellular processes such as differentiation, proliferation and apoptosis (Blaukat *et al*., 2000). While the activation of MAPK pathway could be through activation of PKA by cAMP, it can as well be carried out by the activation of small GTPases, such as RasGEF, RhoGEF and c-Raf, mostly via Gβγ (Ito *et al*., 1995). Activation or inhibition of MAPK pathway by G proteins is not a unidirectional model. Since MAPK pathway is a central signaling cascade, it has several regulators. Different subtypes of G proteins regulate MAPK pathway at opposite directions. For example, $G\alpha_s$ can inhibit MAPK pathway by inhibiting C-Raf that triggers MEK1/3-ERK1/2 activation. However, by activation of B-Raf via $G\alpha_s$, MEK1/3-ERK1/2 pathway is activated. This differential regulation of the MAPK pathway via G proteins is due to the different subtypes of G proteins, thus activation of different isoforms of PKAs and ACs (Goldsmith and Dhanasekaran, 2007).

1.3.4. Desensitization and Internalization of GPCRs

Once activated, GPCRs trigger a signaling cascade through G proteins and their effectors. However, GPCRs do not only regulate cellular functions, but its own as well. When a GPCR is exposed to prolonged or repeated exposure by an agonist, it also activates a feedback regulatory mechanism that causes the attenuation of the GPCR-mediated signaling, and consequent desensitization of the receptor. For desensitization, GPCRs need to be phosphorylated. Phosphorylation of GPCRs is mediated by cAMP-activated PKAs and the G protein-coupled receptor kinases (GRKs). It was first thought that not the PKA-mediated phosphorylation, but only GRK activation triggered receptor desensitization (Ferguson and Caron, 1998). However, it was later found that PKA and PKC-dependent phosphorylation of GPCRs were also accelerating GPCR desensitization. However, the main desensitization mechanism is mediated by GRKs (Luttrell and Lefkowitz, 2002).

As schematized in Figure 1.5, when a receptor is bound to its ligand, the Gβγ subunit activates a specific GRK isoform that phosphorylates the active receptor from Ser and Tyr residues at the intracellular loops and the C-terminal region. This phosphorylation

increases the affinity of a class of proteins, called β-arrestins, which binds to the phosphorylated receptor and causes uncoupling of G proteins and binding of clathrin to the receptor. Together with clathrin, binding of the adapter protein 2 (AP-2) targets the receptor-arrestin complex to clathrin-coated pits (CCP) that results in receptor internalization in early endosomes. Receptors in endosomes are then targeted to two pathways: they are either taken up by lysosomes for degradation, or recycled back to the membrane as inactive receptors (Moore *et al*., 2007).

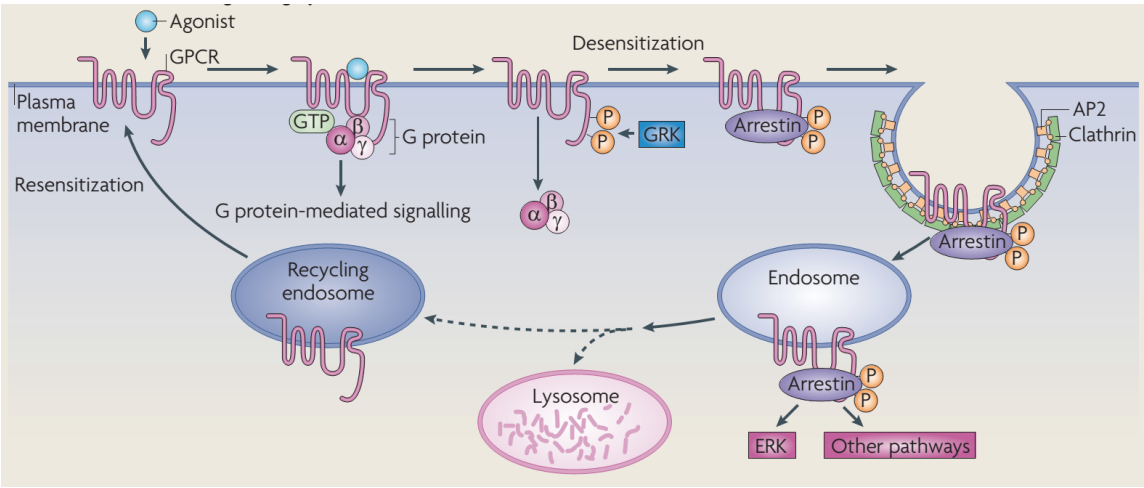

Figure 1.5. Mechanism of GPCR desensitization and internalization. Phosphorylation of the active receptor by GRKs causes G protein de-coupling and β-arrestin recruitment. β-arrestin activates receptor internalization, and then drives the internalized receptor through degradation or recycling. On the other hand, β-arrestin might initiate arrestin-mediated signaling events as well (Ritter and Hall, 2009).

β-arrestins do not only target GPCRs for endocytosis mechanism, but can also activate specific signaling cascades, for example, the RAF-MEK-ERK1/2 pathway (DeFea *et al*., 2000) and the ASK-MKK4-JNK3 (McDonald *et al*., 2000). With the recent evidence, activation of such well-known pathways by β-arrestins show that they are the important players of physiological cellular processes, such as metastasis, chemotaxis, apoptosis and behavior (Lefkowitz *et al*., 2006).

1.4. Insect GPCRs and Neuropeptides

Likewise in mammals, GPCRs play crucial roles in regulating homeostatic, physiological, behavioral and developmental processes in insects, the largest class of Arthropoda. There is growing evidence that GPCR-mediated signaling is involved throughout the insect lifespan. A large number of insect GPCRs are activated by neuropeptides, which are small peptides that are formed by 5-80 amino acids (Bendena, 2010). These neuropeptides are synthetized as larger precursor proteins, but they undergo a number of cleavage that gives rise to active neuropeptides.

The advances in post-genomic era has brought several opportunities to identify orthologous genes within different species. Whole-genome data analyses in insects, such as *Drosophila melanogaster* and *Anopheles gambiae*, provided strong collections of data from which GPCRs could also be explored (Brody and Cravchik, 2000; Hill *et al*., 2002). Studies on classification of insect neuropeptide receptors have shown that these GPCRs can also be classified in a similar fashion as in mammalian GPCRs. There are five different classes of insect GPCRs, namely rhodopsin-like (Family A), secretin-like (Family B), metabotropic glutamate (Family C), frizzled/smoothened and Family F receptors (Adams, 2010). Tremendous effort on transcriptomics studies and verification by proteomics provided very valuable information on insect peptidomes, from which precursors of neuropeptides have been identified precisely (Hummon *et al*., 2006). Combining this genetics, transcriptomics and proteomics data, it is possible to characterize insect GPCRs with their physiological ligands. Studies on insect GPCR physiology have shown that insects also have G protein orthologues of α, β and γ subunits that act in a similar fashion as their mammalian counterparts in terms of signaling pathways they activate (Caers *et al*., 2012).

1.4.1. Allatostatins and Allatostatin Receptors

Allatostatins (ASTs) constitute one of the insect neuropeptide classes inhibiting the synthesis of the juvenile hormone (JH). JH is one of the two main hormones that insect development depends on and it is produced by the *corpora allata* (CA) in the insect brain

(Stay and Tobe, 2007). Allatostatins also have myoinhibitory activity on visceral muscles that regulate feeding behavior (Zandawala and Orchard, 2013). Other than that, they also cause inhibition of fat body-mediated vitellogenin production in cockroaches, inhibition of prothoracicostatic activity, larval heartbeat and regulation of metamorphosis and migratory flight in individual insect species (Tobe and Bendena, 2006). Mode of action for ASTs is schematized in Figure 1.6.

Allatostatins are divided in three groups characterized by their well-conserved domains. The first identified type of ASTs is the cockroach type, FGLa/ASTs (A-type) that are characterized by the conserved Y/F-X-F-G-L-amide sequence at the C-terminal region. The second type is the cricket type, MIP/ASTs (A-type), have conserved W-X_6-W-amide sequence, and the third is the moth type, PISCF/ASTs (C-type) are named after the C-terminal P-I-S-C-F-amide sequence (Woodhead *et al*., 1989). This type of ASTs have been identified in species within Lepidoptera, Diptera and Coleoptera so far. These peptides contain a disulfide bridge between two Cys amino acids, and give rise to a circular peptide structure. Inhibition of JH by PISCF/ASTs was found in moths, but not in *Drosophila melanogaster* (Weaver and Audsley, 2009). Moreover, in mosquitoes PISCF/ASTs were found to be localized at *corpora cardiac* (CC), where no JH synthesis or regulation might occur (Hernández-Martínez *et al*., 2005).

Different types of ASTs exert their activity by binding to their specific GPCRs, namely Allatostatin receptors (AstRs). AstRs fall into rhodopsin-like (Class A) GPCRs and different types of AstRs were identified as human orthologues, due to sequence similarities. While FGLa/AstRs are orthologues of mammalian galanin receptors, MIP/AstRs are orthologues of bombesin receptors and PISCF/AstRs are the orthologues for somatostatin/opioid receptors (H.-J. Kreienkamp *et al*., 2004). The first AST-specific receptor identified in insects was an AstR in *Diploptera punctata* species (Cusson *et al*., 1991). The silkworm orthologue of the PISCF/AstR was found to be expressed abundantly in CC and CA (Yamanaka *et al*., 2008). Later on, with the aid of emerging whole-genome databases, more AstRs were identified genetically and characterized functionally. The first example of such work is the functional characterization of a FGLa/AstR from *Drosophila melanogaster* using a reverse pharmacology approach (Birgül *et al*., 1999). Further work

also revealed that AstRs are functionally expressed in many other insect species, including pests (Audsley and Down, 2015).

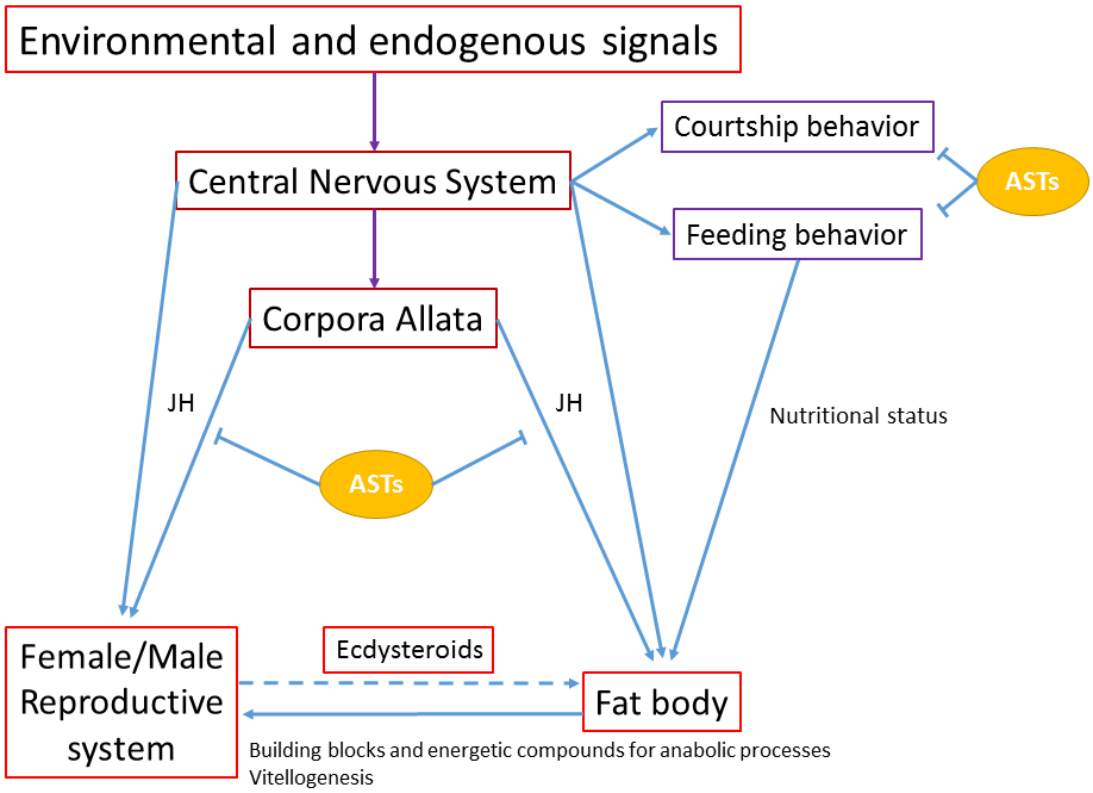

Figure 1.6. Involvement of Allatostatins in the regulation of essential processes in insects. CNS: Central nervous system (Adapted from Van Wielendaele *et al*., 2012).

1.4.2. GPCRs as Potential Targets for Pesticide Applications

Some insect species can be very harmful against crops and even plants in natural forest lands. They can cause reduced growth, and even large-scale loss of trees. Moreover, some insect species are the virus and parasite vectors that cause diseases such as Malaria, Yellow fever, Encephalitis, Typhus, Chagas' disease and Dengue fever (Barrozo *et al*., 2004). Protecting humans, agricultural crops and forests from insect invasion is a challenging problems. Usage of chemical pesticides that mainly target the insect nervous and

hormonal system is the most common way of combatting against pests all around the world (Bendena, 2010). However, the usage of these naturally derived or synthetic chemicals have many drawbacks, such as being harmful to humans, other beneficial insects and whole ecosystem. Another problem is that insects may develop resistance to pesticides after long-term exposure. On the other hand, breakdown products of some of the pesticides may have similar structures to natural plant hormones, which may disturb plant growth and fertilization (Chalubinski and Kowalski, 2006).

Indian stick insect, *Carausius morosus* was also found to synthetize peptides with allatostatic activity *in vitro*. In total, five FGLa/ASTs and six MIP/ASTs were identified (Gäde *et al*., 1997; Matthias W. Lorenz *et al*., 2000). However, *in vivo* experiments have shown that these peptides did not have any effect on JH synthesis in adult stick insect species (M W Lorenz *et al*., 1999). On the other hand, even though not PISCF/AST was isolated from *Carausius morosus*, a PISCF/AstR-like encoding cDNA was partially identified (Auerswald *et al*., 2001). Later, full sequence of this partial cDNA was identified by our group and was named as CamAstR-C. Bioinformatics analysis of the CamAstR-C showed strong resemblance of this receptor to other PISCF/AstRs. Within the same study, a binding case for AST-C was shown on the cells expressing CamAstR-C, by atomic force microscopy. These findings raises up the possibility that the stick insect might synthetize PISCF/AST(s) with their cognate receptor(s) that may be regulating the JH synthesis during vitellogenesis, or other AST-regulated processes.

Because of all above-mentioned drawbacks of insecticides, finding novel targets and designing more environmental-friendly, less harmful insecticides to human health and non-target organisms is now an emerging area. One of the strongest candidate of insecticide targets is insect neuropeptide GPCRs, because they mediate all developmental, physiological and behavioral actions of insects by direct and indirect mechanisms. The reason that several neuropeptides are produced only by insects, targeting the receptors for those peptides might reduce the harm of insecticides on human health (Audsley and Down, 2015).

1.4.3. Potential of Allatostatin Receptors for Insect Control

Because of the inhibitory activity of ASTs on larval development, feeding behavior and metamorphosis, regulation of AstR-mediated mechanisms is thought to be an important candidate for pest control. A number of studies in moths have shown that the knock-down of FGLa/ASTs via double-stranded RNAs caused increased mortality (Griebler *et al*., 2008; Meyering-Vos *et al*., 2006). AstRs were directly targeted by peptidomimetics of ASTs. Regarding this, a study designed and used chemical analogs of FGLa/AST and showed that they were able to inhibit JH synthesis potently in *Diploptera punctata* (Xie *et al*., 2011, 2015). On the other hand, another group used peptide analogues of FGLa/ASTs, instead of the chemical ones. In this study, it was shown that the analog peptide was stable and not degraded by insect proteases. Thus it was able to penetrate through the cuticle and activate its target receptor (Kai *et al*., 2009).

1.5. Methods used in GPCR Characterization

In order to determine on an insect neuropeptide receptor as a target for pesticide design, it is necessary to have information about the biological activity of the natural ligand for that receptor. Next to that, it is also crucial to characterize the existence and function of the receptors that can be the targets for insecticides in individual insect species. For that reason, several groups identified and characterized the functional and pharmacological features of insect neuropeptides using a number of well-established tools.

The process of revealing the natural ligand and functional properties for a receptor is termed as “deorphanizing”. One of the oldest strategies used for receptor deorphanization is the usage of reverse pharmacology approach. In this strategy, heterologous expression systems are used. Cells that heterologously express the orphan receptor of interest is treated with fractions of purified protein extracts and data measurement is performed depending on which secondary messenger is used as a reporter. This approach, to date, is successfully applied on mammalian cell lines and *Xenopus* oocytes by combination of electrophysiological, bioluminescent and fluorescent assays (Caers *et al*., 2012).

Almost all of the insect GPCR deorphanization strategies take the advantage of promiscuous G proteins, namely the human $G\alpha_{16}$ and the murine $G\alpha_{15}$. These Gα subunits can couple with almost all activated GPCRs within the cells, and they activate the PLC-β-mediated pathway that eventually causes an increase in intracellular Ca^{2+} levels. Reporter molecules that can couple with the Ca^{2+}, such as the bioluminescent aequorine protein are used for obtaining readouts to quantify receptor activity (Bender *et al*., 2002). Another reporter molecule that can be used for Ca^{2+} readout is the a mutant of green fluorescent protein (GFP) that becomes fluorescent upon Ca^{2+} binding (Tian *et al*., 2009).

Another widely-used assay for measuring the ligand-specific G protein activation takes the advantage of GDP-GTP exchange of Gα subunits for activation. In this assay, a radioactive GTP analog, guanosine-5'-O-(3'-[^{35}S]thio)-triphosphate ([^{35}S]GTPγS) is used. This analog of GTP can bind to activated Gα, but cannot be hydrolyzed. Thus, radiolabel on the bound [^{35}S]GTPγS can be quantified by scintillation proximity assays (SPA) (DeLapp, 2004). Using the same technique, the levels of IP_3 (activated by $G\alpha_q$), and cAMP (activated by $G\alpha_s$) can be measured using the analogs [^{3}H]inositol and [^{125}I]cAMP, respectively (Horton *et al*., 2005).

In order to characterize G protein specificity of a receptor, assays such as cAMP measurement and GIRK channel activity are used, since their activity solely depends on $G\alpha_s$ and $G\alpha_{i/o}$, respectively. Intracellular cAMP levels can be measured using both a luciferase-based assay that utilizes a reporter gene with the promoter for cAMP response element (CRE) (George *et al*., 1997).

Similar luciferase-based assays are also used to measure activity of other G protein-specific pathways. For example, $G\alpha_{q/11}$-mediated PLC activity was measured via nuclear factor of activated T-cells response element (NFAT-RE)-reporter gene. Likewise, $G\alpha_{12/13}$ activity was measured via RhoGEF-activated serum response element (SRE)-reporter gene (Z. Cheng *et al*., 2010).

1.5.1. FRET-Based Analysis of GPCR Signaling

Several physiological and biochemical techniques that are used to characterize GPCRs are versatile tools to characterize receptor signaling in quantitative terms. Even though these tools were able to determine the components that play important roles in GPCR activation and signaling, they provide poor information about the kinetics and localization of the signaling events. On the other hand, these tools require long times of sample preparation and measurements, and the signals collected using these techniques may contain non-specific signals, because the readouts are downstream signaling molecules that may be activated by non-GPCR-specific cellular processes (Black, 1996).

The principle of FRET is basically the non-radiation transfer of energy from an excited fluorescent molecule to another proximate one. There are certain conditions that should be met for FRET, as schematized in Figure 1.7. Occurrence of FRET requires spectral overlap of a donor emission and acceptor excitation spectra. When the donor fluorophore is excited with a certain wavelength of light, it emits the light at a higher wavelength. If another fluorophore that can be excited that can be excited with the emitted light of donor is at a certain proximity, it can be excited and emits the light with higher wavelength. Another requirement for FRET is the correct orientation of fluorophores in space, in case of using GFP variants as FRET pairs, for example CFP and YFP (Selvin, 2000). In recent years, engineered versions of these fluorescent proteins with improved quantum yields are used to measure FRET at higher resolution (Spiess *et al.*, 2005). These features of FRET makes this technique ideal to study conformational changes within a protein and interactions between two proteins.

Since GPCR-mediated signaling contains several protein-protein interactions, and GPCR activation consists of a number of conformational changes within the receptor protein, signaling and activation properties of GPCRs have been analyzed spatio-temporally at high resolution using FRET (Lohse *et al.*, 2008). Using intramolecular FRET (donor/acceptor labeling a of receptor at two different domains that become proximate to/distant from each other upon conformational changes in an activated receptor), kinetic analyses

of receptor activation can be successfully measured, as proved for several well-studied GPCRs (Hoffmann *et al*., 2005; J.-P. Vilardaga *et al*., 2003). Another intramolecular FRET sensor was designed in order to measure the changes in intracellular cAMP levels. This was achieved by engineering a cAMP binding protein, namely Epac1. Genetically-engineered Epac1-camps carries two fluorophores, YFP at N-terminus, and CFP at C-terminus (Nikolaev *et al*., 2004; Nikolaev and Lohse, 2006). When they are not bound to cAMP, two fluorophores on Epac1-camps are in close proximity, so a high FRET signal is observed. Once it binds with cAMP, two fluorophores move away from each other, and it causes a decrease in FRET signal over the time.

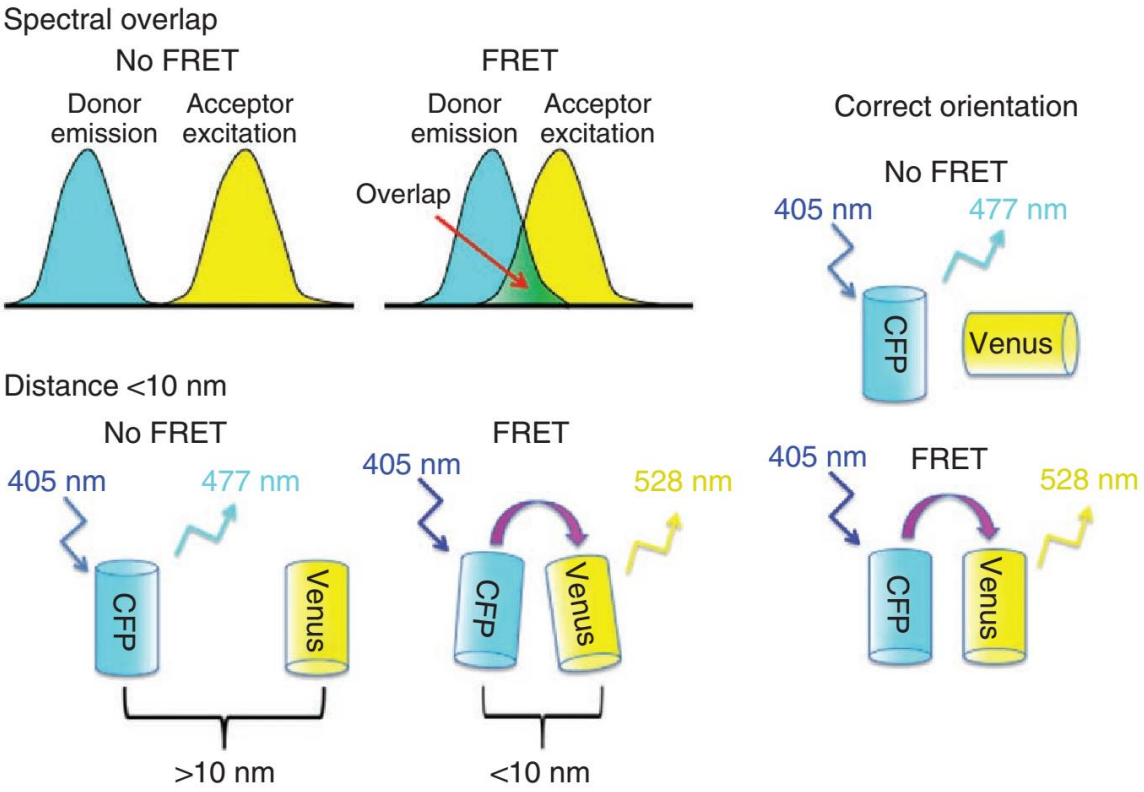

Figure 1.7. Three essential requirements for FRET. Donor emission and acceptor excitation spectra should overlap. The distance between donor and acceptor fluorophores should be less than 10 nm. Dipoles of the fluorophores should be parallel to each other (Adapted from Broussard, Rappaz, Webb, & Brown, 2013).

Next to the intramolecular interactions, FRET has been used in order to determine the kinetics and duration of the interactions between the activated receptor and its interaction partners, such as G proteins, GRKs and β-arrestins (Breton *et al*., 2010; Peter Hein *et al*., 2005; Krasel *et al*., 2005). On the other hand, measurement of G protein activation kinetics, as well as analyses of G protein subunit disassociation/molecular rearrangement have also been studies by FRET using fluorescent-labeled G protein subunits (Bünemann *et al*., 2003; J.-P. Vilardaga *et al*., 2003). Very recently, labeling of different downstream effectors of GPCR-mediated signaling events have elucidated the dynamics of effector activation with G protein interaction, as well as detecting novel pathways for effector regulation (Bodmann *et al*., 2014; Reddy *et al*., 2015).

2. PURPOSE

A transcript from *Carausius morosus* was recently identified and analyzed *in silico* and *in vitro*. This transcript was found to show high sequence similarity to PISCF-AST receptors of other insect species. Therefore, it was thought to be a transcript encoding for a same class of protein in *C. morosus*. Thus, this receptor was named CamAstR-C. Upon bioinformatics analyses, a binding pocket for common PISCF-AST peptide was proposed, and binding studies via Atomic Force Microscopy validated this binding pocket to be specific for PISCF-type of ASTs. However, further evidence was needed in order to prove whether this transcript was encoding for a 7-transmembrane protein, which could bind to a PISCF-AST in *Carausius morosus* and become activated upon ligand binding. The goal of this study is characterizing the cellular localization, functionality and signaling properties of this receptor. Our aim was also to study the signal transduction properties of the mutated receptors, in order to better understand the importance of those domains that were predicted to be important for receptor-agonist interaction. Furthermore, the downstream signaling pathways that are the targets of activated G proteins was also another target of this study, in order to expand the map of CamAstR-C signaling and reveal its ability to trigger various signal transduction pathways in a heterologous expression system.

3. MATERIALS

3.1. General Kits, Enzymes and Reagents

Table 3.1. List of kits, enzymes and reagents.

BCA Protein Assay Kit	Pierce, USA
Dulbecco's Modified Eagle Medium (DMEM)	PAN, Germany
Effectene Transfection Reagent	QIAGEN, Germany
Fetal Bovine Serum (FBS)	Gibco, USA
Genopure Plasmid Midi Kit	Roche, Switzerland
Hank's Buffered Salt Solution (HBSS)	Gibco, USA
High Pure Plasmid Isolation Kit	Roche, Switzerland
Lipofectamine 2000 Transfection Reagent	Invitrogen, USA
Penicillin Streptomycin 10X	Gibco, USA
Phosphate Buffered Saline (PBS)	Gibco, USA
Phusion High-Fidelity DNA Polymerase	Thermo Scientific, USA
PageRuler Unstained Low Range Protein Ladder	Fermentas, USA
QIAquick Gel Extraction Kit	QIAGEN, Germany
Restriction Enzymes	Fermentas, USA
RNase A	Roche, Switzerland
T4 DNA Ligase	New England Biolabs Inc., USA
Taq DNA Polymerase	Fermentas, USA
Trypsin-EDTA (0.53 mM EDTA, 0.05 % Trypsin)	Gibco, USA
Turbofect Transfection Reagent	Fermentas, USA
Vectashield Antifade Mounting Medium	Vector Laboratories, USA

3.2. Chemicals and Disposable Lab ware

3.2.1. Chemicals

Table 3.2. List of chemicals used in this study.

Acrylamide	AppliChem, Germany
Agar	Conda, Spain
Agarose E	Conda, Spain
Ammonium Persulfate (APS)	Sigma-Aldrich, USA
Ampicillin	AppliChem, Germany
β-Mercaptoethanol	Merck, USA
Bovine Serum Albumin (BSA)	Sigma-Aldrich, USA
Bromophenol Blue	Fluka, USA
Calcium Chloride dehydrate	AppliChem, Germany
D-Glucose	Sigma-Aldrich, USA
Dimethyl Sulfoxide (DMSO)	Sigma-Aldrich, USA
EDTA	AppliChem, Germany
Ethanol	Emsure, Germany
Ethidium Bromide	Promega
Formaldehyde	Sigma-Aldrich, USA
Glycerol	Sigma-Aldrich, USA
Glycine	Fisher Scientific, USA
HEPES	Sigma-Aldrich, USA
Isopropanol	Emsure, Germany
Magnesium Chloride	Sigma-Aldrich, USA
Methanol	Emsure, Germany
N, N, N', N'-tetramethylethylenediamine (TEMED)	AppliChem, Germany
NP-40	Roche, Switzerland

Table 3.2. List of chemicals used in this study (cont.).

para-Nitrophenylphospate (p-NPP)	Gold Bio, USA
Phorbol-12-Myristat-13-Acetate (PMA)	Santa Cruz Biotechnology, USA
Poly-L-Lysine Hydrobromide (PLL)	Sigma-Aldrich, USA
Sodium Dodecyl Sulfate (SDS)	AppliChem, Germany
Tris	AppliChem, Germany
Triton X-100	AppliChem, Germany
Tryptone	Conda, Spain
Yeast Extract	Conda, Spain

3.2.2. Consumable Materials

Table 3.3. List of consumable materials used in this study.

Cell Culture Plates, 100 mm, 60 mm, 6-well, 12-well, 96-well	TPP, Switzerland
Assay Plates, 96-well	TPP, Switzerland
Centrifuge Tubes (15 ml, 50 ml)	TPP, Switzerland
Cover Slips	VWR, USA
Cryo Tubes	Greiner Bio One, UK
Filter Tips	CAPP, Denmark
Micropipette Tips	Axygen, USA
Pasteur Pipettes	Hartenstein
Petri Dishes	Fırat Plastik, Turkey
Serological Pipets	VWR, USA
Syringe Filter Units (0.22 μm, 0.45 μm)	EMD Millipore, USA
Test Tubes (0.2 ml, 0.5 ml, 1.5 ml, 2 ml)	Axygen, USA

3.3. Biological Materials

3.3.1. Bacterial Strains

Bacterial strain used in this study was E. coli TOP10 (genotype: F- mcrA Δ(mrrhs-dRMS-mcrBC) ϕ80lacZΔM15 ΔlacX74 recA1 araD139 Δ(araleu) 7697 galU galK rpsL (StrR) endA1 nupG).

3.3.2. Cell Lines

Human embryonic kidney cell lines used in this study, HEK293FT was kindly provided by Prof. Nesrin Özören, Boğaziçi University, and HEK293T was kindly provided by Prof. Moritz Bünemann, Philipps University Marburg, Germany.

3.3.3. Antibodies

Table 3.4. List of antibodies used in this study.

Antibody	**Host/Isotype**	**Company**	**Concentration**	**Purpose**
β-actin	Rabbit	Cell Signaling	1:1000	WB
p44/42 MAPK (Erk1/2)	Rabbit	Cell Signaling	1:1000	WB
Phospho-p44/42 MAPK (Erk1/2) (Thr202/Tyr204)	Rabbit	Cell Signaling	1:1000	WB
Rabbit IgG	HRP	Cell Signaling	1:5000	WB
ZO-1	Rabbit	Thermo Fisher	1:1000	IF
Rabbit IgG	AlexaFluor 555	Abcam	1:500	IF

3.3.4. Peptides

Custom peptides were designed in silico and obtained by custom synthesis from Biomatik, Canada. Peptides that were used in this study are as follows: *Drosophila melanogaster* Allatostatin-C (AST-C) (pQVRYRQCYFNPISCF) and *Drosophila melanogaster* Allatostatin-3A (AST-3A) (SRPYSFGL-NH_2).

3.3.5. Plasmids

Table 3.5. List of plasmids used in this study.

Construct	**Species**	**Origin**	**Vector**
Empty pcDNA3		Invitrogen, USA	pcDNA3
CamAstRC	*C. morosus*	(Duan Sahbaz, 2013)	pcDNA3
CamAstRC-SYFP2	*C. morosus*	This study.	pcDNA3
CamAstRC-sensor	*C. morosus*	This study.	pcDNA3
pcFb2AR-SYFP2	Human	(Krasel *et al*., 2005)	pcDNA3
α_{2A}-AR (HA-tagged)	Mouse	(Bünemann *et al*., 2003)	pcDNA3
$G\alpha_{i1}$ C351I	Rat	(Bünemann *et al*., 2003)	pcDNA3
$G\alpha_o$	Rat	(Frank *et al*., 2005)	pcDNA3
$G\alpha_s$	Rat	(Hein *et al*., 2006)	pcDNA3
$G\alpha_q$	Mouse	(Adjobo-Hermans *et al*., 2011)	pcDNA3
$G\alpha_{i1}$-YFP C351I	Rat	(Bünemann *et al*., 2003)	pcDNA3
$G\alpha_o$-YFP	Rat	(Frank *et al*., 2005)	pcDNA3
$G\alpha_s$-YFP	Rat	(Hein *et al*., 2006)	pcDNA3
$G\alpha_q$-YFP	Mouse	(Adjobo-Hermans *et al*., 2011)	pcDNA3

Table 3.5 List of plasmids used in this study (cont.).

$G\beta_1$	Human	(Bünemann *et al*., 2003)	pcDNA3
$G\beta_1$-Cerulian	Human	(Bünemann *et al*., 2003)	pcDNA3
$G\gamma_2$	Bovine	(Ruiz-Velasco *et al*., 2001)	pcDNA3
CFP-$G\gamma_2$	Bovine	(Ruiz-Velasco *et al*., 2001)	pcDNA3
GRK2	Human	(Krasel *et al*., 2005)	pcDNA3
Arrestin3-CFP	Bovine	(Krasel *et al*., 2005)	pcDNA3
AC5	Human	(Milde *et al*., 2014)	pcDNA3
Epac1-camps	Human	(Nikolaev *et al*., 2004)	pcDNA3
$G\alpha_{q/i1}$	Human	(Inoue *et al*., 2012)	pCAGGS
$G\alpha_{q/i3}$	Human	(Inoue *et al*., 2012)	pCAGGS
$G\alpha_{q/o}$	Human	(Inoue *et al*., 2012)	pCAGGS
$G\alpha_{q/s}$	Human	(Inoue *et al*., 2012)	pCAGGS
$G\alpha_{16}$	Human	(Inoue *et al*., 2012)	pCAGGS
AP-TGFα	Human	(Inoue *et al*., 2012)	pcDNA3

3.3.6. Primers

Table 3.6. List of primers used in this study.

Primer Name	**Aim**	**Sequence**	**RE Cutting Site**
CamAstRC_F	Cloning	CCCAAGCTT ATGTCTGTGGAACAAGTGACG	HindIII
CamAstRC_R_NS	Cloning	TGCTCTAGA CACCTGGGTCGGCTGCTG	XbaI

Table 3.6. List of primers used in this study (cont.).

CamAstRC-R	Cloning	TGCTCTAGA CTACACCTGGGTCGGCTGCTG	XbaI
FLAG-CamAstRC_F1	Cloning	CCCAAGCTT ATGGACTACAAGGACGATGATGAC-GCC	HindIII
FLAG-CamAstRC_F2	Cloning	GGACGATGATGACGCC ATGTCTGTGGAACAAGTGACG	-
SYFP2_F	Cloning	CGGGATCC GTGAGCAAGGGCGAGGAGCTG	BamHI
SYFP2_R	Cloning	CTAGCTAGC CTTGTACAGCTCGTCCATGCC	NheI
SYFP2_AstRC_F	Cloning	CTAGCTAGC AAGAACAAGTCCAAGGAGAAG	NheI
SYFP2_AstRC_R	Cloning	CGGGATCC GGGCCCGACGGTCTTCAGCTTC	BamHI

3.4. Buffers and Solutions

3.4.1. DNA Gel Electrophoresis

Table 3.7. Preparations of buffers and solutions used in DNA gel electrophoresis.

Solution	**Content**
50X Tris-Acetic acid EDTA (TAE)	2 M Tris-acetate 50 mM EDTA pH 8.5
Ethidium Bromide (EtBr)	Merck, USA

3.4.2. Bacterial Media

Table 3.8. Preparations of buffers and solutions used in bacterial culture.

Luria Bertani Medium (LB)	10 g Tryptone 5 g Yeast Extract 5 g NaCl Distilled water up to 1 L, autoclaved
LB Agar	1 L LB medium 15 g Agar
Ampicillin stock (1000X = 100 mg/ml in 70% EtOH)	100 mg/ml in 50% ethanol Sterilized by filtration and stored at -20˚C 100 µg/ml (1X) working concentration

3.4.3. Polyacrylamide Gel Electrophoresis (PAGE) and Western Blotting

Table 3.9. Preparations of buffers and solutions used in PAGE and Western Blotting.

10% SDS-PAGE gel (Running gel)	10%Acrylamide : Bisacrylamide (37.5:1) 375mM Tris-HCl (pH 8.8) 0.1% SDS 0.1% APS 0.1% N, N, N, N-Tetramethylethylenedia-mine (TEMED)
4% SDS-PAGE gel (Stacking gel)	5%Acrylamide : Bisacrylamide (37.5:1) 125mM Tris-HCl (pH 6.8) 0.1% SDS 0.1% APS 0.1% TEMED

Table 3.9. Preparations of buffers and solutions used in PAGE and Western Blotting (cont.).

Running Buffer	25 mM Tris 192 mM Glycine 0.1% SDS
Transfer Buffer	25 mM Tris 200 mM Glycine 10% Methanol
Tris Buffered Saline with Tween 20 (TBS-T)	150 mM NaCl 20 mM Tris-HCl pH 8.0 0.1% Tween 20
Western Blot Blocking Solution	5% non-fat milk powder in TBS-T
4X Protein Loading Dye	200 mM Tris-Cl pH 6.8 8% SDS 40% Glycerol 4% β-Mercaptoethanol 50 mM EDTA 0.8% Bromophenol Blue
Cell Lysis Buffer	137 mM NaCl 20 mM Tris-Cl pH 7.4 2 mM EDTA 0.2% NP-40 5 mM NaF
SOC Medium	20 g Tryptone 5 g Yeast extract 2 ml of 5M NaCl 2.5 ml of 1M KCl 10 ml of 1M $MgCl_2$ 10 ml of 1M $MgSO_4$

3.4.4. Immunofluorescence

Table 3.10. Preparations of buffers and solutions used in Immunofluorescence.

10X PBS	81.8 g NaCl 2 g KCl 14.2 g Na_2HPO_4 2.45 g KH_2PO_4 Up to 1 L with distilled water, autoclaved
4% Paraformaldehyde (PFA) Solution	40 g Paraformaldehyde 1 ml of 10 M NaOH Up to 1 L with distilled water
Immunofluorescence Blocking Solution	3% Bovine Serum Albumin (BSA) in PBS

3.5. Equipment

Table 3.11. Equipment used in this study.

Agarose Gel Electrophoresis System	Mini-sub Cell GT, Bio-Rad, USA
Autoclaves	MAC 601, Eyela, Japan ASB260T, Astell, UK
Carbon dioxide Tank	2091, Habaş, Turkey
Cell Culture Incubator	Hepa Class 100, Thermo, USA
Centrifuges	Centrifuge 5415R, Eppendorf, USA Allegra X22-R, Beckman, USA J2-21 Centrifuge, Beckman, USA
Documentation System	G:BOX Chemi XX6, Syngene, UK
Freezers	2021D, Arçelik, Turkey ULT Freezer, ThermoForma, USA

Table 3.11. Equipment used in this study (cont.).

Incubator	Hepa ClassII Forma Series, Thermo, USA
Heat Block	DRI-Block DB-2A, Techne, UK
Laminar Flow Cabinets	Labcaire BH18, UK
Magnetic Stirrers	M221 Elektro-mag, TURKEY Clifton Hotplate Magnetic Stirrer, HS31, UK
Microscopes	Axioplan, Zeiss, Germany Observer.Z1, Zeiss, Germany TCSSP5II, Leica, Germany
Micropipettes	Finnpipette, Thermo, USA
Microwave Oven	M1733N, Samsung, MALAYSIA
pH Meter	H221, Hanna Instr., USA
Power Supply	Bio-Rad, USA
Plate reader	VersaMax, Molecular Devices, USA
Spectrofluorometer	Cary Eclipse, Agilent Technologies, USA
Pipettors	Greiner-bio one, UK RatioLab acupetta, Germany
Power Supplies	EC135-90, Thermo Electron Corp Power Pac Universal, BIO-RAD, USA
Scales	Precisa XT4200C, Germany
SDS-PAGE Electrophoresis System	Mini-PROTEAN 4Cell, BIO-RAD, USA
SDS-PAGE Transfer System	Trans-Blot Semi-Dry, USA
Shakers	VIB Orbital Shaker, InterMed, Denmark Lab-Line Universal Oscillating Shaker, USA
Spectrophotometer	Nanodrop ND-100 Thermo, USA
Vortex	Vortexmixer VM20, Chiltern Scientific, UK
Water Bath	TE-10A, Techne, UK

3.6. Technical Equipment for FRET Measurements: Visitron Setup

Table 3.12. Equipment mounted together with the Visitron setup.

Inverted Microscope	Axiovert 100, Zeiss, Germany
Micromanipulator	MM33, Merzhäuser, Germany
Perfusion System	VX3-8xP, ALA Scientific Instruments, USA
Light source CFP excitation	PrecisExcite-100, 440 nm, CoolLED, UK
Light source YFP excitation	PrecisExcite-100, 500 nm, CoolLED, UK
Excitation filter CFP	436/20 nm, Chroma, USA
Dichroic	458LP, Semrock, USA
Beam splitter (to split off YFP)	505 LP and 416;500;582;657, Chroma, USA
CFP emission filter	470/24 nm, Chroma, USA
YFP emission filter	525/39 nm, Semrock, USA
Dualband excitation filter CFP/YFP	416;501 nm, Semrock, USA
Dichroic	440;520 nm, Semrock, USA
Dualband emission filter	464;547 nm, Semrock, USA
High performance CCD-camera	SPOT Pursuit, SPOT Imaging Solutions, USA
Objective	Plan/Apo N 60x/1.45 Oil, Nikon, Japan
Optical table	Vision IsoStation, Newport Corporation, USA
Cell chamber for microscopy	Attofluor, Invitrogen, USA

3.7. Software and Databases

Table 3.13 Software and databases used in this study.

Image Analysis	ImageJ, http://imagej.nih.gov/ij
Tracing live FRET signals	Visiview, Visitron Systems
Generation of overlay traces and graphs	GraphPad Prism 6, Graph Pad Software
Bleach corrections of raw FRET traces	Origin Pro 9, OriginLab
Construction of plasmid maps	SnapGene Viewer, GSL Biotech, USA
Preparation of images and figures	Inkscape, GNU General Public License

4. METHODS

4.1. Molecular Biology Methods

4.1.1. Preparation of Chemically Competent *E. coli* cells

5 ml of LB medium supplemented with 25 µg/ml streptomycin was inoculated with a 100 µL aliquot of *E. coli* TOP10 strain from glycerol stock, and grown at 37˚C overnight with shaking at 200 rpm. Next day, 25 ml LB medium was inoculated with 0.25 ml overnight culture and grown at 37˚C overnight with shaking at 200 rpm to an optical density at 600 nm (OD_{600}) of 0.3-0.6. Cells were harvested by centrifugation at 6000 rpm for 10 minutes at 4˚C. Pellet was re-suspended with 12.5 ml of autoclaved and ice-cold 50 mM $CaCl_2$, and then incubated on ice for 30 minutes. Cells were centrifuged again at 6000 rpm for 10 minutes at 4˚C, and then the pellet was re-suspended in 2.5 ml autoclaved ice-cold cold 50 mM $CaCl_2$. For long term storage at -80˚C, glycerol was added to the final concentration of 10%. Aliquots of cell mixtures were prepared in 500 ml tubes and frozen in liquid nitrogen, and then stored at -80˚C.

4.1.2. Transformation of the Chemically Competent *E. coli* TOP10 cells

An aliquot of the competent cells were thawed on ice for 15 minutes and 1 µl plasmid or ligation mixture was added into the tube. Cells were incubated on ice for 20 minutes, and then placed on a heat block set at 42˚C for 45 seconds, and then immediately on ice for 2 minutes. 500 µl of LB medium was added and the cells were incubated for 1 hour at 37˚C with shaking at 200 rpm. After incubation, a 100 µl fraction of the cell suspension was spread on selective LB-agar plates containing appropriate antibiotic, and grown overnight at 42˚C.

4.1.3. Preparation of Plasmid DNA from *E. coli*

All plasmid purifications were performed using Genopure or High Pure Plasmid Isolation Kits (Roche, Germany) according to the manufacturer's instructions. Colonies of transformed bacteria were picked from the LB-agar plate using a micropipette tip and inoculated in LB medium (5 ml for mini prep and 50 ml for midi prep isolation). Plasmid concentrations and purities were assessed by spectrophotometric measurements and by agarose gel electrophoresis. Mini prep isolation was performed for sequencing and quality assessment analyses, and midi prep scale isolation was performed to obtain high yield, endotoxin-free plasmid for transfection. Only endotoxin-free plasmids were used for transfection purposes.

4.1.4. Primer Design and Standard Polymerase Chain Reaction (PCR)

Primers were designed in silico using CLC Bio Workbench software (http://www.clcbioworkbench.com). For cloning purposes, appropriate restriction endonuclease sites were attached to the 5' ends of the primers. Melting temperatures of primers for PCR with Taq or Phusion polymerase were calculated with CLC Bio Workbench software.

Polymerase chain reactions were performed to amplify DNA fragments for cloning into different plasmids. *Taq* polymerase or Phusion DNA polymerase were used for DNA amplification, as described in Table 4.1 and Table 4.2, respectively. PCR reactions were prepared in 0.2 ml plastic tubes, spinned down, and a thermal cycler was used to perform the reaction. Amounts of $MgCl_2$, primers, DMSO, and conditions of the annealing temperature and time were optimized in order to obtain a single, specific amplicon of the target DNA fragment.

Table 4.1. PCR reaction mix for *Taq* DNA Polymerase.

Component	**Volume**	**Final concentration**
Template DNA	1 µl	1 µg
10X Taq Buffer	5 µl	1X
$MgCl_2$	4 µl	2 mM
DMSO	2.5 µl	5%
25 mM dNTP mix	1 µl	0.5 mM
Forward primer	1 µl	0.2 µM
Reverse Primer	1 µl	0.2 µM
Taq Polymerase	0.5 µl	0.5 Unit (U)
Distilled water	34 µl	

Table 4.2. PCR reaction mix for Phusion DNA Polymerase.

Component	**Volume**	**Final concentration**
Template DNA	1 µl	1 µg
5X Phusion Buffer	10 µl	1X
DMSO	1.5 µl	3%
10 mM dNTP mix	1 µl	0.2 mM
Forward primer	2.5 µl	0.5 µM
Reverse Primer	2.5 µl	0.5 µM
Taq Polymerase	0.5 µl	0.5 Unit (U)
Distilled water	31 µl	

When setting up the thermal cycling conditions, melting temperatures of primer pairs were considered in order to determine the optimal primer annealing temperature. It

was also considered to set the primer annealing temperature at least 4˚C below the elongation temperature.

Table 4.3. Standard PCR programs to amplify CamAstR-C.

	Taq		**Phusion**	
Step	**Temperature**	**Time**	**Temperature**	**Time**
Initial denaturation	95˚C	5 minutes	98˚C	30 seconds
Denaturation	95˚C	45 seconds	98˚C	10 seconds
Primer annealing	57˚C	30 seconds	66˚C	15 seconds
Elongation	72˚C	1.45 minutes	72˚C	20 seconds
Final elongation	72˚C	7 minutes	72˚C	7 minutes
Hold	4˚C	∞	4˚C	∞

4.1.5. Restriction Enzyme Digestion of DNA

Restriction enzyme digestion reactions were prepared by mixing appropriate enzymes and their respective buffers, DNA fragments or vectors in 0.2 ml PCR tubes to a final volume of 20 µl, and were carried out at 37˚C for 30 minutes using FastDigest Restriction Enzymes (Fermentas, USA). One unit from each restriction enzyme was used for the digestion of 1 µg of DNA. Subsequently, inhibition of the restriction enzyme was performed at 65˚C for 15 minutes.

4.1.6. Agarose Gel Electrophoresis

To prepare 1% Agarose gel, 0.5 g of Agarose was melted in 50 ml 1X TAE buffer by heating using a microwave oven and after cooling the solution to room temperature 5 µl ethidium bromide (final concentration of 0.5 µg/ml) was added to allow UV-light detection of the DNA. Mixture was cast in an agarose tray. After the gel was polymerized, it was placed in an electrophoresis chamber containing 1X TAE buffer. 6X loading dye was mixed with DNA samples to a final concentration of 1X. Samples were loaded in the gel and it was run at 100 Volt constant voltage for 40 minutes.

4.1.7. DNA Extraction from Agarose Gel

After resolving PCR product or digested DNA fragment on agarose gel, bands of interest on the gel were excised using a scalpel and placed into a 1.5 ml micro centrifuge tube, and then extraction of the DNA fragment was performed using QIAquick Gel Extraction Kit (QUAGEN, Germany) according to the manufacturer's instructions.

4.1.8. Ligation of DNA fragments

Ligation of digested vectors and DNA fragments were performed using T4 DNA Ligase (NEB, USA). In this reaction, ligase enzyme was mixed with its appropriate buffer, 100 ng digested plasmid with insert with 1:3 or 1:5 molar ratio, and the reaction was carried out at room temperature for one hour.

4.1.9. Colony PCR and Sequencing

Colonies that were grown on selective agar plates were inoculated in 5 ml LB overnight. Next day, a 1 µl amount of the overnight culture was added to a PCR mix as summarized on Table 4.1, using the universal primers T7 and SP6. Plasmid isolation was

carried out for positive cultures as described in section 4.1.3. Extracted plasmids were sent to Macrogen, Korea for sequencing with universal primers SP6 and T7.

4.2. Cell Culture Methods

4.2.1. Growth and Maintenance of HEK293 Cells

HEK293FT and HEK293T cells were grown in DMEM containing 10% FBS and 1% Penicillin/Streptomycin on 10 cm cell culture dishes in an incubator at 37˚C with 5% CO_2 and 95% air. Culture media were stored at 4˚C and warmed to 37˚C in a water bath prior to use. Containers were wiped with 70% ethanol before using. Cells were passaged every 2-3 days when they reached ~90% confluency on plates. In order to passage cells, DMEM was aspirated and cells were briefly washed with PBS. Cells were treated with 1 ml Trypsin-EDTA (0.53 mM EDTA, 0.05 % Trypsin) and briefly incubated until all cells were detached from the surface. After resuspension with 5 ml DMEM, cells were collected into a 15 ml centrifuge tube and centrifuged at 1200 rpm for 3 minutes at room temperature. Medium was aspirated and cells were again suspended in 5 ml DMEM, and then the cells were transferred to a new 10 cm dish in 1:10 ratio.

4.2.2. Transfection of HEK293 cells

For FRET measurements, HEK293T cells were seeded in 6 cm dishes 16 hours before transfection and transfected using the Effectene Transfection Reagent (QIAGEN, Germany) according to the manufacturer's instructions. In general, a four-day transfection protocol was used in order to prepare transiently transfected cells for FRET measurements, as described in Table 4.4.

For TGFα shedding assay, western blotting and immunofluorescence, HEK293FT cells were grown in 12-well plates and transfected using Lipofectamine 2000 (Invitrogen, USA) according to the manufacturer's instructions.

Table 4.4 Transfection protocol of HEK293T for FRET measurements.

Day, time	**Step**
Day 1, morning	Passage cells from 10 cm dish to 6 cm dish
Day 1, evening	Transfect cells
Day 2, morning	Stop transfection by changing the medium
Day 2, evening	Split cells onto cover slips coated with Poly-L-Lysine
Day 3, morning	FRET measurement

4.3. Biochemical Methods

4.3.1. Agonist Treatment of HEK293FT Cells and Preparation of Cell Lysates

On 6-well plates, HEK293FT cells were transfected as described in section 4.2.2. After 24 hours of transfection, growth medium was replaced with DMEM without FBS and antibiotics. After 2 hours serum starvation, cells were treated with 100 µl of 5 mM Allatostatin-C (AST-C) solution (final concentration of AST-C is 50 µM) prepared in 0.1% BSA in 1X PBS. After 5-10-15-20 minutes of incubations, media were aspirated and cells were briefly washed with 3 ml 1X PBS once. 1 ml lysis buffer was added into wells and plate was placed on ice. Cells were collected using a scraper and they were collected into 1.5 ml micro centrifuge tubes, and then incubated on ice for 30 minutes for cell lysis. Cell lysates were centrifuged at 14000 rpm for 10 minutes at 4˚C. Supernatants were collected into fresh 1.5 ml micro centrifuge tubes and directly used or stored at -20˚C for short term storage.

4.3.2. Quantification of Protein Concentrations in Lysates

Protein quantification was performed using BCA Protein Assay Kit (Thermo, USA). 2000 µg/ml stock BSA solution was serially diluted to obtain BSA standards of

different concentrations (250, 500, 750, 1000, 1500, and 2000 µg/ml). Protein samples were prepared in triplicates of 1/5 dilutions in PBS at a total volume of 20 µl. To prepare the BCA Working Reagent, 50 volumes Reagent A was mixed with 1 volume Reagent B. For each sample, 150 µl of BCA Working Reagent was added into the wells of a 96-well plate. The plate was placed on ice, and then 5 µl of protein and BSA standard samples were mixed with the reagent in the plate. The plate was then incubated at 37˚C for 30 minutes, and then cooled down at room temperature for 5 minutes. The absorbance of the samples was measured versus a water reference at 562 nm using a plate reader. The absorbance values of blank samples were subtracted from the absorbance values of samples and a standard curve was prepared by plotting the average blank corrected absorbance for each BSA standard versus its concentration in µg/ml. Using the standard curve, the protein concentrations for each unknown sample was determined.

4.3.3. SDS-PAGE and Wet Transfer of Proteins

Concentrations of protein samples were made equal according to the lowest amount of protein sample by addition of lysis buffer. 4X protein loading dye was added into each sample and samples were heated at 95˚C for 5 minutes for protein denaturation.

For western blotting, 10% separating gels were cast up to 3 cm from the top of gel cassettes and layered with isopropanol and polymerized for approximately 30 minutes. After polymerization, isopropanol was removed and the 4% stacking gels were cast on the polymerized separating gels. Combs of appropriate width and size were inserted immediately after casting the stacking gel. Gels were assembled onto the electrophoresis modules of Mini PROTEAN 4Cell system. Modules were placed into an electrophoresis tank and the assemblies and the tank were filled with 1X Running Buffer. Combs were removed and samples were loaded into the wells. The lid of the electrophoresis tank was placed and the electrical leads were inserted into a power supply. Electrophoresis was performed at 200V constant voltage for 35 minutes. After electrophoresis was complete, gels were removed from the gel cassette and the stacking gel was discarded.

4.3.4. Western Blotting

Separating gels, PVDF membranes, sponges and blotting papers were immersed in transfer buffer for 10 minutes. The gel cassette was placed into running buffer, with the black side down. Respectively, one fiber pad, a sheet of filter paper, equilibrated gel, pre-wetted PVDF membrane, a sheet of filter paper and one fiber pad were placed onto each other, and then the cassette was closed firmly, being careful not to move any components in the sandwich. The cassette was placed in the transfer module and the module was placed in the tank. A frozen cooling unit and a magnetic stir bar was added into the tank and it was filled with Transfer Buffer. The blot was run at 100V for 90 minutes. Upon completion of the run, blotting sandwiches were disassembled.

Membranes were placed in a TBST solution with 5% non-fat milk and blocked for 1 hour at room temperature by shaking. After blocking, membranes were washed with TBST for 5 minutes. Washing step was repeated three times. After washing, primary antibody solution, prepared in 5% BSA in TBST or 5% non-fat milk in TBST, was added onto the membranes and incubated at 4˚C overnight by shaking. After incubation with primary antibodies, membranes were washed three times with TBST for 5 minutes each. HRP-linked secondary antibodies were diluted in 5% non-fat milk in TBST and added in the membranes, and then incubated at room temperature for 1 hour by shaking. Membranes were again washed three times with TBST for five minutes each. In order to visualize the protein blots, HRP substrate-containing Super Signal West Femto Sensitivity Kit (Thermo, USA) was used. Solution A and Solution B of this kit were mixed at 1:1 ratio and protected from light. Membrane blots were visualized by addition of the HRP substrate on the membranes and imaging with G:BOX Chemi XX6 device.

4.3.5. Immunofluorescence of HEK293FT Cells

HEK293FT cells were grown in 6-well plates were transfected as described in section 4.2.2. Twenty four hours after transfection, cells were detached and split to a 24-well

plate containing PLL-coated cover slips and incubated overnight. In case of agonist treatment before specimen preparation, cells were serum-starved for 2 hours, and then agonist solution was added to the wells. After treatment, growth media was aspirated, cells were washed once with pre-warmed 1X PBS and 1 ml ice-cold 4% PFA was added to each well, incubated for 20 minutes at room temperature, and then aspired. Cells were washed three times with 1X PBS and blocked with 1 ml Immunofluorescence Blocking Solution for 1 hour. After blocking, cells were washed three times with 1X PBS and incubated with 1:500 dilution of anti-ZO-1 antibody in blocking solution for one hour. After incubation, cells were washed three times with 1X PBS and incubated with 1:250 dilution of anti-rabbit antibody conjugated with Alexa Fluor 555 in blocking solution for 90 minutes. After incubation, cover slips were washed once with 1X PBS, 1 μg/ml DAPI and three times with 1X PBS, respectively. Cover slips were mounted with a drop of Vectashield Antifade Medium and place on a glass slide, and then sealed with nail polish. Slides were stored at 4˚C.

4.4. TGFα Shedding Assay

4.4.1. Passage of HEK293FT Cells

The method was adapted and modified from the original protocol published by Inoue *et al*., 2012. HEK293FT cells were grown in 10-cm plates until they reached approximately 90% confluency.

The morning when the cells reached this confluency, growth medium was aspirated, cells were washed once with 1X PBS, and then detached using 1 ml Trypsin-EDTA (0.53 mM EDTA, 0.05% Trypsin). After brief incubation with Trypsin-EDTA, 5 ml DMEM was added to stop trypsin activity. Cells were suspended and collected into a 15 ml centrifugation tube, and then centrifuged at 1200 rpm for 5 minutes at room temperature. Supernatant was aspirated and cells were suspended in complete DMEM medium at a concentration of 2×10^5 cells/ml, seeded at 1 ml to each well of 12-well plates and placed in a cell culture incubator for 24 hours.

4.4.2. Transfection of Plasmids

Opti-MEM Reduced Serum Medium was pre-warmed to room temperature. 125 µl Opti-MEM per well was added in a 1.5 ml tube and mixed with plasmids (250 ng of AP-TGFα, 100 ng of CamAstR-C, and 50 ng of chimeric Gα). In a different tube, Opti-MEM (125 µl per well) and Lipofectamine 2000 (1.25 µl per well) were mixed and briefly vortexed. After 30 minutes of incubation of Lipofectamine mixture, it was combined with the plasmid mixture (125 µl per tube) and incubated further for 20 minutes, added to wells containing cells, and transfected for 24 hours.

4.4.3. Re-seeding of Cells

Growth medium was aspirated and 1 ml 1X PBS was added to each well of transfected HEK293FT cells for washing. Cells were detached with 250 µl Trypsin-EDTA (0.53 mM EDTA, 0.05% Trypsin) and 1 ml DMEM was added to stop trypsin activity. Cells were suspended and collected in 15 ml centrifuge tubes and centrifuged at 1200 rpm for 3 minutes at room temperature. Supernatant was aspirated and cells were suspended in 3 ml 1X PBS. After 10 minutes of incubation at room temperature, cells were centrifuged again at 1200 rpm for 3 minutes. Supernatant was aspirated and cells were suspended in pre-warmed (37˚C) HBSS containing 5 mM HEPES (pH 7.4).

24 wells (3 columns, 8 wells at each column) of a 96-well plate were used for seeding 90 µl of each transfection condition per well. Cells were incubated in a cell culture incubator for 30 minutes prior to addition of ligands.

4.4.4. TGFα Shedding Assay

Five different concentrations of AST-C was prepared at 10X concentration using HBSS as diluent. Thirty minutes after re-seeding, cells were treated with 10 µl AST-C as

schematized in Table 4.5. Plates were gently tapped in order to mix ligand and placed in a cell culture incubator for 1 hour.

After one hour incubation with the ligand, plates were centrifuged using a S2096 microplate centrifuge rotor (Beckman Coulter, USA) at 1200 rpm for 3 minutes at room temperature. From each well, 80 µl cell media were transferred into 96-well assay plates using a multichannel micropipette. p-NPP containing solution (10 mM p-NPP, 40 mM Tris-HCl (pH 9.5), 40 mM NaCl, and 10 mM $MgCl_2$) was prepared during the agonist treatment and incubated at 37˚C. 80 µl of p-NPP solution was added to each well on collected media plates and to cell plates. Plates were incubated at 37˚C for 5 minutes and absorbance values were measured at 405 nm using VersaMax plate reader (Molecular Devices, USA). After 1 hour incubation, absorbance values were measured again.

Table 4.5. Scheme of agonist treatment for TGFα Shedding Assay.

Well	**Compound**	**Concentrations**	
		Preparation (10X)	Final
A	HBSS (Vehicle control)	-	-
B		-	-
C	Ligand	20 nM	2 nM
D		200 nM	20 nM
E		2 µM	200 nM
F		20µM	2 µM
G		200 µM	20 µM
H	TPA (Positive control)	1 µM	100 nM

4.5. Immunofluorescence and Confocal Microscopy

Immunofluorescence labelled cells that were prepared on glass slides for visualization were imaged using a Leica TSC SP5 confocal microscopy setup equipped with a 20x/1.3 oil CS HC x PL APO objective. Water was used between the specimen and cover slips in order to obtain better resolution. YFP was illuminated with a 514 nm 40 mW Diode laser and YFP emission was detected at 518-580 nm range. CFP was illuminated 458 nm with a 65 mW Argon laser and CFP emission was detected at 462-510 nm range. Images were obtained with the LAS AF software in a 1024 x 1024 and 512 x 512 pixel format, consisting of 4 to 32 averaged line scans. The scan speed was set to 400 Hz and pinhole was set to airy 1 in general. Images were saved in "lif" and "tiff" file formats.

4.6. FRET Measurements

4.6.1. PLL-Coating of Coverslips and Re-Seeding Cells

Transiently transfected HEK293T cells were re-seeded to 6-well plates containing PLL-coated coverslips. In advance, coverslips were rinsed once with ethanol, dried and placed into the wells of a fresh 6-well plate. Approximately 150 µl PLL was added onto each cover slip and incubated at room temperature for 20 minutes. Coverslips were washed 3 times with 3 ml PBS and dried. Cells were detached and re-seeded on PLL-coated coverslips as described in 4.4.1.

4.6.2. Preparation of Agonist Solutions, Perfusion System and Cell Chamber

Peptide ligand solutions were prepared in FRET buffer with 0.1% fatty acid-free BSA, and the syringes of the perfusion system was filled with maximum 5 ml of the agonist solutions. 1.5 ml of the samples were run into a collection tube and syringes were refilled to 5 ml again. In order to perform FRET measurements, growth media on coverslips were aspirated and coverslips were placed in an Attofluor cell chamber and the

chamber was filled with FRET buffer (137 mM NaCl, 5.4 mM KCl, 10 mM HEPES, 2 mM $CaCl_2$, 1 mM $MgCl_2$ in ultrapure water, pH 7.35).

4.6.3. FRET Measurement

For FRET measurements, one cell from the mounted coverslip was chosen depending on the intensity and the localization of the CFP and YFP using the dual excitation mode of the fluorescent microscope. After choosing a cell, the tip of the perfusion manifold was positioned close to the chosen cell. During all measurements, cells were continuously superfused with agonist solution and/or the FRET buffer using a valve controller. Depending on the assay, cells were superfused with different concentrations of agonists and FRET buffer, or two different agonists at the same time. For the measurements, cells were excited with 440 nm for 60 milliseconds (ms) at 1 Hertz (Hz) frequency. $F_{CFP\ (440\ nm,\ 480nm)}$ (CFP emission) and $F_{YFP\ (440\ nm,\ 535nm)}$ (YFP emission) were recorded simultaneously at split channels with a CCD-camera. After each measurement, direct YFP emission was measured using 500 nm light for excitation, for the correction of direct excitation of YFP by 440 nm. Background fluorescence was corrected by manually choosing a blank area near the measured cells using the VisiView software.

4.7. FRET Data Analysis

4.7.1. Correction Factors for Bleed Through and False Excitation

The excitation and emission spectra of YFP and CFP overlap partly at 440 nm excitation light and 535 nm emission channel. Due to these overlapping spectra, when cells are excited with 440 nm light, YFP is also partly excited alongside CFP. This excitation of YFP is detected at 535 nm channel, and called as false excitation (FE). Moreover, tailing of CFP emission into the 535 nm channel, which is used to detect acceptor emission, causes a spillover signal that is referred to as bleed through (BT). In order to correct

the false signals caused by the spectral cross-talk, correction factors were determined previous to the measurements.

In order to determine a correction factor for FE, HEK293T cells were transfected with an YFP-only containing plasmid. Fluorescence intensity was measured at 535 nm channel, for excitation at 440 nm (F_{YFP440}) and 500 nm (F_{YFP500}), both values were corrected for background and YFP FE factor was determined by dividing F_{YFP440} by F_{YFP500}. In order to calculate detect a correction factor for CFP BT, cells were transfected with a CFP-only containing plasmid. One cell was measured in FRET measurement mode, excited at 440 nm and the intensity in YFP (F_{CFP480}) and CFP (F_{CFP535}) channels were measured. CFP bleed-through factor was calculated by dividing F_{CFP480} by F_{CFP535}.

After background correction, simply by subtracting the intensity of a background region from both CFP and YFP fluorescence values, corrected YFP was calculated with the following equation:

$$F_{YFP(corr)} = F_{YFP(440,535)} - BT \times F_{CFP(440,480)} - DE \times F_{YFP(500,535)} \qquad (4.1)$$

When obtained $F_{YFP(corr)}$ value for each time point, FRET ratio is obtained by dividing $F_{YFP(corr)}$ by F_{CFP}.

4.7.2. Correction of Photo Bleaching

Illumination of cells with high intensities and at high frequencies for long times during FRET measurements causes a decrease in fluorescence over time. This decrease in fluorescence is called photo bleaching of fluorophores, and is described by mono-exponential decrease of the signal over time. In order to correct the FRET ratio traces, a mono-exponential function was fitted to the manually chosen baseline of the trace, and then the fitted function was subtracted from the measured FRET ratio trace, using Origin Pro 9 software.

4.7.3. Normalization of FRET Ratio Traces

Because FRET measurements are performed on single cells, and every single measured cell have different basal FRET ratios due to differential heterologous expression of fluorophore tagged proteins, measured FRET values vary at each cell. Therefore, FRET ratio traces were normalized to minimum and maximum values. Normalized FRET ratio for each time point were calculated with the following equation:

$$\Delta(F_{YFP}/F_{CFP}) = \frac{((F_{YFP}/F_{CFP}) - (F_{YFP}/F_{CFP})_{min})}{((F_{YFP}/F_{CFP})_{max} - (F_{YFP}/F_{CFP})_{min})} \quad (4.2)$$

4.7.4. Calculation of the Onset and Offset Kinetics

In order to determine the kinetic values for G protein activation and receptor-arrestin interaction, FRET measurements for both conditions were plotted using Origin Pro 9 software. Data points from the plots that corresponded to agonist application (from the beginning until the end) for each individual cell measurement were copied to another data sheet on GraphPad Prism 6 software. Mean values were calculated with standard error, and then those values were plotted against time in seconds. A mono-exponential decay curve and formula was calculated using the one-phase association analysis model on GraphPad Prism 6, and $t_{1/2}$ (time point at half-maximum/minimum of the response) values were automatically calculated and displayed as a bar graph.

Analysis of the G protein deactivation and receptor-arrestin disassociation were also carried out using the same method. Analysis of the data with exponential one phase decay mode was the only difference from the method described above.

5. RESULTS

5.1. Generation of Fluorescently Labelled CamAstR-C

The cDNA encoding for CamAstR-C was identified and cloned into pcDNA3 vector previously by our group (Duan Sahbaz, 2013). Since the initial goal of this work was to study the receptor signal transduction by means of FRET, it was necessary to label CamAstR-C fluorescently. Therefore, a YFP-encoding sequence was fused directly to the C-terminus of CamAstR-C gene using molecular techniques, in order to study the activation-mediated interaction of the receptor with its intracellular interaction partners.

The pcFb2AR-SYFP2 vector was kindly provided by Prof. Moritz Bünemann. This pcDNA3-based vector carries a β_2-adrenergic receptor gene tagged with SYFP2, a yellow fluorescence protein with enhanced brightness, protein folding, and Förster radius (Kremers *et al*., 2006). In order to replace the β_2-adrenergic receptor gene with CamAstR-C in this vector, a restriction digestion reaction was performed to excise the β_2-adrenergic receptor gene, using HindIII and XbaI restriction enzymes. Later, the digested vector was visualized on agarose gel. Figure 5.1 displays the two fragments of the digested circular vector. The upper band, which is the vector backbone with SYFP2, was isolated using QIAquick Gel Extraction Kit (QIAGEN, Germany).

CamAstR-C gene was amplified from pcDNA3-CamAstRC vector using the primers CamAstRC_F and CamAstRC_R_NS, in the presence of Phusion DNA polymerase (Thermo Scientific, USA) in the PCR. The primers carry the restriction enzyme recognition sites for HindIII (CamAstRC_F) or XbaI (CamAstRC_R_NS) at their 5’ end. Next to that, the reverse primer, CamAstRC_R_NS does not align with the last three nucleotides of the CamAstR-C gene, which translate the stop codon (TAG). Therefore, when the amplified gene is fused at its C-terminus with SYFP2, they will be translated and expressed together as a fusion protein.

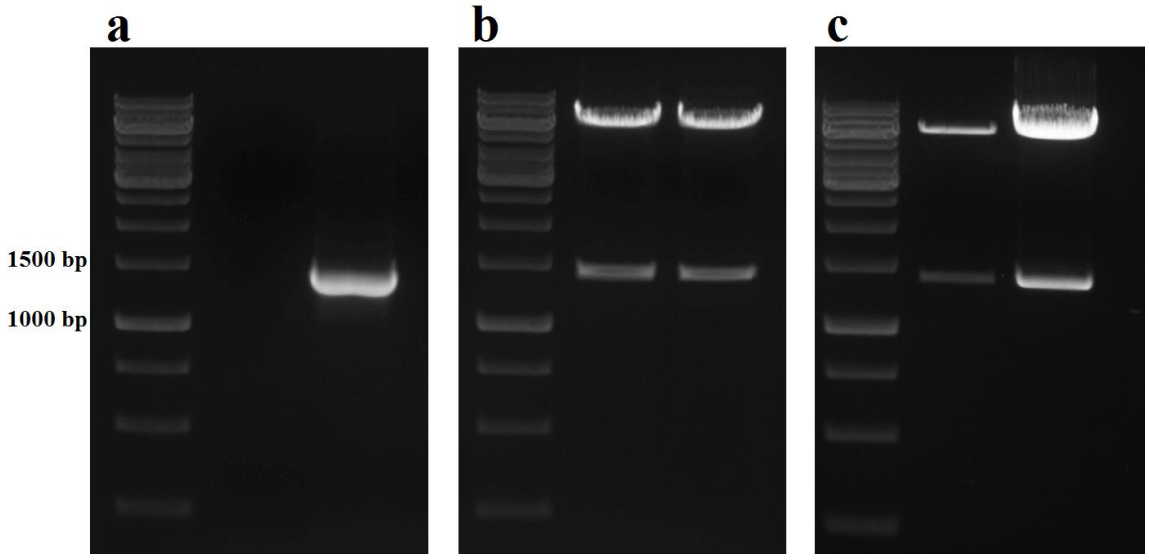

Figure 5.1. a) PCR amplification of CamAstR-C gene from pcDNA3-CamAstRC vector. Lane 1 is the negative control, where no template was added, whereas it was added in lane 2. b) Restriction enzyme digestion of pcFb2AR-SYFP2 vector with conventional HindIII+XbaI (Lane 1) and FastDigest equivalents (Lane 2). c) Restriction enzyme digestion of two isolated plasmids from positive colony cultures. Digested CamAstR-C is observed between 1000-1500 bp lanes.

The annealing temperature for the primer pair was 66˚C. After the PCR, reaction mix was loaded and visualized on agarose gel. The only band appeared on the gel was corresponding between 1000bp and 1500bp (Figure 5.1b). This band was excised from the gel and purified using QIAquick Gel Extraction Kit (QIAGEN, Germany). Later, the PCR product was digested with HindIII and XbaI enzymes, in order to obtain this gene with sticky ends that are complementary with the sticky ends of the digested vector. After restriction digestion, the digested fragment was visualized and purified from the gel.

Concentrations of both the digested vector and CamAstR-C insert were measured using a spectrophotometer (Nanodrop ND-100, Thermo, USA). Ligation reaction was set up by mixing 100 ng digested plasmid with insert at 1:3 or 1:5 molar ratio. Later, the reaction mix was used for bacterial transformation. The next day, a colony PCR was performed in order to determine the colonies that were actually transformed with the ligated

plasmid. Positive colonies were then grown in LB, a small volume of the culture was stored with glycerol at -80˚C, and then plasmid isolation was performed using the rest of the culture. Isolated plasmids were sent to Macrogen Korea for DNA sequencing. Sequencing was requested to be performed using T7 and SP6 primers, which span the whole area where inserts are ligated in pcDNA3-based vectors. Depending on the sequencing results, plasmids that contain SYFP2 fused at the C-terminus of CamAstR-C with no mutation were picked from the -80˚C stocks and cultured in higher volumes for plasmid isolation.

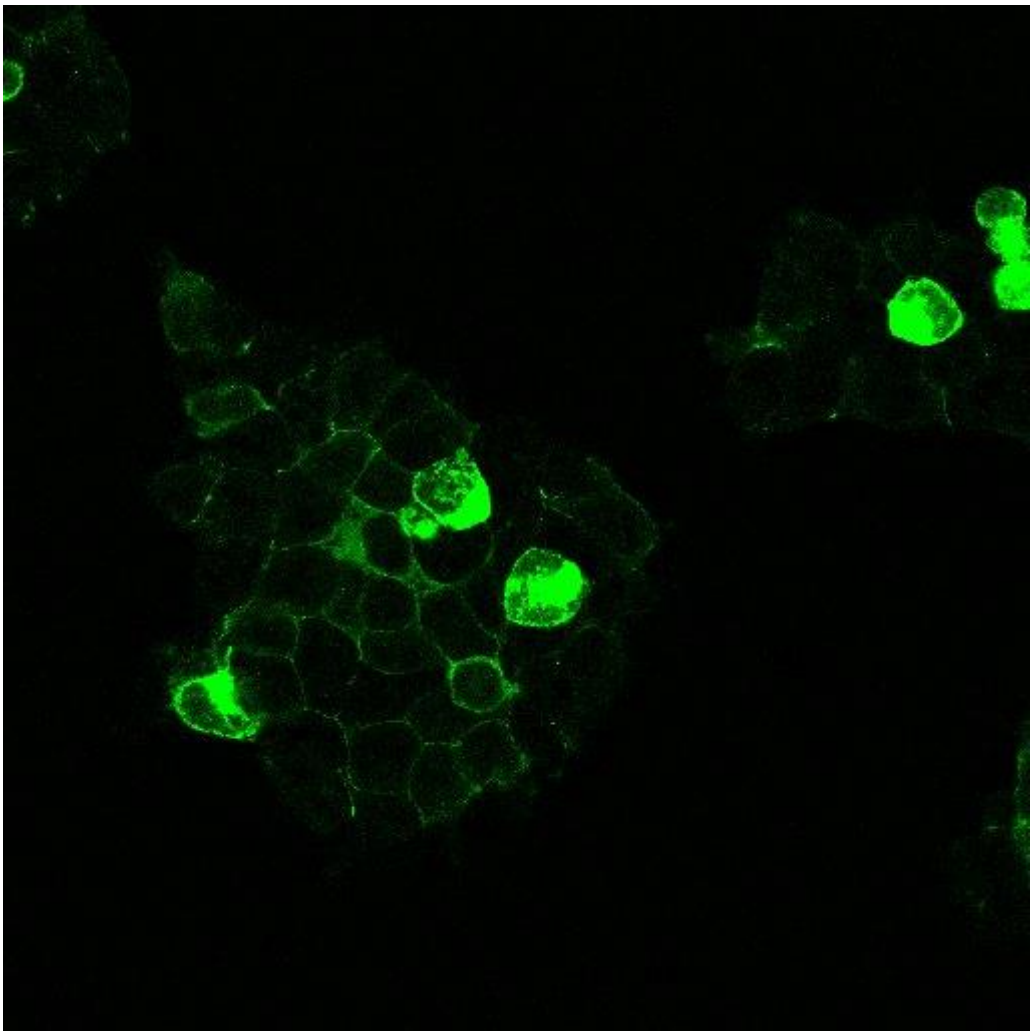

Figure 5.2. Confocal image of expression and localization of CamAstRC-SYFP2 in HEK293T cells.

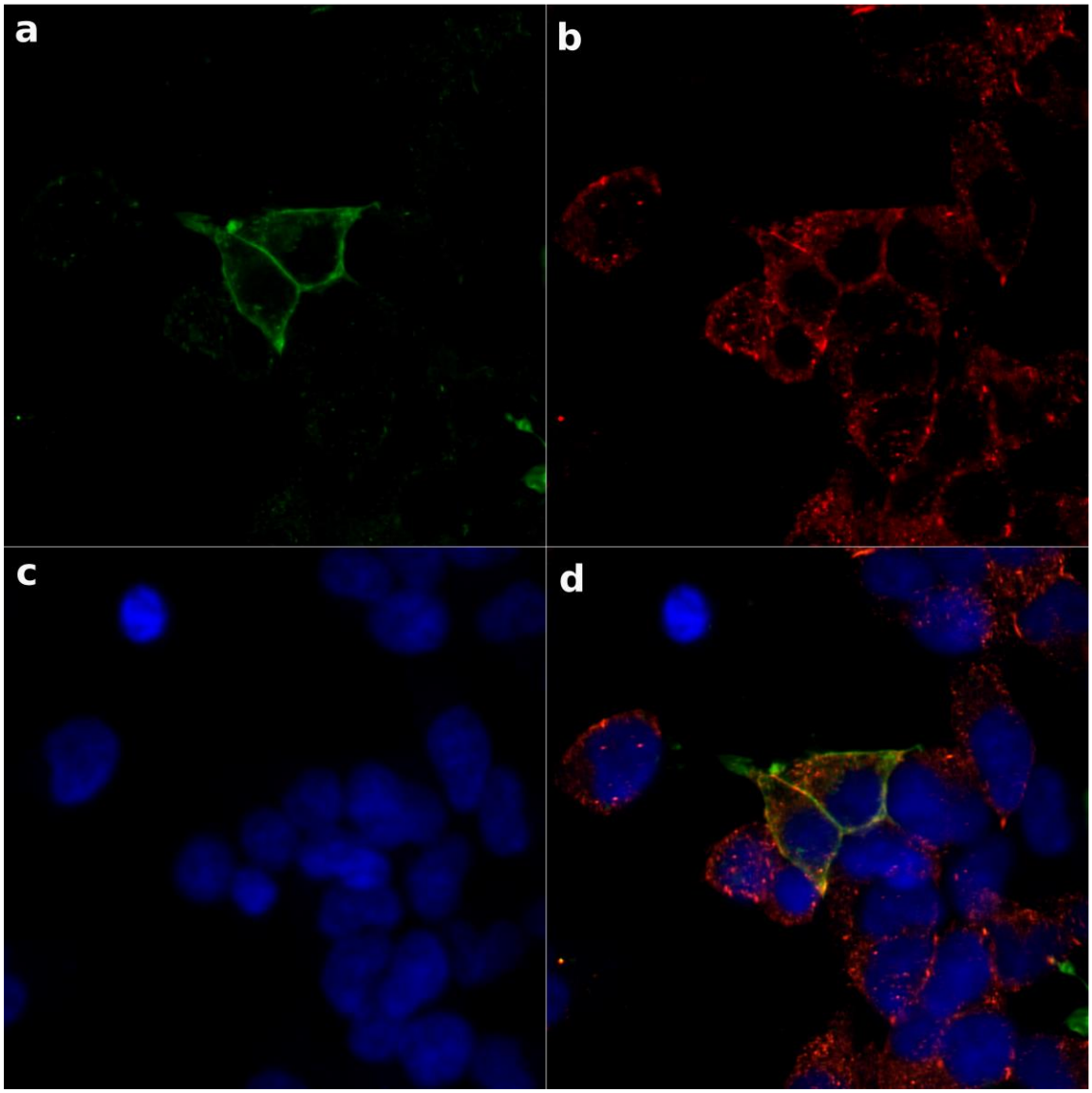

Figure 5.3. CamAstR-C co-localized with ZO-1. Confocal images of transfected and immunostained HEK293 cells show: a) expression and localization of CamAstRC-SYFP2 (green), b) localization of immunostained ZO-1 (red) c) cell nucleus stained with DAPI (blue) and d) three-colors merged together. Membrane expression of CamAstRC-SYFP2 and its co-localization with ZO-1.

5.2. Expression of Fluorescent CamAstR-C in HEK293T Cells

HEK293T cells were transfected with endotoxin-free CamAstRC-SYFP2 plasmid, using Lipofectamine 2000 transfection reagent (Invitrogen, USA) and cells were visualized 24 hours after transfection. It was observed that the expression of the fluorescent-labelled receptor was well-tolerated by HEK293T cells. The fluorescent signal was predominantly localized at the cell membrane region, and also at intracellular region, especially in cells expressing high amounts of protein (Figure 5.2).

After optimization of the transfection with a lower amount of the vector, immunofluorescence experiment was performed on cells expressing CamAstRC-SYFP2. Cell nucleus and ZO-1 (zona occludens 1, a protein located on a cytoplasmic membrane surface of intercellular tight junctions) were also stained with anti-ZO1 antibody and DAPI, respectively. Confocal images revealed that the CamAstRC-SYFP2 was co-localized with immunostained ZO-1, on the cell membrane specifically (Figure 5.3).

5.3. Functionality of CamAstR-C

Previous studies by our group proved AST-C binding to CamAstR-C by means of atomic force microscopy (Duan Sahbaz, 2013). In order to investigate whether CamAstR-C was responsive to AST-C stimulation, we used a method called TGFα-shedding assay. The principle of this assay is measuring the GPCR activation as ectodomain shedding of a membrane bound TFGα, which is fused with alkaline phosphatase (AP). Quantification of the GPCR activity is carried out by measuring released TGFα through the enzymatic activity of the AP. In endogenous conditions, shedding of AP-TGFα is solely dependent on the activation of $G\alpha_q$ and $G\alpha_{12}$ mediated pathways. However, using chimeric Gα proteins that can couple with $G\alpha_i$ or $G\alpha_s$-coupled receptors and activate $G\alpha_q$-mediated pathway, the coverage of the assay was expanded for GPCRs that couple with Gα subunits other than $G\alpha_q$ and $G\alpha_{12}$.

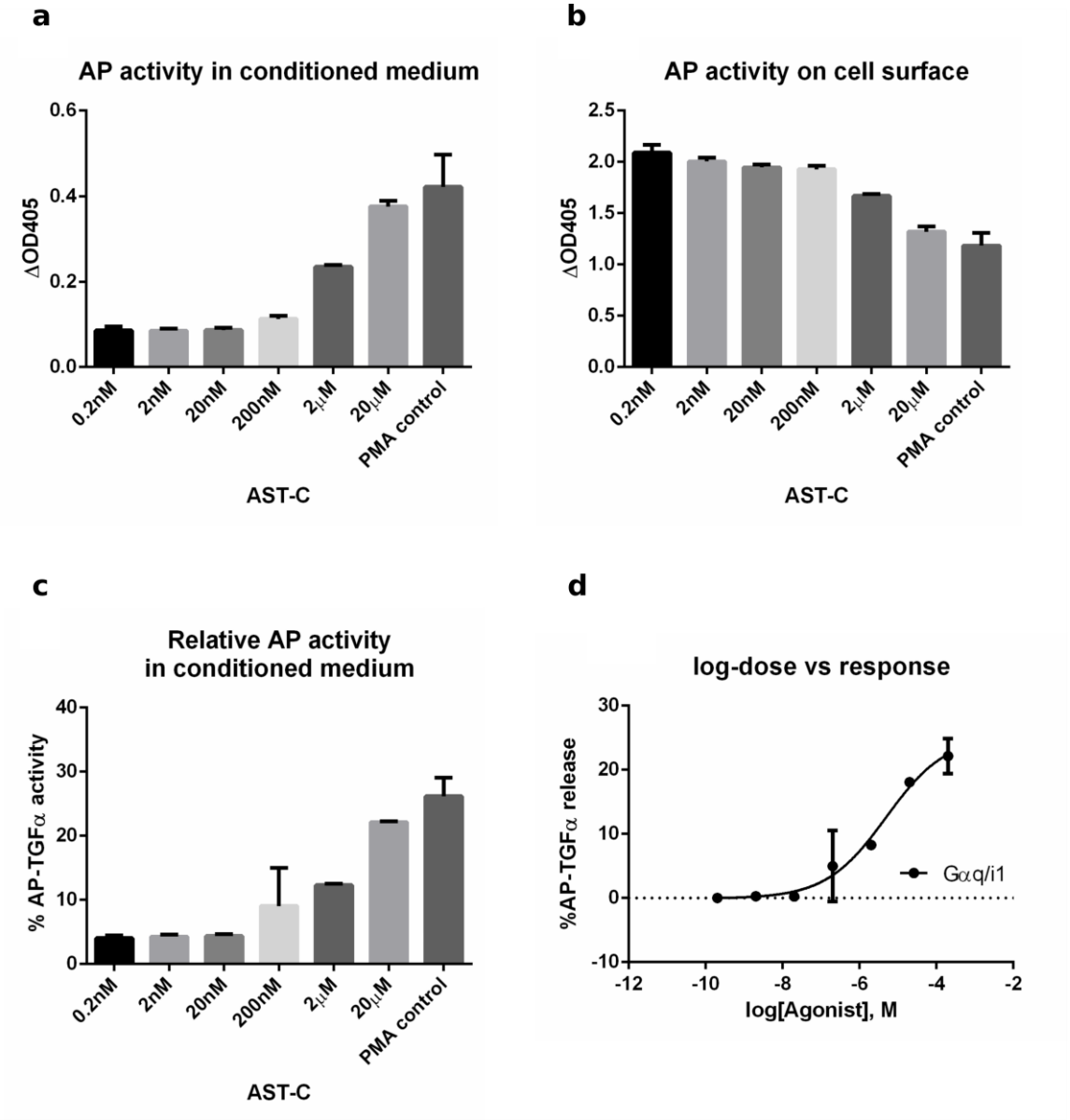

Figure 5.4. Data processing of the TGFα-shedding assay for CamAstR-C. AP-TGFα activity in the conditioned medium: (a) and on the cell plate (b) are normalized against the vehicle-treated condition, and then the increase of the AP-TGFα activity was quantified as percentage AP-TGFα release (c). A dose-response graph was plotted and EC50 value was calculated as 5 μM. Error bars for standard error of mean. Data are representative for 3 assay replicates from one experiment.

For the assay, HEK293FT cells were transfected with 0.1 µg wild-type CamAstR-C, 0.25 µg AP-TGFα and various chimeric Gα subunit for each transfection condition ($G\alpha_{q/i1}$, $G\alpha_{q/i3}$, $G\alpha_{q/o}$ or $G\alpha_{16}$). Cells were treated with different concentrations of AST-C ranging between 2 nM-20 µM. After 1 hour treatment with agonist, conditioned medium was collected into a 96-well assay plate, and AP substrate solution was added both on the cell plate and conditioned medium plate. Plates were further incubated at 37˚C for 2 hours and OD values were measured at 405 nm. AP activity on both plates were calculated from the OD. Depending on these responses, a logarithmic concentration-response curve was plotted and EC50 value for the TGFα-shedding was calculated as 5 µM for $G\alpha_{q/i1}$-mediated activity (Figure 5.4). This assay showed that CamAstR-C was activated and increased an indirect pathway dose-dependently. Also, AP-TGFα-shedding was only observed when $G\alpha_{q/i1}$, $G\alpha_{q/i3}$, $G\alpha_{q/o}$ or promiscuous $G\alpha_{16}$ was transfected (Figure 5.5), even though unexpectedly high EC50 values were obtained. In order to validate the G protein-coupling and downstream signaling properties of the CamAstR-C further investigation was needed.

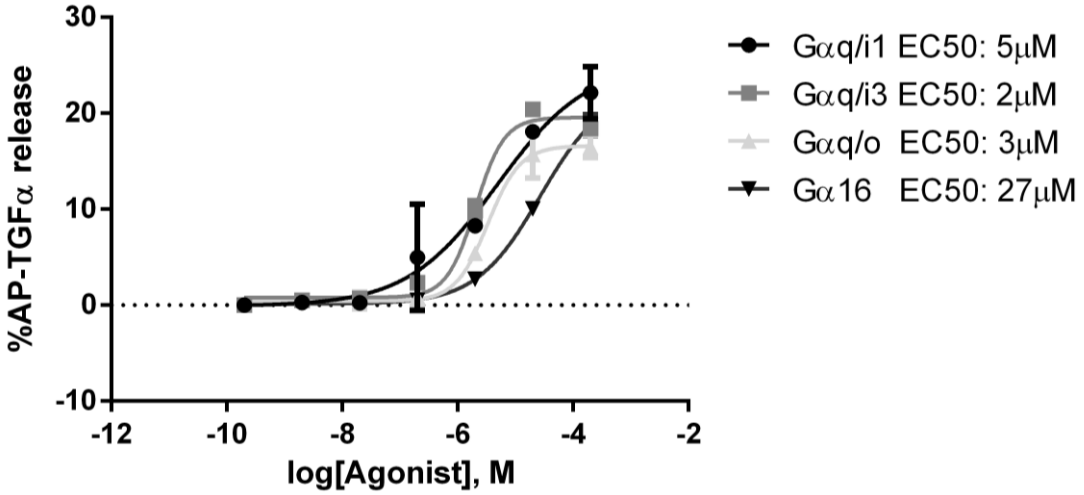

Figure 5.5. Comparison of logarithmic dose-response curves for percentage AP-TGFα release via activation of $G\alpha_{q/i1}$, $G\alpha_{q/i3}$, $G\alpha_{q/o}$ and $G\alpha_{16}$ proteins. Error bars for standard error of mean.

5.4. FRET-Based Detection of the Activation and Signaling of CamAstR-C

In order to confirm the native agonist and characterize the signaling properties of the CamAstR-C, we performed a number of FRET-based experiments in collaboration with Prof. Moritz Bünemann at Philipps Universität Marburg, Germany. For these studies, cells were transfected with fluorescent labeled proteins and grown on coverslips. Then, live measurements were taken using a FRET-compatible fluorescent microscopy setup with a high magnification objective and a dualband emission photometric system. It is important to note that the fluorescent-labelled proteins that were used for studying PPIs via FRET in this study are well-established and their efficacy are documented (Lohse *et al*., 2008).

5.4.1. G Protein Activation by CamAstR-C

Measurement of FRET between YFP-labeled Gα subunits and a variant of CFP, Cerulean (Cer)-labeled Gβγ subunits is a well-established method to determine the Gα activation. Therefore, we used this method in order to determine which Gα subunit is activated upon CamAstR-C activation with AST-C.

Activation of G proteins is followed by dissociation of Gα and Gβγ. Several FRET experiments have shown this dissociation as a decrease in FRET ratio between fluorescently labelled $G\alpha_s$, $G\alpha_q$, $G\alpha_o$ and Gβ/Gγ subunits. However, activation of $G\alpha_{i1}$ was shown as an increase in FRET. In this case, $G\alpha_{i1}$-Gβγ trimer was shown to undergo a molecular rearrangement upon activation, and in the end, YFP within the $G\alpha_{i1}$ and Cerulean at the N-terminus of $G\beta_1$ are positioned at close proximity, as shown in Figure 5.6 (Bünemann *et al*., 2003).

In order to perform the FRET measurements expressing CamAstR-C and fluorescent-labelled G protein subunits, HEK293T cells were grown on 6-cm plates and transfected with plasmids according to Table 5.1. Twenty four hours after transfection, these

cells were re-seeded on PLL-coated coverslips and incubated overnight. Next day, coverslips were placed onto a cell chamber and chamber was filled with FRET buffer (as prepared according to the recipe on the section 4.6.2.

Table 5.1. Transfection conditions for G protein activation FRET.

$G\alpha_{i1}$ activation	**$G\alpha_{o}$ activation**	**$G\alpha_{s}$ activation**	**$G\alpha_{q}$ activation**
0.5 µg CamAstR-C	0.5 µg CamAstR-C	0.5 µg CamAstR-C	0.5 µg CamAstR-C
0.8 µg $G\alpha_{i1}$-YFP	0.8 µg $G\alpha_{o}$-YFP	0.8 µg $G\alpha_{s}$-YFP	0.8 µg $G\alpha_{q}$-YFP
0.5 µg Cer-$G\beta_1$	0..5 µg $G\beta_1$	0.5 µg $G\beta_1$	0.5 µg $G\beta_1$
0.2 µg $G\gamma_2$	0.2 µg $G\gamma_2$-Cer	0.2 µg $G\gamma_2$-Cer	0.2 µg $G\gamma_2$-Cer

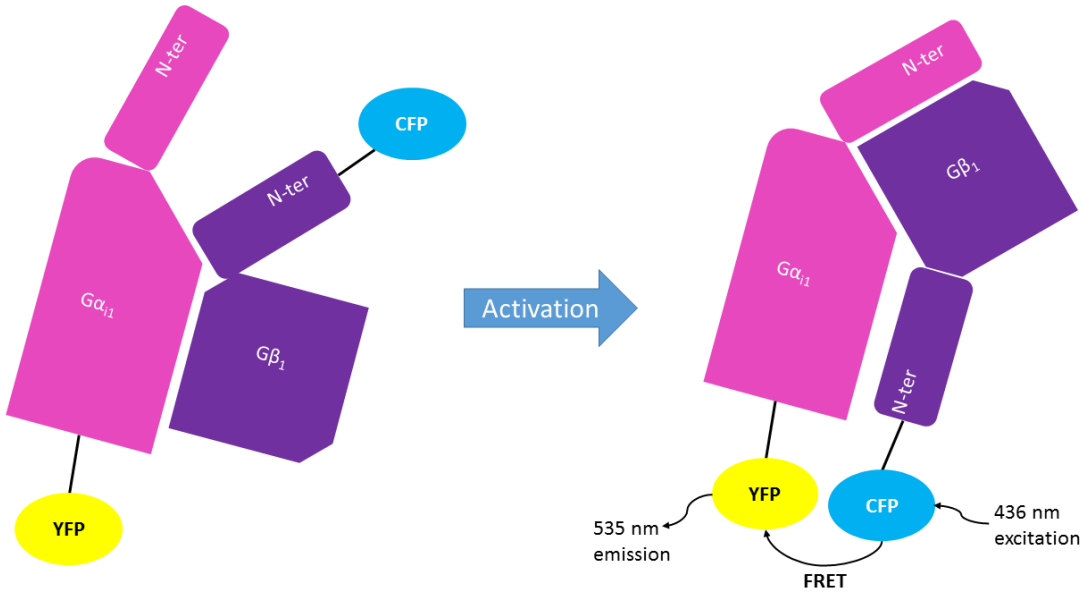

Figure 5.6. Conformational rearrangement of heteromeric Gi protein. Upon activation, loosely interacting $G\alpha_{i1}/G\beta_1$ undergoes a molecular switch, which can be measured as an increase in FRET from CFP at the N-terminus of $G\beta_1$ and YFP fused to $G\alpha_{i1}$ (Adapted from Bünemann *et al.*, 2003).

Using the dual excitation mode of the fluorescent microscope at 63X magnification, an individual cell that expressed both of the fluorescent proteins with correct localization was picked, and FRET measurement was started with excitation of CFP at 440 nm for 60 seconds at sampling rate of 1 Hz (for $G\alpha_o$, $G\alpha_q$ and $G\alpha_s$) or 2 Hz (for $G\alpha_{i1}$). After application of FRET buffer during the first 60 seconds of the measurement, AST-C solution at increasing concentrations were applied on the same cell for 90 or 60 seconds, with 60 seconds of buffer application in between each concentration. Both YFP and CFP emission were recorded simultaneously by a CCD-camera, and FRET ratio was calculated and plotted automatically by the Visiview software (Visitron, Germany).

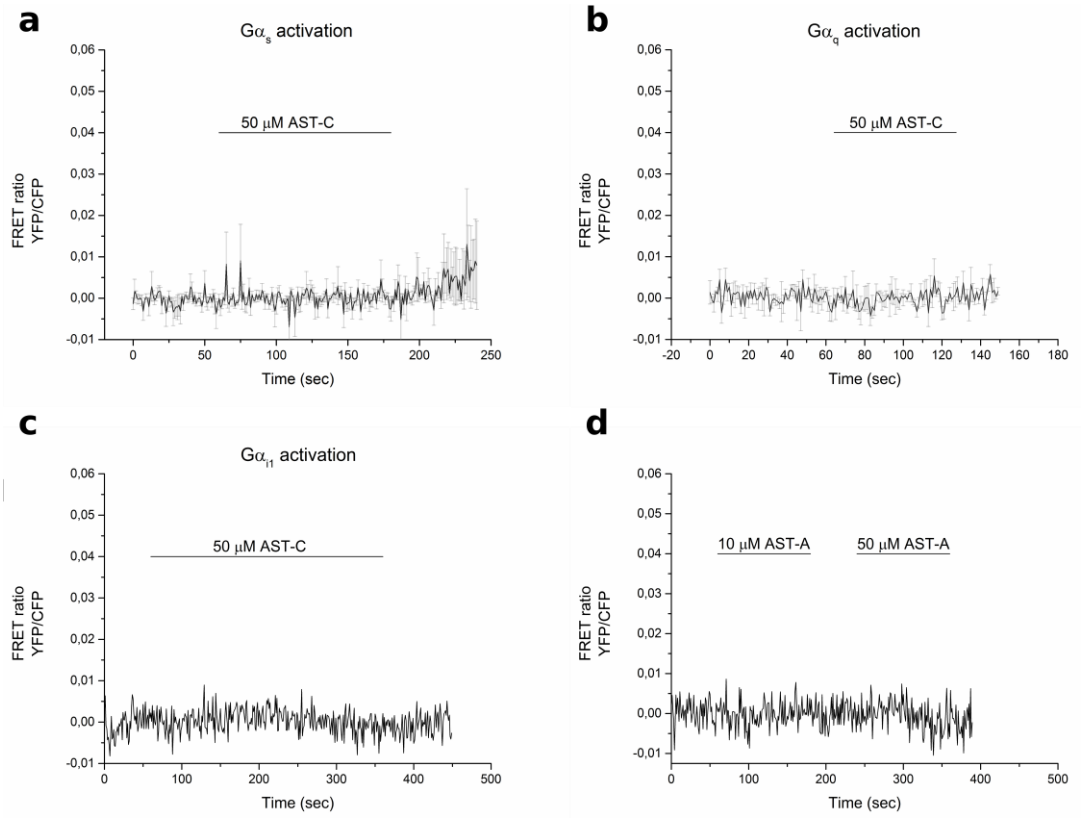

Figure 5.7. FRET measurements of heterotrimeric G protein activation. No FRET between $G\alpha_s$-YFP/$G\gamma_2$-Cer (a) or $G\alpha_q$-YFP/$G\gamma_2$-Cer (b) was observed. AST-C activation of the cells transfected with empty pcDNA3 (instead of pcDNA3-CamAstRC) did not trigger $G\alpha_{i1}$ activation. AST-A had no effect on $G\alpha_{i1}$ activation in cells expressing CamAstR-C. Error bars for standard error of mean for 3 measurements.

Measurements of the cells transfected with the mix for $G\alpha_s$ or $G\alpha_q$ activation did not display any change in FRET ratio (Figure 5.7a, b). However, cells transfected with the mix for $G\alpha_{i1}$ activation displayed a dose-dependent increase in FRET. On the other hand, a dose-dependent increase in FRET ratio was observed in $G\alpha_{i1}$-transfected cells (Figure 5.8a). Supporting this, measurement of the cells transfected with $G\alpha_o$ mix displayed a concentration-dependent decrease in FRET ratio (Figure 5.8b). Conversely, no change on FRET was observed when these cells were treated with AST-A (Figure 5.7d). These results clearly show that CamAstR-C is $G\alpha_{i/o}$ coupled, like its orthologues in other insects. Next to that, a concentration-response curve was fitted for these measurements, and it was found that AST-C triggered $G\alpha_{i1}$ activation with an EC50 value around 15.7 nM (Figure 5.9). In order to confirm that the activation of $G\alpha_{i1}$ and $G\alpha_o$ were both mediated by activation of CamAstR-C, the same experiments were performed by replacing the CamAstR-C vector with empty pcDNA3.1. FRET measurements of these cells did not reveal any change in FRET ratio (Figure 5.7c).

In a previous study performed by our group, a binding pocket for AST-C was predicted by docking the AST-C on CamAstR-C (Duan Sahbaz, 2013). In this study, IFTPPK (residues from 292-297) motif on ECL3 of CamAlstR-C was predicted to be a potential conserved binding motif for AST-C, and the N-terminus region of the receptor was proposed to have a role in strengthening the binding pocket (Figure 5.10). Atomic force microscopy studies previously performed by our group proved that the alanine scanning of the whole motif (F11211R11211 mutant) and deletion of the N-terminus (Ndel mutant) caused a decrease in the affinity of CamAstR-C to AST-C. In order to investigate the validity of this decreased affinity of the above-mentioned mutant receptors, $G\alpha_i$ protein activation was measured by means of FRET. When FRET responses were plotted as concentration-response curves, it was noticed that they were right-shifted compared to the wild type-receptor, and the EC50 values were calculated approximately 758,1 nM for Ndel mutant and 15 μM for F11211R11211 mutant (Figure 5.9).

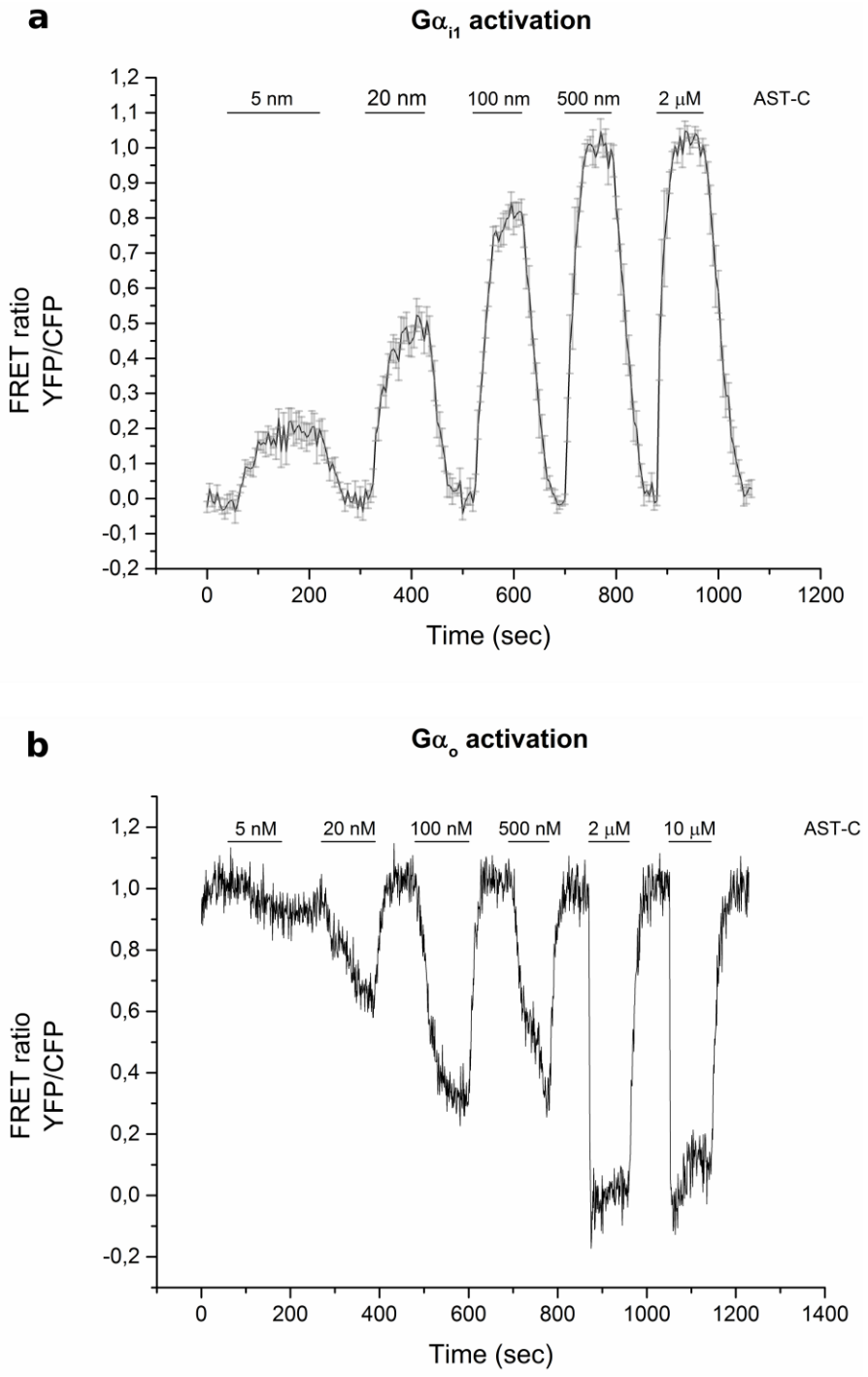

Figure 5.8. FRET measurements of $G\alpha_{i1}$ and $G\alpha_{o}$ activation. While a dose-dependent increase of the signal was observed for $G\alpha_{i1}$-YFP/Cer-$G\beta_1$ FRET (due to the molecular switch upon activation), $G\alpha_{o}$-YFP/$G\gamma_2$-Cer FRET displayed a dose-dependent decrease of FRET. Error bars for standard error of mean were derived from 12 measurements.

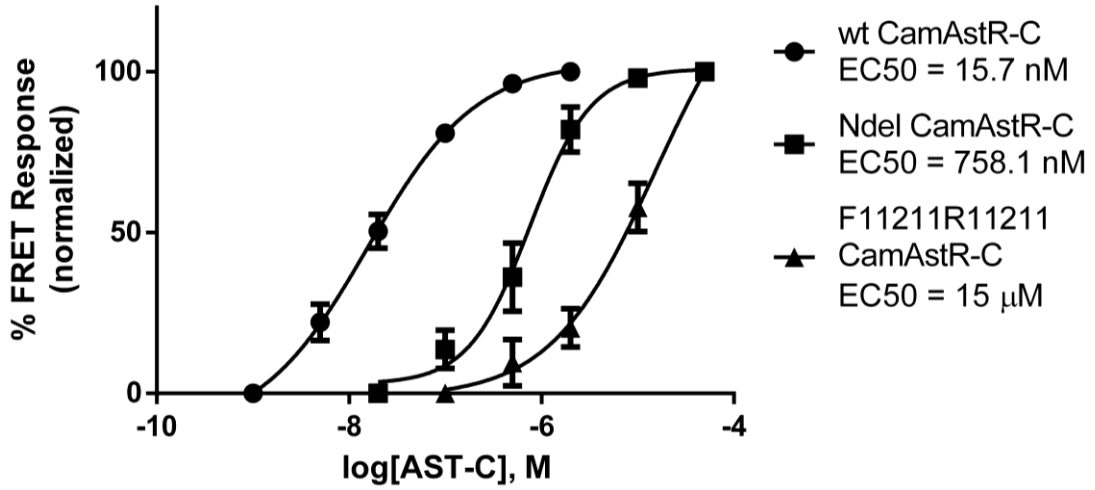

Figure 5.9. Logarithmic dose-response curves calculated from FRET measurements of G protein activation by wild-type CamAstR-C, NdeI mutant CamAstR-C and binding pocket mutant CamAstR-C. Error bars for standard error of mean were calculated from at least 3 independent measurements for each receptor.

5.4.2. Interaction between CamAstR-C and G Protein Subunits

Upon activation with an agonist, GPCRs interact with heterotrimeric G proteins. With regard to the results obtained from the previous section, we suggested that CamAstR-C was a $G\alpha_{i/o}$ protein-coupling receptor. To confirm this, we performed another real-time FRET assay, in which the interaction between (C-terminally) SYFP2-tagged CamAstR-C and (N-terminally) Cerulean-tagged $G\gamma_2$ in single cells. HEK293T cells were transfected with 0.5 μg CamAstRC-SYFP2, 0.8 μg $G\alpha_{i1}$, 0.5 μg Gβ1 and 0.2 μg Cer-Gγ2. FRET measurements were performed in a similar way as in G protein activation assay. Only upon stimulation of the cells with AST-C, a concentration-dependent increase on FRET ratio was recorded. When the same experiment was performed with the $G\alpha_o$ plasmid, concentrate-dependent increase in FRET was observed again. These results confirmed that CamAstR-C was able to interact with $G\alpha_{i1}$ and $G\alpha_o$ upon stimulation with AST-C (Figure 5.11).

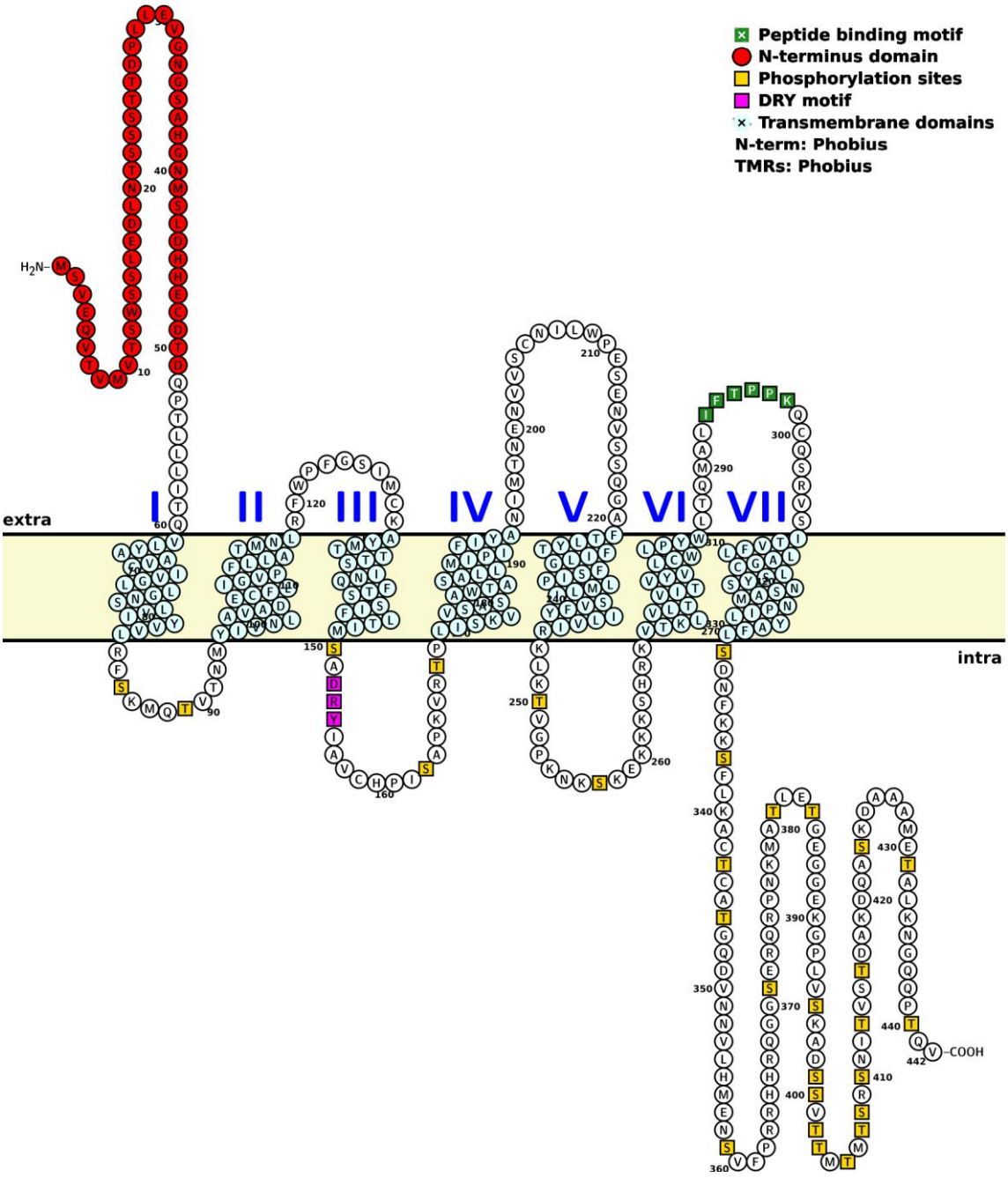

Figure 5.10. Snake-plot representation of CamAstR-C on the cell membrane. Deleted residues in the Ndel mutant of the receptor are shown in red. IFTTPK motif, which was mutated in F11211R11211 mutant is shown in green. GPCR Class A-specific DRY motif is shown in magenta. Potential GRK phosphorylation sites (serine and threonine residues) are shown in yellow. Transmembrane domains are depicted in light cyan color. Image created using Protter software (Omasits *et al*., 2014).

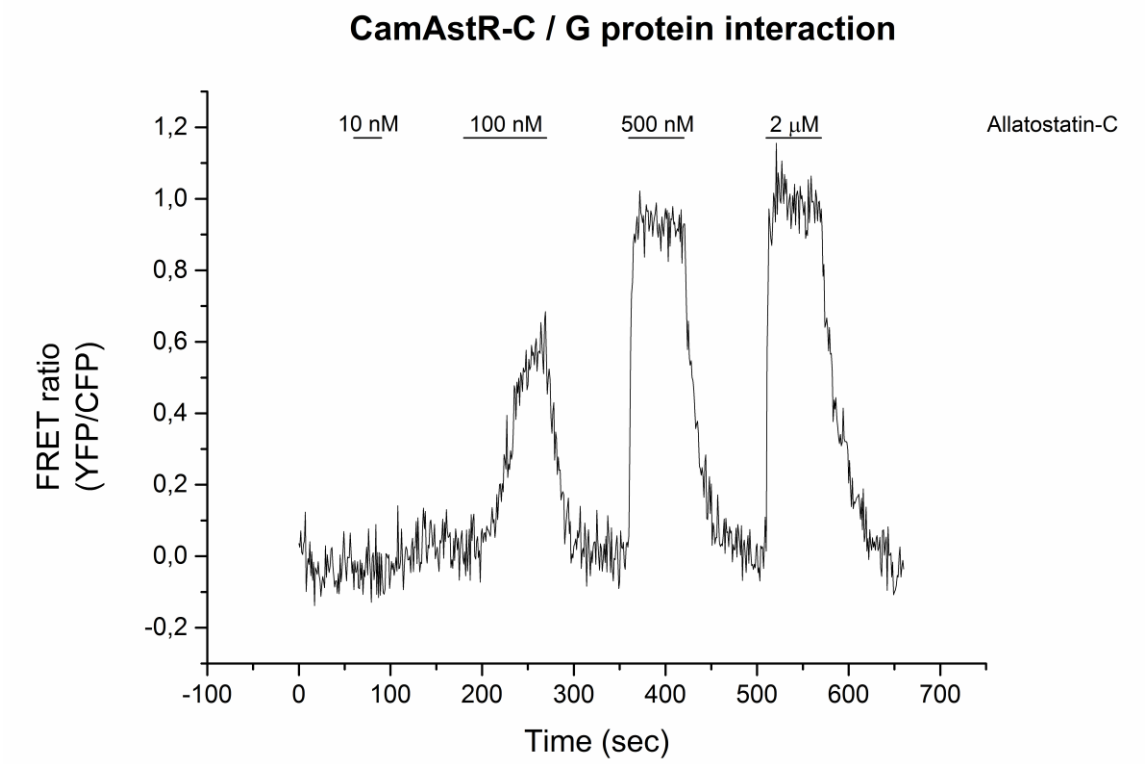

Figure 5.11. A representative time-resolved FRET measurement of CamAstR-C/G protein interaction. FRET between CamAstRC-SYFP2 and $G\gamma_2$-Cer was measured. Dose-dependent increase of FRET in high doses of AST-C was observed.

5.4.3. Interaction between CamAstR-C and β-Arrestin2

GPCRs are prone to GRK-mediated phosphorylation and recruitment of β-arrestins to the phosphorylated receptors after activation with an agonist. Interaction with β-arrestins is the major mechanism of receptor desensitization (Krasel *et al*., 2005). However, it is also known that the internalization of a receptor after β-arrestin is followed up by receptor degradation or recycling, as well as transmission of β-arrestin-mediated signaling (Violin *et al*., 2006). It was previously shown that upon treatment with AST-C, β-arrestin2 was recruited to the cell membrane and translocated back to the cytoplasm as pits in HEK293 cells expressing Drosophila C-type AstR1 and 2 (Johnson *et al*., 2003).

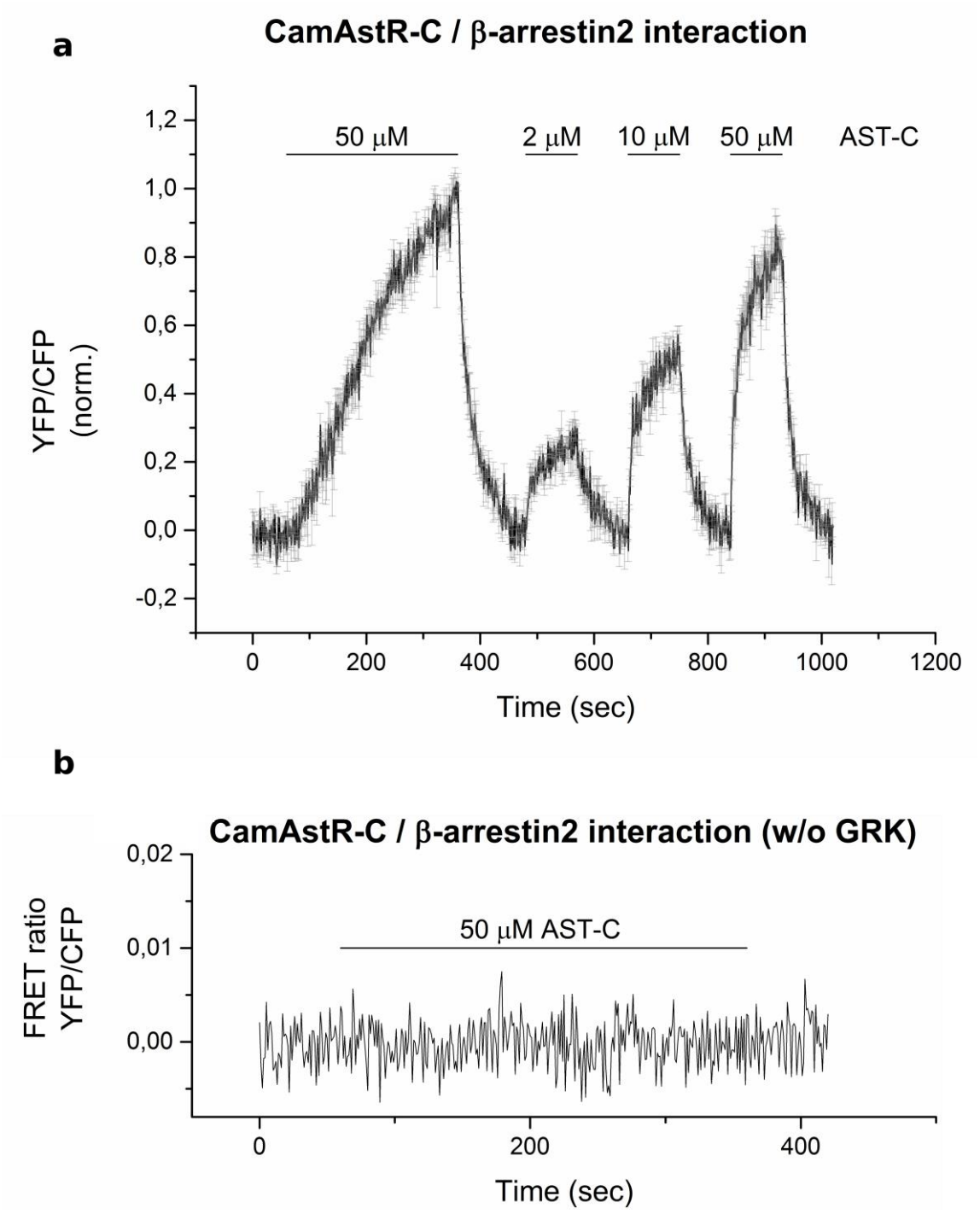

Figure 5.12. FRET measurements of CamAstR-C interaction with β-arrestin. Here, FRET between CamAstRC-SYFP2 and β-arrestin2-Cer was measured. (a) When GRK2 was overexpressed along with the fluorophore-labelled receptors, a dose-dependent FRET increase was detected upon AST-C treatment. (b) No FRET was observed in the cells that did not overexpress GKR2.

Since G protein activation and interaction with CamAstR-C was proven in HEK293T cells, it was also of our interest whether CamAstR-C interacts with β-arrestins upon AST-C treatment. To test this, we studied the interaction between CamAstR-C and β-arrestin2 (Arrestin3) by means of FRET. HEK293T cells transfected cells with 0.5 µg CamAstRC-SYFP2, 0.6 µg β-arrestin2-Cer and 0.6 µg GRK2 were grown on coverslips and used for FRET measurements. Measured cells were initially stimulated with a super-saturating concentration of AST-C (50µM), and the bound ligand was washed out with the FRET buffer superfusion. After the first washout, increasing concentrations of AST-C were applied on the measured cell with wash-out intervals. Results of this assay showed that receptor-arrestin interaction occurred in a dose-dependent manner (Figure 5.12a). On the other hand, the initial application of AST-C showed slower kinetics than the latter agonist stimulations. This result suggested that the kinetics of the receptor-arrestin interaction was enhanced by prior agonist stimulation. To our surprise, oversaturating concentrations of AST-C were needed to obtain significant results for this assay.

Since it is known that phosphorylation of the agonist-activated receptor by GRK is the rate-limiting step for β-arrestin binding, we repeated this experiment by excluding the GRK2-carrying plasmid from the reaction mix. As expected, results showed no significant change in time-resolved FRET measurements, even when the cells were superfused with 50 µM AST-C (Figure 5.12b). Thus, it was shown that receptor phosphorylation by GRK was indeed necessary for β-arrestin recruitment to CamAstR-C.

5.4.4. Regulation of Adenylyl Cyclase Activity by CamAstR-C

The main effector that is regulated by $G\alpha_{i/o}$ is adenylyl cyclases (ACs). Activation of $G\alpha_{i/o}$ results in inhibition of AC activity, thus causes a decrease in intracellular cAMP levels. Since CamAstR-C was found to be a $G\alpha_{i/o}$-coupled receptor, its activation is also expected to inhibit cAMP production. Therefore, we used a previously established FRET-based protocol using Epac1-camps, in order to measure the $G\alpha_i$-protein-dependent inhibition of cAMP production (Milde *et al*., 2014). Epac1-camps is an engineered form of the Epac1 protein. It carries a YFP and a CFP at its N- and C-terminus. In free form, two

fluorophores on Epac1-camps are in enough proximity to generate FRET. When bound to cAMP, the protein undergoes a conformational change, which increases the distance between two fluorophores, causing the loss of FRET. Here, we used this sensory protein in order to test the inhibitory effect of CamAstR-C on cAMP production.

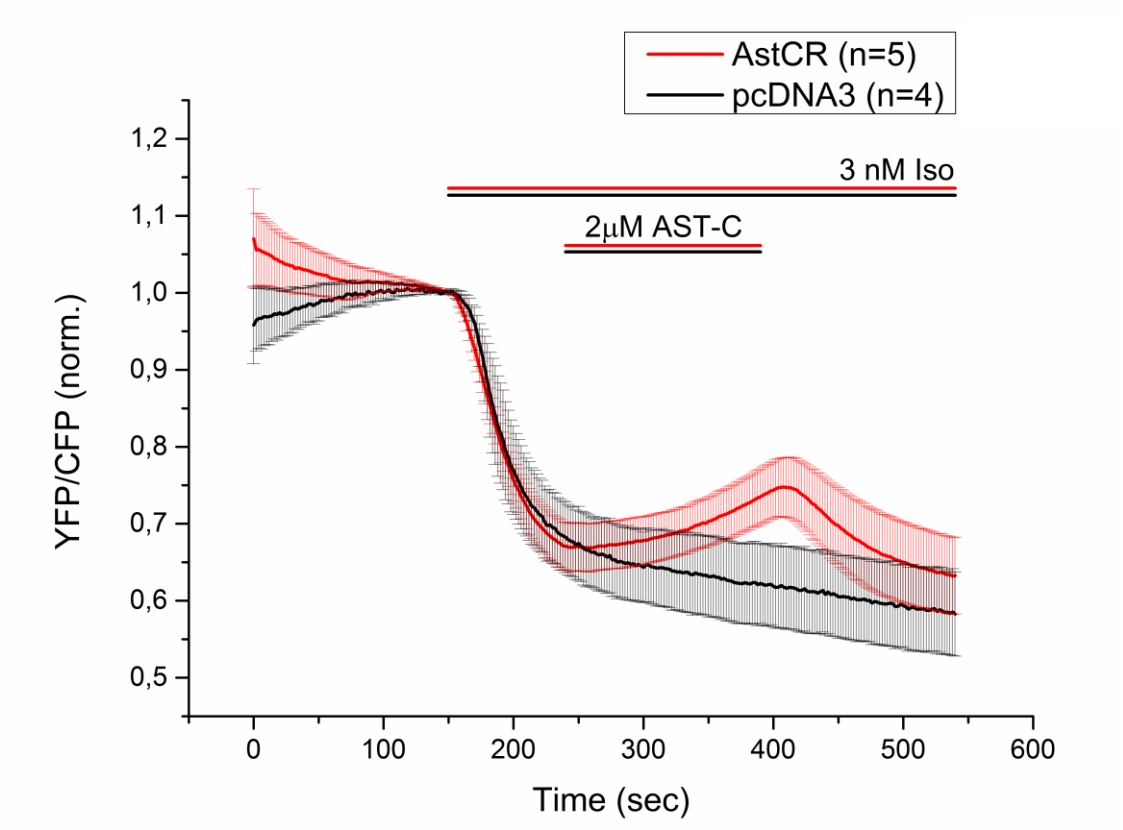

Figure 5.13. FRET-based measurements of changes in cAMP in single cells expressing Epac1-camps. Increase in intracellular cAMP level is measured as decrease in FRET, since Epac1-camps sensor protein binds to cAMP and intramolecular FRET decreases. Comparison of cAMP alterations in mock-transfected and CamAstR-C-expressing HEK293T cells displayed an ability of CamAstR-C activation on inhibition of AC5.

In this protocol, cells were transfected with 0.1 µg CamAstR-C, 0.25 µg Epac1-camps and 0.3 µg AC5. In control experiments, CamAstR-C was replaced with empty pcDNA3. Measurements were performed first with buffer application, followed by superfusion of 3 nM isoprenaline for 90 seconds, in order to stimulate cAMP production via

endogenous β_2-adrenergic receptors. After stimulation of cAMP production, isoprenaline was competed with 2 μM AST-C, in order to stimulate endogenous $G\alpha_{i/o}$ via CamAstR-C.

Results of this experiment showed that 3nM isoprenaline mediated a robust decrease in FRET ratio, meaning that it potently promoted cAMP production. Application of 2 μM AST-C reversed the direction of cAMP levels, but it could not inhibit isoprenaline-mediated response potently. Yet, rebound stimulus after withdrawal of AST-C stimulation was clearly observed. Control experiments showed that application of AST-C on the cells that did not express CamAstR-C had no effect on intracellular cAMP production stimulated by isoprenaline (Figure 5.13). All together, these results indicate that CamAstR-C can be fully activated by AST-C in HEK293T cells, and trigger $G\alpha_i$- mediated inhibition of AC5.

5.4.5. Kinetics of the Protein-Protein Interactions Activated by CamAstR-C

To determine the kinetics of the $G\alpha_i$ protein activation by CamAstR-C, cells were transfected with the plasmid mix as shown on Table 5.1. For the FRET measurements of $G\alpha_i$ activation, cells were stimulated with different concentrations of AST-C, ranging from 5 nM to 2 μM. The same measurement conditions were used in terms of agonist application times, wash-out times and each measurement was overlaid. Kinetics of $G\alpha_i$ activation/deactivation were calculated by fitting of mono-exponential curves on the overlaid measurements. From the equations obtained from these curves, $t_{1/2}$ values (time until the FRET ratio reached its half-maximum) were calculated. As shown in Figure 5.14a, kinetics of the G protein activation (on-rate kinetics) was dose-dependent. The higher dose of AST-C resulted in faster increase in FRET. On the other hand, analysis of the off-rate kinetics, reflecting the deactivation of the heterotrimeric G protein, did not seem to be as strictly dose-dependent as G protein activation (Figure 5.14b) and half-life of deactivation varied for each concentration measurement.

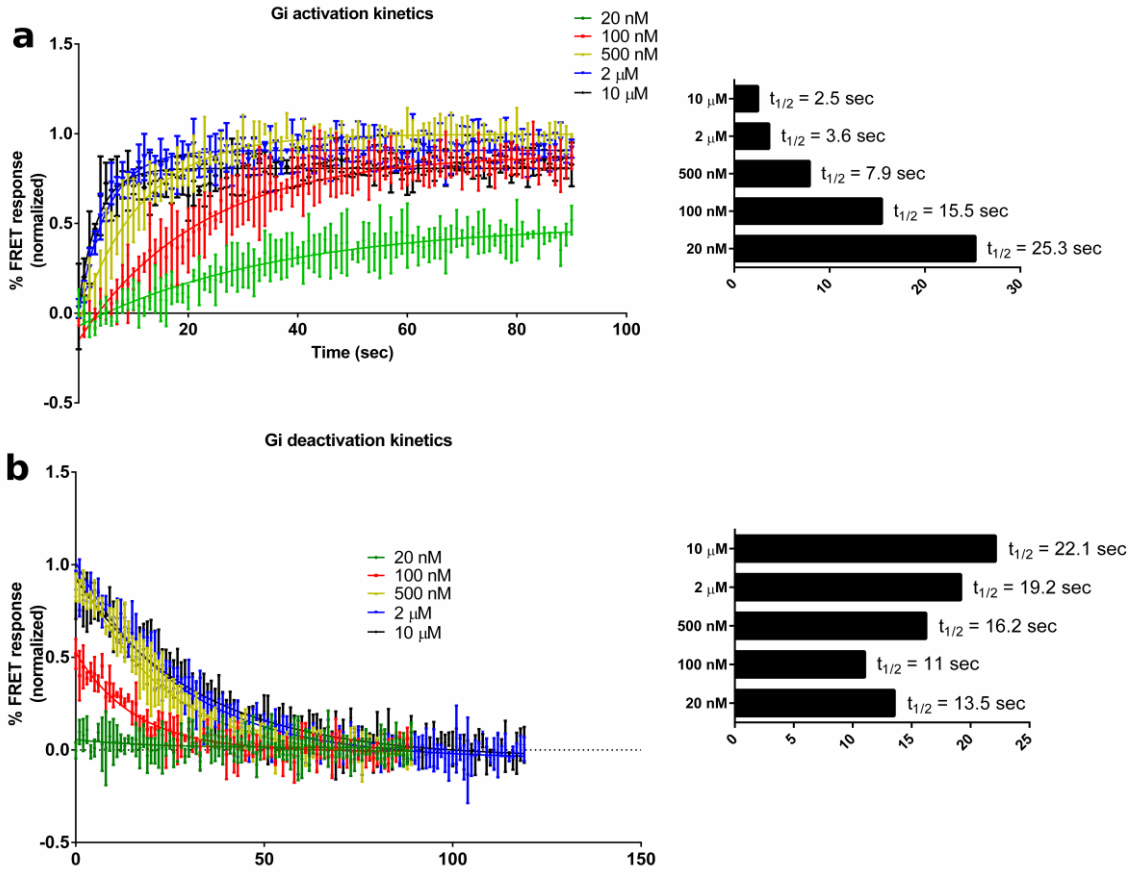

Figure 5.14. CamAstR-C-mediated activation and deactivation kinetics of $G\alpha_{i1}$. Kinetic values were calculated by plotting a nonlinear regression for the FRET measurements.

Next to that, kinetics of β-arrestin2 recruitment to CamAstR-C was also analyzed. It was observed during the first FRET measurements between CamAstR-C and β-arrestin2 that the on-rate kinetics of the second stimulation was always faster than the first stimulus. In order to analyze both the activation and inactivation kinetics of β-arrestin2 recruitment, we stimulated the cells repeatedly with the supersaturating concentrations of AST-C (50 μM) and measured FRET values. Figure 5.15 shows an overlay of measurements from single cells. When two consecutive stimulations of the same cell are overlaid, it was clearly seen that the on-rate kinetics of β-arrestin2 recruitment during second stimulation was faster than the kinetics of the first stimulation. However, comparison of the off-rate kinetics did not show a significant difference, which suggests that the disassociation kinetics of β-arrestin2 from CamAstR-C is not dependent on GRK-mediated phosphorylation of the receptor (Figure 5.15).

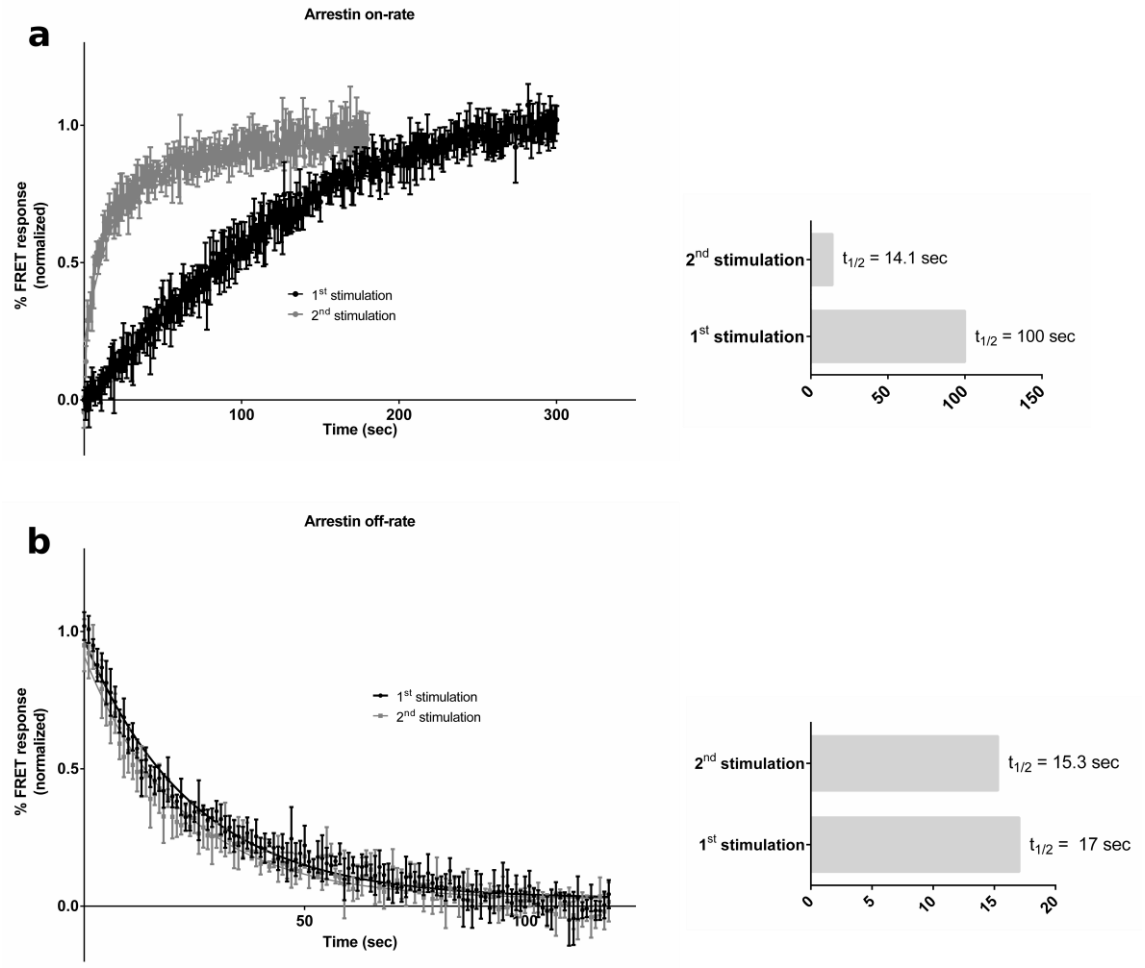

Figure 5.15. Kinetic analysis of CamAstR-C / β-arrestin2 interaction and dissociation. During activation, second stimulus of the cell with agonist causes faster receptor-arrestin interaction, while there is no difference on deactivation kinetics for both stimulations.

5.5. Endocytosis of CamAstR-C upon Activation

Since interaction of a receptor with β-arrestin2 is the major factor of desensitization and subsequent internalization of the receptor, we tested whether CamAstR-C interaction with β-arrestin2 followed this internalization path. In order to investigate this, HEK293T cells were transfected with CamAstRC-SYFP2, β-arrestin2-Cer and GRK2 and re-seeded on PLL-coated coverslips 24 hours after transfection. After another overnight

incubation, cells were treated with 50 μM AST-C for one hour. After the treatment, coverslips were fixed with 4% PFA and mounted on glass slides for immunofluorescence imaging. Images were acquired using 458 nm excitation light and emission detection within 462-510 nm range.

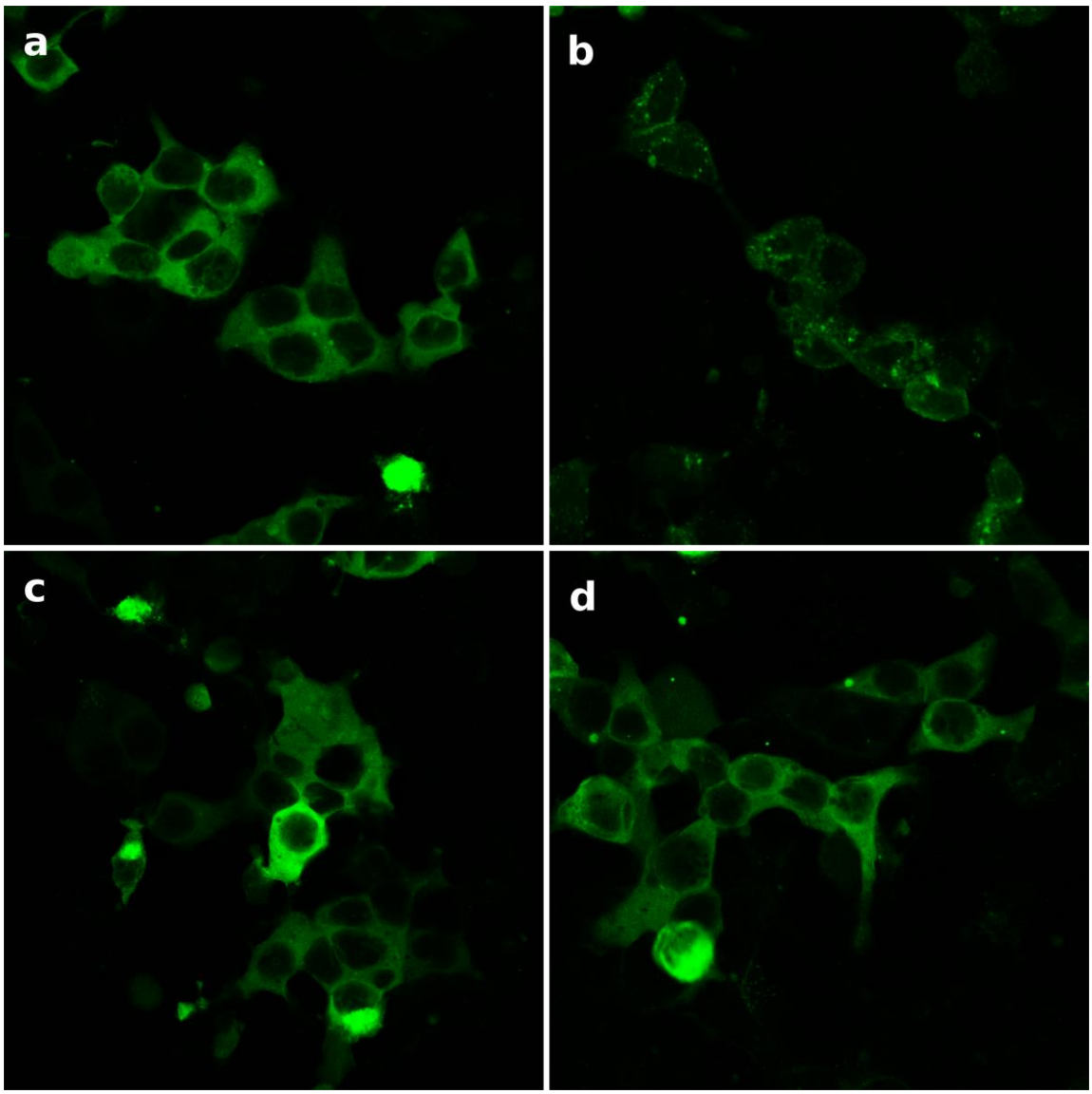

Figure 5.16. Confocal images of arrestin translocation upon AST-C stimulation of HEK293T cells. β-arrestin2-Cer is located in cytoplasm in PBS-treated cells (a). 1 hour treatment of cells with AST-C caused internalization of β-arrestin2, probably with CamAstR-C (b). However, PBS (c) or AST-C (d) treatment of cells without GRK2 over-expression did not exhibit any β-arrestin2 translocation.

When cells were not treated with AST-C, β-arrestin2-Cer was localized in the cytosol (Figure 5.16a). However, treatment of the cells with AST-C for 1 hour caused internalization of the receptor with β-arrestin2 and form dot-like shapes within the cytosol, which were thought to be the clathrin-coated pits (Figure 5.16b). On the other hand, a control experiment, in which GRK2-encoding plasmid was replaced with empty pcDNA3, proved that presence of GRK2 is necessary for receptor internalization (Figure 5.16c and d). These results were in accordance with the results obtained from FRET measurements between CamAstR-C-SYFP2 and β-arrestin2-Cer.

5.6. Further Downstream Effects of CamAstR-C Activation

Activation of a receptor does not only trigger signaling pathways through Gα subunits, as discussed in section 1.3.3. Activation of Gβγ subunits and β-arrestin2 can also initiate alternative signaling pathways, such as the ones mediated by PI3K, PLC, Src, MAPK or Rho (Violin *et al*., 2006). Among these pathways, we tested whether MAPK pathway was affected by CamAstR-C activation. Therefore, we assessed extracellular signal-regulated kinase 1/2 (ERK1/2) activation by quantifying the active form of ERK1/2, namely pERK1/2.

Western blot results indicated that, upon AST-C treatment of the Huh7 cells stably expressing CamAstR-C, pERK1/2 level increased in the first 30 minutes, compared to the control group. Moreover, there was no more increase in pERK1/2 level after the first 30 minutes, in cells expressing the receptor. However, there was no significant change on pERK1/2 level in AST-C-treated cells with no receptor expression, during the whole course of treatment (Figure 5.17).

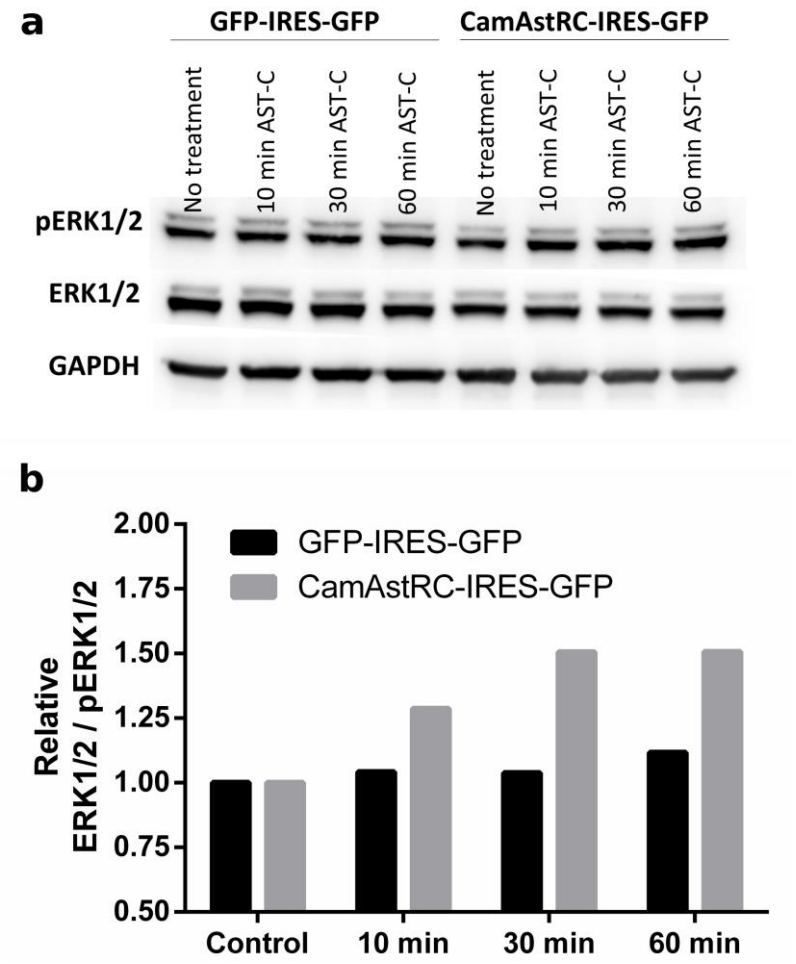

Figure 5.17. Western blot analysis of ERK1/2 phosphorylation upon AST-C treatment of Huh7 cells stably expressing CamAstR-C. (a) Stimulation of the CamAstR-C expressing cells caused increased ERK1/2 phosphorylation within 60 minutes, while no change was observed in control cells. (b) Quantification of the observed blots. pERK1/2 level increased 0.5 fold in 30 minutes and remained at that level until 60th minute.

6. DISCUSSION

Previous work from our group identified and characterized a cDNA from the Indian stick insect, *Carausius morosus*, as a PISCF Allatostatin receptor, and verified binding of PISCF Allatostatin to this receptor using atomic force microscopy (Duan Sahbaz, 2013). Here, in this study, we functionally characterized the PISCF-Allatostatin-specific activation of the CamAstR-C, and analyzed its signaling properties in a spatio-temporal manner, using FRET-based assays.

Firstly, since CamAstR-C was predicted as a GPCR, it was crucial to prove its localization on the cell membrane. Therefore, SYFP2, encoding for an enhanced yellow fluorescent protein (YFP) was fused to the C-terminal region of CamAstR-C gene by molecular cloning methods. After verification of the cloning and purification of the expression plasmid containing this fusion gene, the recombinant protein was produced in HEK293T cells to visualize CamAstR-C expression and localization through its YFP tag. The expressed protein was mainly localized at the cell-cell borders. Immunofluorescence experiments further confirmed that this localization of CamAstR was indeed at the cell membrane, since it co-localized with a well-known membrane protein, zona occludens 1 (ZO-1) (Siliciano and Goodenough, 1988). So, we could conclude that CamAstR-C was a membrane protein.

In order to confirm the predicted GPCR function of the CamAstR-C, we needed to use a functional tool where receptor activity could be measured. For this purpose, we decided to use the novel TGFα-shedding assay. This assay is originated from a $G\alpha_q$-mediated pathway, where the activation of this protein triggers a pathway that in the end causes the ectodomain shedding of TGFα. This assay uses chimeric G proteins that are the mutated version of $G\alpha_q$ subunit, where its last 6 residues are exchanged with the last 6 residues of $G\alpha_s$ or $G\alpha_{i/o}$ class of G proteins. In the end, the chimeric G protein couples with a $G\alpha_s$ or $G\alpha_{i/o}$-coupled receptor, but activates the $G\alpha_q$ pathway that causes TGFα-shedding. In addition, a mutant form of TGFα is used in this assay. This mutant version of the protein

is fused with alkaline phosphatase (AP) at its N-terminus. Therefore, quantification of TGFα-shedding assay could be carried out by measuring the AP activity in the medium. Adaptability, specificity and sensitivity of this assay allow to characterize the function of CamAstR-C. Results of this assay showed that TGFα-shedding increased dose-dependently when the cells were transfected with $G\alpha_{i1,}$ $G\alpha_{i3}$ or $G\alpha_{o}$ and then treated with AST-C. This specified for the first time that CamAstR-C was a $G\alpha_{i/o}$-coupled receptor. However, unexpectedly high EC50 values were obtained for this assay. This is probably due to the reason that peptide solutions were prepared and aliquoted in plastic tubes, to which peptides can stick easily. On the other hand, since the TGFα-shedding assay medium did not contain any serum proteins, peptide might have stuck to the plastic surface of the wells, causing decreased concentrations than it was applied. All in all, these results from TGFα-shedding assay displayed strong evidence for CamAstR-C function and its G-protein specificity. To our knowledge, this is the first time that TGFα-shedding assay was used form pharmacological characterization of an insect GPCR. This suggests that TGFα-shedding assay can be considered as a suitable method for characterization and deorphanization of other invertebrate GPCRs, using potential and known ligands. With this assay, several compounds can be screened in high-throughput manner, and readouts can be obtained using a microplate spectrophotometer.

FRET-based methods were used in this study because of their ability to show receptor interaction with intracellular proteins that are triggered by receptor activation. Another reason that we decided to use FRET is its ability to provide information on where and when the receptor signaling and interactions occur.

G protein activation by CamAstR-C was measured by means of FRET between Gα and Gβγ subunits. The results of this assay showed that the cell stimulation with AST-C only activated $G\alpha_{i1}$ or $G\alpha_{o}$, but not $G\alpha_{s}$ or $G\alpha_{q}$. These data confirmed the results from the TGFα-shedding assay. The EC50 value calculated for $G\alpha_{i1}$ activation was 15,7 nM, which is far lower than what was obtained from the TGFα-shedding assay. This EC50 value for CamAstR-C is in accordance with the widely-accepted phenomena that peptides can activate their cognate GPCRs at low nanomolar-range concentrations. More valuably,

this EC50 value of 15,7 nM is also in accordance with the results for other PISCF/AstRs from different insects, as summarized in Table 6.1.

Table 6.1. EC50 values for insect PISCF-Allatostatin receptors.

Organism	**Peptide**	**EC50**	**Reference**
C. morosus	Pyro-Glu-allatostatin C	15,7 nM	This study
D. melanogaster	Gln-allatostatin C	9,45 nM	(H. J. Kreienkamp *et al*., 2002)
D. melanogaster	Pyro-Glu-allatostatin C	25,4 nM	(H. J. Kreienkamp *et al*., 2002)
A. aegypti	*A. aegypti* allatostatin-C	27,7 nM	(Mayoral *et al*., 2010)
T. castaneum	*Trica*-AST-C	12 nM	(Audsley *et al*., 2013)

G protein activation analysis was also performed with mutants of the CamAstR-C. Results showed that deletion of the N-terminus domain of CamAstR-C caused a shift to right of the dose-response curve, giving an EC50 value of 760 nM. When the binding pocket-mutant receptor (F11211R11211 mutant), where the predicted binding pocket motif, IFTPPK, was mutated to AAAAAA) was assessed for its G protein activation ability, FRET responses displayed a EC50 value of 15,7 μM, which is almost 1000 times higher than the EC50 of the wild type CamAstR-C. Such dramatic increases of EC50 values demonstrate that the mutated domains, N-terminus and IFTPPK motif, are crucial for the ligand accommodation on the receptor. Thus, this results proved that the affinity of the receptor to AST-C significantly decreased when IFTPPK motif was completely mutated to Alanine resides. This is especially important for the IFTPPK motif, since it was proposed as a conserved binding motif for insect PISCF/AstRs, in the previous study by our group (Duan Sahbaz, 2013).

Analysis of the kinetics of G protein activation by CamAstR-C also proved fast on-set and relatively slower off-set kinetics of the G protein activation. Activation kinetics were shown to be increasing parallel to the concentration of applied AST-C. The highest $t_{1/2}$ value for G protein activation was calculated as 2,5 seconds (for 10 μM AST-C). Similar FRET studies proved that activation of G proteins normally occur within milliseconds. These studies were performed by measuring FRET ratio with very high resolution of time (20 Hz) (Bünemann *et al*., 2003; J.-P. Vilardaga *et al*., 2003). Thus, high resolution data points easily depicted fast kinetics. However, in this study, FRET measurements were carried out with lower time resolution (1 or 2 Hz). Therefore, the fastest kinetics we could catch would be only within a second. For that reason, even though we were able to detect that receptor activation became faster with increasing AST-C concentrations, we probably could not detect the real kinetics of this activation. Increasing the frequency of data collection would enhance the resolution of the collected results, thus allowing calculations of millisecond changes of FRET ratio.

Since we were able to identify G protein activation by CamAstR-C, it was also necessary to prove receptor-G protein interactions. To do this, we measured FRET between SYFP2-tagged CamAstR-C and CFP-tagged Gβγ. We proved that SYF2-tagged receptor localized on the cell membrane. Expression of the constructs did not exhibit any specific FRET signal. However, stimulation of the measured cell with AST-C displayed a small, but significant and dose-dependent increase in FRET. Amplitudes of FRET ratios obtained from this measurements were significantly smaller than the ones obtained from FRET between Gα and Gβγ. Because FRET measurement between G protein subunits is already a very well-established method, it was expected to obtain such data with high magnification. On the other hand, measurement of FRET between a receptor and G proteins would result in smaller amplitudes, since the interaction and orientation of the fluorophore at the C-terminus of the receptor and G protein is not always well-established. It might be the case in our experiment that the distance between two fluorophores was not optimal for high FRET occurrence, when CamAstR-C and CFP-$G\gamma_2$ interacted. This aspect can be assessed by truncating the C-terminus of CamAstR-C at different positions and performing the same experiments.

Taken together, this time-resolved, direct FRET measurements revealed that CamAstR-C/G protein interaction was fast, transient and occurred in agonist-dependent manner. On the other hand, these results further supported the phenomena that receptors and G proteins are not pre-coupled (Hein *et al*., 2005).

In the next set of experiments, we were able to show CamAstR-C interaction with β-arrestin2 in single living cells by means of FRET. In this assay, we used N-terminally SYFP2-tagged CamAstR-C and C-terminally Cerulean-tagged β-arrestin2 for FRET measurements. Binding, signaling and internalization properties of the β-arrestin2-Cer were previously shown to be very similar to those of the wild-type β-arrestin2 (J. P. Vilardaga *et al*., 2001). Results of this experiment clearly displayed dose-dependent increase of the receptor interaction with β-arrestin2. Then, it was noticed that β-arrestin2-receptor interaction was strictly dependent on the receptor phosphorylation by GRKs. This dependence on GPCR phosphorylation for β-arrestin2-receptor interaction was in accordance with the β_2-adrenergic receptor/β-arrestin2 interaction (Krasel *et al*., 2005). On the other hand, it was obvious that kinetics of the interaction with the second and later stimulus was always faster than the interaction kinetics of the first stimulus. First agonist stimulation initiates receptor phosphorylation, followed by β-arrestin2 binding. However, during the second stimulus, the receptor is already phosphorylated, so β-arrestin2 binding will not be slowed down by the rate-limiting GRK-mediated phosphorylated step, and its recruitment to the receptor will be faster, since the scaffold of phosphorylated residues will already be present. Kinetic measurements of receptor/β-arrestin2 interaction and dissociation further supported this observation. While $t_{1/2}$ for interaction after first stimulus was 100 seconds, this value was 14,1 seconds for interaction after second stimulus.

Receptor-β-arrestin2 complexes are started to become internalized after prolonged residence of the agonist bound to the receptor. This mechanism is activated in order to desensitize receptor signaling, and degradation/recycling of the receptor. Since CamAstR-C/β-arrestin2 interaction was characterized in this study, we further analyzed via immunofluorescence, whether this complex was internalized. Internalized β-arrestin2 was detected as clathrin-coated pit-like shape in the cytoplasm. When the same experiment was performed in the cells that were not transfected with GRK2 plasmid, no internalization

was detected even after AST-C treatment. As inferred from FRET analysis, these results confirmed the essential requirement of GRK2-mediated receptor phosphorylation for internalization of CamAstR-C/β-arrestin2, as well as their interaction.

Since CamAstR-C was found to be activating $G\alpha_{i/o}$ subunits, it is expected to regulate downstream adenylyl cyclases (ACs) negatively, thus inhibit intracellular cyclic AMP (cAMP) production. Therefore, regulation of the AC5 by CamAstR-C activation was assessed in this study. This experiment was performed by first activating endogenous β_2-adrenergic receptors with 3 nM isoprenaline, and then applying AST-C for competition with isoprenaline. Results from the FRET measurements using the well-established Epac1-camp sensor revealed that CamAstR-C activation reversed isoprenaline-triggered activation of AC5, and reduced the intracellular cAMP levels. However, CamAstR-C activation could not revert the FRET decrease as potent as expected, even with the application of saturating concentrations (2 μM). This might be due to low expression of CamAstR-C. Since a vector including the wild type receptor gene was used for transfection, we could not assess the expression levels of CamAstR-C, nor titer the amounts of plasmids for transfection. Another reason, which is more likely, is that the AST-C used in this study (Pyro-Glu-allatostatin C) might not potently activate the receptor, since it is a PISCF/AST from *D. Melanogaster*. In this case, low potency of the ligand binding will result in low amplification of the downstream signals, therefore cause responses in lower levels.

In order to investigate further downstream pathway activation mediated by CamAstR-C, we have chosen the MAPK pathway, because this pathway is a well-documented target of activated $G\alpha_{i/o}$. It was proven that upon activation of $G\alpha_{i/o}$, disassociated $G\beta\gamma$ subunit activates GRKs. Phosphorylation of the receptor by GRKs trigger β-arrestin2 recruitment, which in turn initiates ERK1/2 activation (Kotecha *et al*., 2002). In our study, Western blot analysis demonstrated time-dependent increase in pERK1/2 levels under treatment of the cells with 50 μM AST-C. Yet, this increase was shown only through one single experiment. Further repetition of this experiment is necessary in order to support the observed result.

Taking together the results of all experiments throughout this study, it was demonstrated that CamAstR-C is a Class A GPCR that is activated by PISCF/ASTs. Using TGFα-shedding assay and FRET-based tools, it was also proven that this receptor can couple with and activate $G\alpha_{i/o}$ subunit in HEK293T cells. Furthermore, activation of $G\alpha_{i1}$ via CamAstR-C triggered negative regulation of AC5, and suppressed its activity of cAMP production. Besides, agonist stimulation of CamAstR-C also caused receptor phosphorylation by GRK2, which stimulated β-arrestin2 recruitment. It was further validated that recruitment of β-arrestin2 to CamAstR-C results in receptor internalization after long exposure (1 hour) of the receptor to AST-C.

In conclusion, for the first time we characterized the pharmacological features and signaling properties of the PISCF-Allatostatin receptor of the Indian stick insect, *Carausius morosus*, by combining optical and biochemical methods. In order to further characterize this receptor, the native PISCF-allatostatin from *Carausius morosus* should be identified. On the other hand, tissue-specific expression pattern and the role of this receptor activity should be investigated in detail, in order to reveal the role of CamAstR-C in adult and/or larval physiology. We also demonstrated the possibility of using two well-established tools, FRET and TGFα-shedding assay for deorphanizing and characterizing invertebrate GPCRs. We believe that these tools will be valuable for further studies to assess invertebrate GPCR signaling in detail, and contribute to the research in pesticide screening, insect physiology and endocrinology.

APPENDIX A: PLASMID MAPS

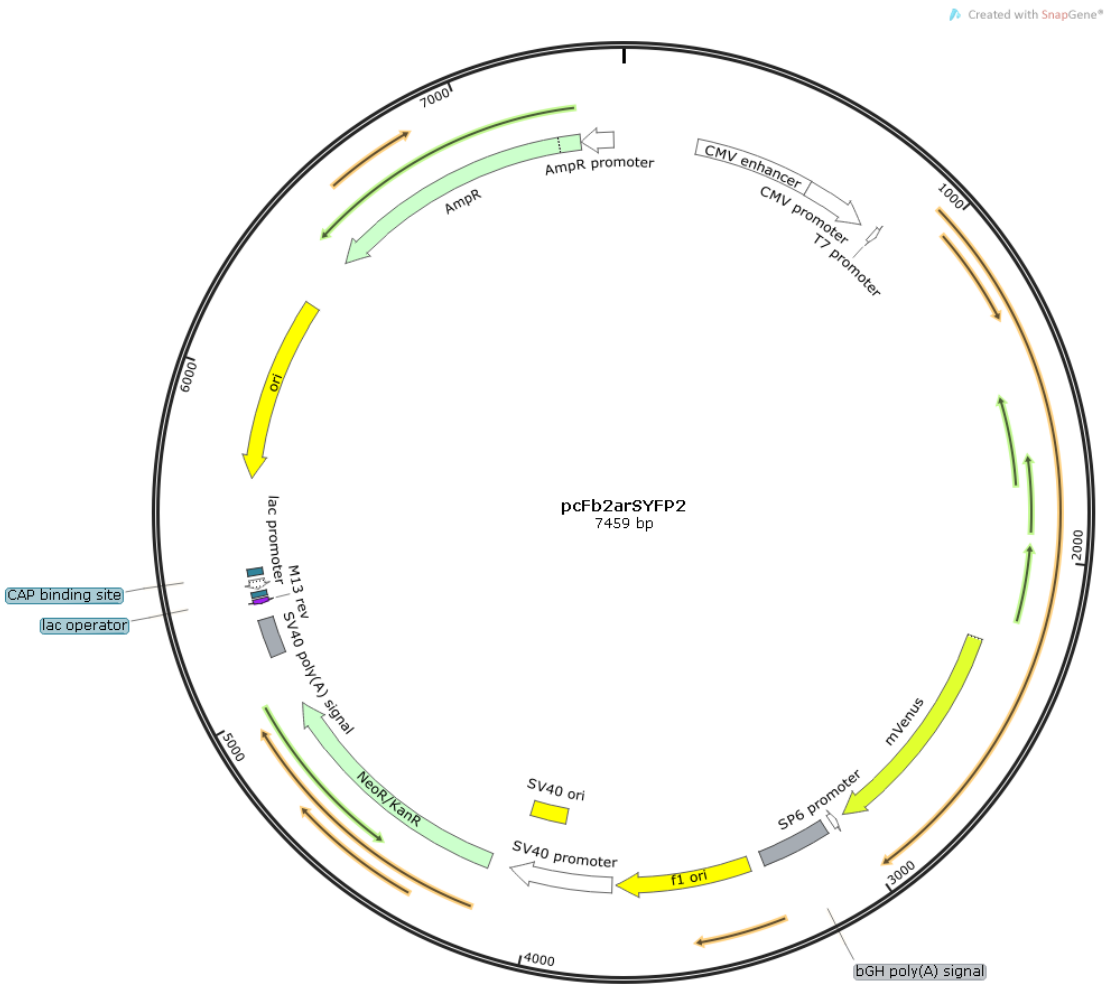

Figure A.1. pcFb2arSYFP2 vector map.

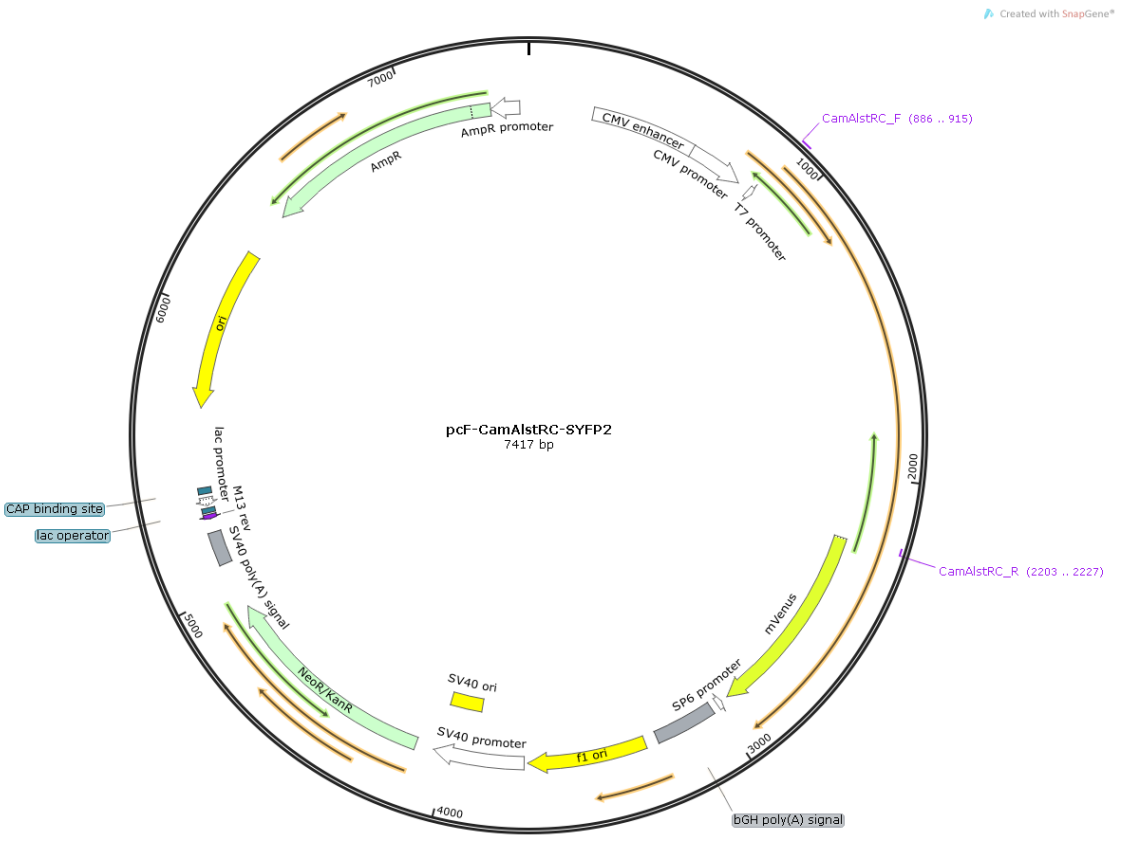

Figure A.2. pcDNA3-CamAstRC vector map and alignment sites of the cloning primers.

Name: pCAGGS/AP-TGFα
ORF: Fusion protein consisting of human TGFα (Gene Symbol, TGFA; NCBI accession number, NM_003236) and human placental alkaline phosphatase (Gene Symbol, ALPP; NCBI accession number, NM_001632)
Nucleotide sequences are synthesized upon codon optimization. Amino acid sequences are unchanged from the original one, Tokumaru et al. 151, 209-220 (2000))
Expression: Mammalian cells (CAG promoter)
Bacterial selection marker: Ampicillin (100 μg/mL)

Reference: Unpublished
Please inform A. Inoue and J. Aoki prior to submission of your papers using the construct.
Note: plasmids will be used for research purpose only and should not be distributed without permission of A. Inoue and J. Aoki.
Contact info: iaska@m.tohoku.ac.jp, jaoki@m.tohoku.ac.jp

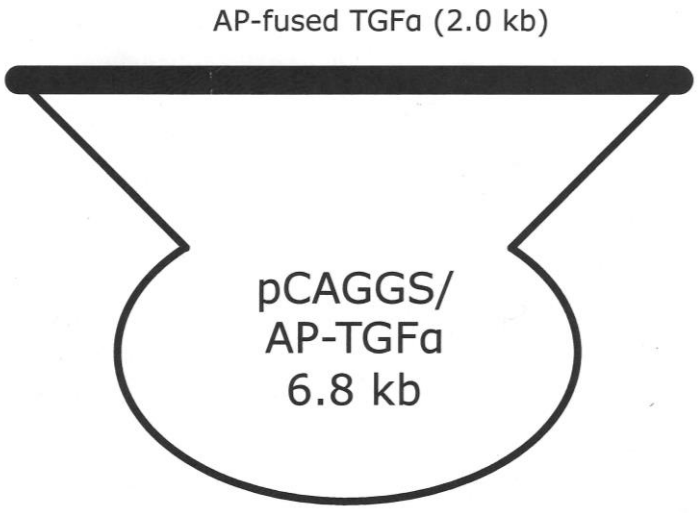

Figure A.3. pCAGGS/AP-TGFα vector map, obtained from Dr. Asuka Inoue (Inoue *et al.*, 2012)

Name: pCAGGS/$G\alpha_{q/s}$
ORF: human $G\alpha_q$ (GNAQ) with C-terminal human $G\alpha_s$ (GNAS, 6 aa)
Tag: None
Expression: Mammalian cells (CAG promoter)
Bacterial selection marker: Ampicillin (100 μg/mL)

Reference: Inoue et al. Nat. Methods 9, 1021 (2012)
Note: plasmids will be used for research purpose only and should not be distributed without permission of A. Inoue and J. Aoki.
Contact info: iaska@m.tohoku.ac.jp, jaoki@m.tohoku.ac.jp

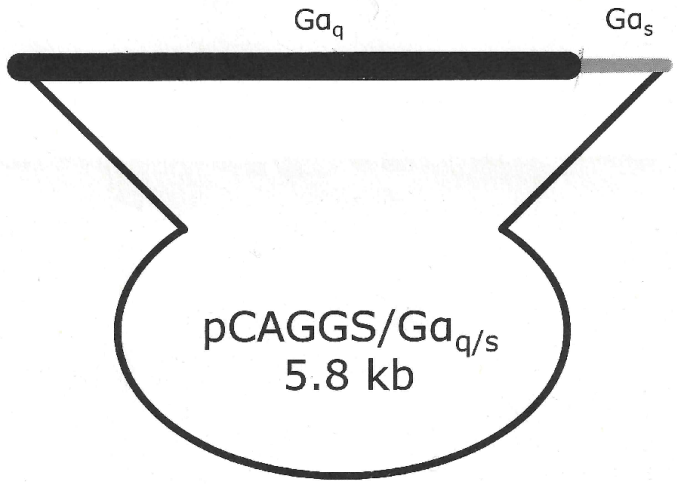

Junction (5′ side)

```
      1710       1720       1730       1740       1750       1760       1770       1780       1790       1800
tctcatcattttggcaaagaattgagctcccgggtaccgccaccATGACTCTGGAGTCCATCATGGCGTGCTGCCTGAGCGAGGAGGCCAAGGAAGCCCG
                                          M  T  L  E  S  I  M  A  C  C  L  S  E  E  A  K  E  A  R
```

Junction (3′ side)

```
      2710       2720       2730       2740       2750       2760       2770       2780       2790       2800
CAGTGACAAAATTATCTACTCCCACTTCACGTGCGCCACAGACACCGAGAATATCCGCTTTGTCTTTGCTGCCGTCAAGGACACCATCCTCCAGTTGAAC
  S  D  K  I  I  Y  S  H  F  T  C  A  T  D  T  E  N  I  R  F  V  F  A  A  V  K  D  T  I  L  Q  L  N

      2810       2820       2830       2840       2850       2860       2870       2880       2890       2900
CTGCGTCAGTACGAGCTGCTCTGActcgagatcgatggccaatgccctggctcacaaataccactgagatctttttccctctgccaaaaattatggggac
 L  R  Q  Y  E  L  L  *
```

Figure A.4. pCAGGS/$G\alpha_{q/s}$ vector map and sequence of the junction sites, obtained from (Inoue *et al.*, 2012).

Name: pCAGGS/$G\alpha_{q/i1}$
ORF: human $G\alpha_q$ (GNAQ) with C-terminal human $G\alpha_{i1}$ (GNAI1, 6 aa)

```
Junction (3' side)
      2810      2820      2830
CTGAAAGATTGTGGTCTCTTTTGActcgag
 L  K  D  C  G  L  F  *
```

Name: pCAGGS/$G\alpha_{q/i3}$
ORF: human $G\alpha_q$ (GNAQ) with C-terminal human $G\alpha_{i3}$ (GNAI3, 6 aa)

```
Junction (3' side)
      2810      2820      2830
CTGAAGGAATGTGGACTTTATTGActcgag
 L  K  E  C  G  L  Y  *
```

Name: pCAGGS/$G\alpha_{q/o}$
ORF: human $G\alpha_q$ (GNAQ) with C-terminal human $G\alpha_o$ (GNAO1, 6 aa)

```
Junction (3' side)
      2810      2820      2830
CTGCGGGGCTGCGGCTTGTACTGActcgag
 L  R  G  C  G  L  Y  *
```

Name: pCAGGS/$G\alpha_{q/z}$
ORF: human $G\alpha_q$ (GNAQ) with C-terminal human $G\alpha_z$ (GNAZ, 6 aa)

```
Junction (3' side)
      2810      2820      2830
CTGAAGTACATTGGCCTTTGCTGActcgag
 L  K  Y  I  G  L  C  *
```

Name: pCAGGS/$G\alpha_{q/12}$
ORF: human $G\alpha_q$ (GNAQ) with C-terminal human $G\alpha_{12}$ (GNA12, 6 aa)

```
Junction (3' side)
      2810      2820      2830
CTGAAGGACATCATGCTGCAGTGActcgag
 L  K  D  I  M  L  Q  *
```

Name: pCAGGS/$G\alpha_{q/13}$
ORF: human $G\alpha_q$ (GNAQ) with C-terminal human $G\alpha_{13}$ (GNA13, 6 aa)

```
Junction (3' side)
      2810      2820      2830
CTGAAGCAGCTTATGCTACAGTGActcgag
 L  K  Q  L  M  L  Q  *
```

Figure A.5. Junction sites for other chimeric $G\alpha_q$ constructs, obtained from (Inoue *et al.*, 2012).

Name: pCAGGS/$G\alpha_{16}$
ORF: human $G\alpha_{16}$ (GNA15)
Tag: None
Expression: Mammalian cells (CAG promoter)
Bacterial selection marker: Ampicillin (100 μg/mL)

Reference: Inoue et al. Nat. Methods 9, 1021 (2012)
Note: plasmids will be used for research purpose only and should not be distributed without permission of A. Inoue and J. Aoki.
Contact info: iaska@m.tohoku.ac.jp, jaoki@m.tohoku.ac.jp

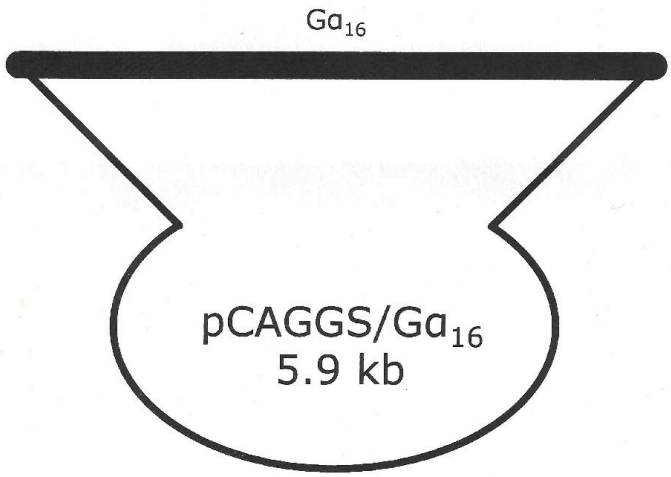

Junction (5′ side)

```
      1710       1720       1730       1740       1750       1760       1770       1780       1790       1800
tctcatcattttggcaaagaattgagctcccgggtaccgccaccATGGCCCGCTCGCTGACCTGGCGCTGCTGCCCCTGGTGCCTGACGGAGGATGAGAA
                                                M  A  R  S  L  T  W  R  C  C  P  W  C  L  T  E  D  E  K
```

Junction (3′ side)

```
      2810       2820       2830       2840       2850       2860       2870       2880       2890       2900
CGCAAGGTCTTCAAGGACGTGCGGGACTCGGTGCTCGCCCGCTACCTGGACGAGATCAACCTGCTGTGActcgagatcgatggccaatgccctggctcac
 R  K  V  F  K  D  V  R  D  S  V  L  A  R  Y  L  D  E  I  N  L  L  *
```

Figure A.6. pCAGGS/Gα_{16} vector map and junction sites, obtained from (Inoue *et al.*, 2012)

REFERENCES

Adams, M. E., 2010, "9) Insect G Protein-Coupled Receptors: Recent Discoveries and Implications", *Insect Pharmacology: Channels, Receptors, Toxins and Enzymes*.

Adjobo-Hermans, M. J. W., J. Goedhart, L. van Weeren, S. Nijmeijer, E. M. M. Manders, S. Offermanns, and T. W. J. Gadella, 2011, "Real-Time Visualization of Heterotrimeric G Protein Gq Activation in Living Cells.", *BMC biology*, Vol. 9, No. 1, pp. 32.

Alewijnse, A. E., H. Timmerman, E. H. Jacobs, M. J. Smit, E. Roovers, S. Cotecchia, and R. Leurs, 2000, "The Effect of Mutations in the DRY Motif on the Constitutive Activity and Structural Instability of the Histamine H(2) Receptor.", *Molecular pharmacology*, Vol. 57, No. 5, pp. 890–8.

Audsley, N., and R. E. Down, 2015, "G Protein Coupled Receptors as Targets for next Generation Pesticides", *Insect biochemistry and molecular biology*, Vol. 67, No. 1, pp. 27–37.

Audsley, N., H. P. Vandersmissen, R. Weaver, P. Dani, J. Matthews, R. Down, K. Vuerinckx, Y.-J. Kim, and J. Vanden Broeck, 2013, "Characterisation and Tissue Distribution of the PISCF Allatostatin Receptor in the Red Flour Beetle, Tribolium Castaneum.", *Insect biochemistry and molecular biology*, Vol. 43, No. 1, pp. 65–74.

Auerswald, L., N. Birgül, G. Gäde, H. J. Kreienkamp, and D. Richter, 2001, "Structural, Functional, and Evolutionary Characterization of Novel Members of the Allatostatin Receptor Family from Insects.", *Biochemical and biophysical research communications*, Vol. 282, No. 4, pp. 904–909.

Barrozo, R. B., P. E. Schilman, S. A. Minoli, and C. R. Lazzari, 2004, "Daily Rhythms in Disease-Vector Insects", *Biological Rhythm Research*, Vol. 35, No. 1-2, pp. 79–92.

Bendena, W. G., 2010, "Neuropeptide Physiology in Insects.", *Advances in experimental medicine and biology*, Vol. 692, pp. 166–191.

Bender, E., A. Buist, M. Jurzak, X. Langlois, G. Baggerman, P. Verhasselt, M. Ercken, H.-Q. Guo, C. Wintmolders, and I. Van den Wyngaert, 2002, "Characterization of an Orphan G Protein-Coupled Receptor Localized in the Dorsal Root Ganglia Reveals Adenine as a Signaling Molecule", *Proceedings of the National Academy of Sciences*, Vol. 99, No. 13, pp. 8573–8578.

Birgül, N., C. Weise, H. J. Kreienkamp, and D. Richter, 1999, "Reverse Physiology in Drosophila: Identification of a Novel Allatostatin-like Neuropeptide and Its Cognate Receptor Structurally Related to the Mammalian Somatostatin/galanin/opioid Receptor Family", *EMBO Journal*, Vol. 18, No. 21, pp. 5892–5900.

Black, J., 1996, "A Personal View of Pharmacology.", *Annual review of pharmacology and toxicology*, Vol. 36, pp. 1–33.

Blake, B. L., M. R. Wing, J. Y. Zhou, Q. Lei, J. R. Hillmann, C. I. Behe, R. A. Morris, T. K. Harden, D. A. Bayliss, and D. P. Siderovski, 2001, "Gβ Association and Effector Interaction Selectivities of the Divergent Gγ Subunit Gγ13", *Journal of Biological Chemistry*, Vol. 276, No. 52, pp. 49267–49274.

Blaukat, A., A. Barac, M. J. Cross, S. Offermanns, and I. Dikic, 2000, "G Protein-Coupled Receptor-Mediated Mitogen-Activated Protein Kinase Activation through Cooperation of Galpha(q) and Galpha(i) Signals.", *Molecular and cellular biology*, Vol. 20, No. 18, pp. 6837–48.

Bodmann, E.-L., A. Rinne, D. Brandt, S. Lutz, T. Wieland, R. Grosse, and M. Bünemann, 2014, "Dynamics of Gαq-Protein-p63RhoGEF Interaction and Its Regulation by RGS2.", *The Biochemical journal*, Vol. 458, No. 1, pp. 131–40.

Bouvier, M., 2013, "Unraveling the Structural Basis of GPCR Activation and Inactivation.", *Nature structural & molecular biology*, Vol. 20, No. 5, pp. 539–41.

Breton, B., M. Lagacé, and M. Bouvier, 2010, "Combining Resonance Energy Transfer Methods Reveals a Complex between the α2A-Adrenergic Receptor, Gαi1β1γ2, and GRK2", *The FASEB Journal*, Vol. 24, No. 12, pp. 4733–4743.

Brody, T., and A. Cravchik, 2000, "Drosophila melanogasterG Protein–Coupled Receptors", *The Journal of cell biology*, Vol. 150, No. 2, pp. F83–F88.

Broussard, J. a, B. Rappaz, D. J. Webb, and C. M. Brown, 2013, "Fluorescence Resonance Energy Transfer Microscopy as Demonstrated by Measuring the Activation of the Serine/threonine Kinase Akt.", *Nature protocols*, Vol. 8, No. 2, pp. 265–81.

Bünemann, M., M. Frank, and M. J. Lohse, 2003, "Gi Protein Activation in Intact Cells Involves Subunit Rearrangement rather than Dissociation.", *Proceedings of the National Academy of Sciences of the United States of America*, Vol. 100, No. 26, pp. 16077–16082.

Caers, J., H. Verlinden, S. Zels, H. P. Vandersmissen, K. Vuerinckx, and L. Schoofs, 2012, "More than Two Decades of Research on Insect Neuropeptide GPCRs: An Overview", *Frontiers in Endocrinology*, Vol. 3, No. NOV, pp. 1–30.

Chalubinski, M., and M. L. Kowalski, 2006, "Endocrine Disrupters-Potential Modulators of the Immune System and Allergic Response", *Allergy*, Vol. 61, No. 11, pp. 26–35.

Cheng, X., Z. Ji, T. Tsalkova, and F. Mei, 2008, "Epac and PKA: A Tale of Two Intracellular cAMP Receptors.", *Acta biochimica et biophysica Sinica*, Vol. 40, No. 7, pp. 651–62.

Cheng, Z., D. Garvin, A. Paguio, P. Stecha, K. Wood, and F. Fan, 2010, "Luciferase Reporter Assay System for Deciphering GPCR Pathways", *Current chemical genomics*, Vol. 4, No. 12, pp. 84.

Cusson, M., G. D. Prestwich, B. Stay, and S. S. Tobe, 1991, "Photoaffinity Labeling of Allatostatin Receptor Proteins in the Corpora Allata of the Cockroach, Diploptera Punctata", *Biochemical and Biophysical Research Communications*, Vol. 181, No. 2, pp. 736–742.

Dascal, N., 2001, "Ion-Channel Regulation by G Proteins.", *Trends in endocrinology and metabolism*, Vol. 12, No. 9, pp. 391–398.

DeFea, Vaughn, O'Bryan, Nishijima, Déry, and Bunnett, 2000, "The Proliferative and Antiapoptotic Effects of Substance P Are Facilitated by Formation of a Beta -Arrestin-Dependent Scaffolding Complex", *Proceedings of the National Academy of Sciences of the United States of America*, Vol. 97, No. 20, pp. 11086–11091.

DeLapp, N. W., 2004, "The Antibody-Capture [35 S] GTPgS Scintillation Proximity Assay: A Powerful Emerging Technique for Analysis of GPCR Pharmacology", *Neuroscience*, Vol. 98, No. 8, pp. 201–206.

Deupi, X., and B. K. Kobilka, 2007, "Activation of G Protein-Coupled Receptors", *Advances in Protein Chemistry*, Vol. 74, pp. 137 – 166.

Dorsam, R. T., and J. S. Gutkind, 2007, "G-Protein-Coupled Receptors and Cancer.", *Nature reviews. Cancer*, Vol. 7, No. 2, pp. 79–94.

Duan Sahbaz, B., 2013, "Identification and Docking Analysis of Allatostatin Receptor in Carausius morosus.", Master of Science, Bogazici University.

Ferguson, S. S., and M. G. Caron, 1998, "G Protein-Coupled Receptor Adaptation Mechanisms.", *Seminars in cell & developmental biology*, Vol. 9, No. 2, pp. 119–127.

Flower, D. R., 1999, "Modelling G-Protein-Coupled Receptors for Drug Design", *Biochimica et Biophysica Acta - Reviews on Biomembranes*, Vol. 1422, No. 3, pp. 207–234.

Frank, M., L. Thümer, M. J. Lohse, and M. Bünemann, 2005, "G Protein Activation without Subunit Dissociation Depends on a Gαi-Specific Region", *Journal of Biological Chemistry*, Vol. 280, No. 26, pp. 24584–24590.

Fredriksson, R., M. C. Lagerström, L.-G. Lundin, and H. B. Schiöth, 2003, "The G-Protein-Coupled Receptors in the Human Genome Form Five Main Families. Phylogenetic Analysis, Paralogon Groups, and Fingerprints.", *Molecular pharmacology*, Vol. 63, No. 6, pp. 1256–72.

Fritze, O., S. Filipek, V. Kuksa, K. Palczewski, K. P. Hofmann, and O. P. Ernst, 2003, "Role of the Conserved NPxxY(x)5,6F Motif in the Rhodopsin Ground State and during Activation.", *Proceedings of the National Academy of Sciences of the United States of America*, Vol. 100, No. 5, pp. 2290–2295.

Gäde, G., M. W. Lorenz, and K.-H. Hoffmann, 1997, "Stick Insect (Carausius Morosus; Phasmatodea: Lonchodidae) Brain Extract Contains Multiple Fractions with Allatostatic Activity", *European Journal of Entomology*, Vol. 94, No. 3, pp. 361–368.

George, S. E., P. J. Bungay, and L. H. Naylor, 1997, "Evaluation of a CRE-Directed Luciferase Reporter Gene Assay as an Alternative to Measuring cAMP Accumulation", *Journal of Biomolecular Screening*, Vol. 2, No. 4, pp. 235–240.

Goldsmith, Z. G., and D. N. Dhanasekaran, 2007, "G Protein Regulation of MAPK Networks.", *Oncogene*, Vol. 26, No. 22, pp. 3122–3142.

Griebler, M., S. A. Westerlund, K. H. Hoffmann, and M. Meyering-Vos, 2008, "RNA Interference with the Allatoregulating Neuropeptide Genes from the Fall Armyworm Spodoptera Frugiperda and Its Effects on the JH Titer in the Hemolymph", *Journal of Insect Physiology*, Vol. 54, No. 6, pp. 997–1007.

Grigoriadis, D. E., S. R. J. Hoare, S. M. Lechner, D. H. Slee, and J. A. Williams, 2009, "Drugability of Extracellular Targets: Discovery of Small Molecule Drugs Targeting Allosteric, Functional, and Subunit-Selective Sites on GPCRs and Ion Channels.", *Neuropsychopharmacology : official publication of the American College of Neuropsychopharmacology*, Vol. 34, No. 1, pp. 106–25.

Hanoune, J., and N. Defer, 2001, "Regulation and Role of Adenylyl Cyclase Isoforms.", *Annual review of pharmacology and toxicology*, Vol. 41, pp. 145–174.

Hein, P., M. Frank, C. Hoffmann, M. J. Lohse, and M. Bünemann, 2005, "Dynamics of receptor/G Protein Coupling in Living Cells.", *The EMBO journal*, Vol. 24, No. 23, pp. 4106–4114.

Hein, P., Rochais, C. Hoffmann, S. Dorsch, V. Nikolaev, S. Engelhardt, Berlot, M. Lohse, and M. Bünemann, 2006, "Gs Activation Is Time-Limiting in Initiating Receptor-Mediated Signaling", *The Journal of biological chemistry*, Vol. 281, No. 44, pp. 33345–33351.

Hernández-Martínez, S., Y. Li, H. Lanz-Mendoza, M. H. Rodríguez, and F. G. Noriega, 2005, "Immunostaining for Allatotropin and Allatostatin-A and -C in the Mosquitoes Aedes Aegypti and Anopheles Albimanus", *Cell and Tissue Research*, Vol. 321, No. 1, pp. 105–113.

Hill, C. A., A. N. Fox, R. J. Pitts, L. B. Kent, P. L. Tan, M. A. Chrystal, A. Cravchik, F. H. Collins, H. M. Robertson, and L. J. Zwiebel, 2002, "G Protein Coupled Receptors in Anopheles Gambiae", *Science*, Vol. 298, No. 5591, pp. 176–178.

Hillenbrand, M., C. Schori, J. Schöppe, and A. Plückthun, 2015, "Comprehensive Analysis of Heterotrimeric G-Protein Complex Diversity and Their Interactions with GPCRs in Solution.", *Proceedings of the National Academy of Sciences of the United States of America*, Vol. 112, No. 11, pp. 1181–1190.

Hoffmann, C., G. Gaietta, M. Bünemann, S. R. Adams, S. Oberdorff-Maass, B. Behr, J.-P. Vilardaga, R. Y. Tsien, M. H. Ellisman, and M. J. Lohse, 2005, "A FlAsH-Based FRET Approach to Determine G Protein-Coupled Receptor Activation in Living Cells.", *Nature methods*, Vol. 2, No. 3, pp. 171–176.

Horton, J. K., S. J. Capper, M. J. Price Jones, and K. T. Hughes, 2005, "Assays for Drug Screening Applications and Research", *Wild D (ed)*, pp. 854–884.

Hummon, A. B., T. a Richmond, P. Verleyen, G. Baggerman, J. Huybrechts, M. A. Ewing, E. Vierstraete, S. L. Rodriguez-Zas, L. Schoofs, J. V Sweedler, 2006, "From the Genome to the Proteome", *Science (New York, N.Y.)*, Vol. 314, No. 5799, pp. 647–649.

Ijzerman, A. P., V.-P. Jaakola, V. Cherezov, R. C. Stevens, M. T. Griffith, J. R. Lane, M. A. Hanson, and E. Y. T. Chien, 2008, "The 2.6 Angstrom Crystal Structure of a Human A2A Adenosine Receptor Bound to an Antagonist", *Science*, Vol. 322, No. 5905, pp. 1211–1217.

Inoue, A., J. Ishiguro, H. Kitamura, N. Arima, M. Okutani, A. Shuto, S. Higashiyama, T. Ohwada, H. Arai, J. Aoki, 2012, "TGFα Shedding Assay: An Accurate and Versatile Method for Detecting GPCR Activation", *Nature Methods*, Vol. 9, No. 10, pp. 1021–1029.

Ito, A., T. Satoh, Y. Kaziro, and H. Itoh, 1995, "G Protein Bg Subunit Activates Ras, Raf, and MAP Kinase in HEK 293 Cells", *FEBS Letters*, Vol. 368, No. 1, pp. 183–187.

Johnson, E. C., L. M. Bohn, L. S. Barak, R. T. Birse, D. R. Nässel, M. G. Caron, and P. H. Taghert, 2003, "Identification of Drosophila Neuropeptide Receptors by G Protein-Coupled Receptors-β-Arrestin2 Interactions", *Journal of Biological Chemistry*, Vol. 278, No. 52, pp. 52172–52178.

Jordan, J. D., K. D. Carey, P. J. Stork, and R. Iyengar, 1999, "Modulation of Rap Activity by Direct Interaction of Galpha(o) with Rap1 GTPase-Activating Protein", *J Biol Chem*, Vol. 274, No. 31, pp. 21507–21510.

Kai, Z., J. Huang, Y. Xie, S. S. Tobe, Y. Ling, L. Zhang, Y. Zhao, and X. Yang, 2009, "Synthesis, Biological Activity, and Hologram Quantitative Structure− Activity Relationships of Novel Allatostatin Analogues†", *Journal of agricultural and food chemistry*, Vol. 58, No. 5, pp. 2652–2658.

Karnik, S. S., and H. G. Khorana, 1990, "Assembly of Functional Rhodopsin Requires a Disulfide Bond between Cysteine Residues 110 and 187", *J Biol Chem*, Vol. 265, No. 29, pp. 17520–17524.

Katritch, V., V. Cherezov, and R. C. Stevens, 2013, "Structure-Function of the G Protein-Coupled Receptor Superfamily.", *Annual review of pharmacology and toxicology*, Vol. 53, pp. 531–56.

Khan, S. M., R. Sleno, S. Gora, P. Zylbergold, J. Laverdure, J. Labbé, G. J. Miller, and T. E. Hébert, 2013, "The Expanding Roles of Gβγ Subunits in G Protein-Coupled Receptor Signaling and Drug Action.", *Pharmacological reviews*, Vol. 65, No. 2, pp. 545–77.

Kobilka, B. K., and X. Deupi, 2007, "Conformational Complexity of G-Protein-Coupled Receptors", *Trends in Pharmacological Sciences*, Vol. 28, No. 8, pp. 397–406.

Kotecha, S. A., J. N. Oak, M. F. Jackson, Y. Perez, B. a Orser, H. H. M. Van Tol, and J. F. MacDonald, 2002, "A D2 Class Dopamine Receptor Transactivates a Receptor Tyrosine Kinase to Inhibit NMDA Receptor Transmission.", *Neuron*, Vol. 35, No. 6, pp. 1111–22.

Krasel, C., M. Bünemann, K. Lorenz, and M. J. Lohse, 2005, "β-Arrestin Binding to the β2-Adrenergic Receptor Requires Both Receptor Phosphorylation and Receptor Activation", *Journal of Biological Chemistry*, Vol. 280, No. 10, pp. 9528–9535.

Kreienkamp, H. J., H. J. Larusson, I. Witte, T. Roeder, N. Birgül, H. H. Hönck, S. Harder, G. Ellinghausen, F. Buck, and D. Richter, 2002, "Functional Annotation of Two Orphan G-Protein-Coupled Receptors, drostar1 and -2, from Drosophila Melanogaster and Their Ligands by Reverse Pharmacology", *Journal of Biological Chemistry*, Vol. 277, No. 42, pp. 39937–39943.

Kreienkamp, H.-J., C. W. Liew, D. Bächner, M.-G. Mameza, M. Soltau, A. Quitsch, M. Christenn, W. Wente, and D. Richter, 2004, "Physiology of somatostatin receptors: from genetics to molecular analysis", *Somatostatin*, pp. 185–202.

Kremers, G. J., J. Goedhart, E. B. Van Munster, and T. W. J. Gadella, 2006, "Cyan and Yellow Super Fluorescent Proteins with Improved Brightness, Protein Folding, and FRET Forster Radius", *Biochemistry*, Vol. 45, No. 2, pp. 6570–6580.

Kunishima, N., Y. Shimada, Y. Tsuji, T. Sato, M. Yamamoto, T. Kumasaka, S. Nakanishi, H. Jingami, and K. Morikawa, 2000, "Structural Basis of Glutamate Recognition by a Dimeric Metabotropic Glutamate Receptor.", *Nature*, Vol. 407, No. 6804, pp. 971–977.

Lanctot, P. M., P. C. Leclerc, M. Clément, M. Auger-Messier, E. Escher, R. Leduc, and G. Guillemette, 2005, "Importance of N-Glycosylation Positioning for Cell-Surface Expression, Targeting, Affinity and Quality Control of the Human AT1 Receptor.", *The Biochemical journal*, Vol. 390, No. Pt 1, pp. 367–76.

Lanzafame, A. A., A. Christopoulos, and F. Mitchelson, 2003, "Cellular Signaling Mechanisms for Muscarinic Acetylcholine Receptors.", *Receptors & channels*, Vol. 9, No. 4, pp. 241–260.

Lebon, G., T. Warne, P. C. Edwards, K. Bennett, C. J. Langmead, A. G. W. Leslie, and C. G. Tate, 2011, "Agonist-Bound Adenosine A2A Receptor Structures Reveal Common Features of GPCR Activation.", *Nature*, Vol. 474, No. 7352, pp. 521–5.

Lefkowitz, R. J., K. Rajagopal, and E. J. Whalen, 2006, "New Roles for Beta-Arrestins in Cell Signaling: Not Just for Seven-Transmembrane Receptors.", *Molecular cell*, Vol. 24, No. 5, pp. 643–52.

Lohse, M., V. Nikolaev, P. Hein, C. Hoffmann, J. Vilardaga, and M. Bünemann, 2008, "Optical Techniques to Analyze Real-Time Activation and Signaling of G-Protein-Coupled Receptors", *Trends in Pharmacological Sciences*, Vol. 29, No. 3, pp. 159–165.

Lorenz, M. W., K. H. Hoffmann, and G. Gade, 1999, "Juvenile Hormone Biosynthesis in Larval and Adult Stick Insects, Carausius Morosus", *J Insect Physiol*, Vol. 45, No. 5, pp. 443–452.

Lorenz, M. W., R. Kellner, K. H. Hoffmann, and G. Gäde, 2000, "Identification of Multiple Peptides Homologous to Cockroach and Crick*et* Allatostatins in the Stick Insect Carausius Morosus", *Insect Biochemistry and Molecular Biology*, Vol. 30, No. 3, pp. 711–718.

Luttrell, L. M., and R. J. Lefkowitz, 2002, "The Role of Beta-Arrestins in the Termination and Transduction of G-Protein-Coupled Receptor Signals.", *Journal of cell science*, Vol. 115, No. Pt 3, pp. 455–465.

Mayoral, J. G., M. Nouzova, A. Brockhoff, M. Goodwin, S. Hernandez-Martinez, D. Richter, W. Meyerhof, and F. G. Noriega, 2010, "Allatostatin-C Receptors in Mosquitoes", *Peptides*, Vol. 31, No. 3, pp. 442–450.

McDonald, P. H., C. W. Chow, W. E. Miller, S. A. Laporte, M. E. Field, F. T. Lin, R. J. Davis, and R. J. Lefkowitz, 2000, "Beta-Arrestin 2: A Receptor-Regulated MAPK Scaffold for the Activation of JNK3.", *Science (New York, N.Y.)*, Vol. 290, No. 5496, pp. 1574–1577.

Meyering-Vos, M., S. Merz, M. Sertkol, and K. H. Hoffmann, 2006, "Functional Analysis of the Allatostatin-A Type Gene in the Cricket Gryllus Bimaculatus and the Armyworm Spodoptera Frugiperda", *Insect Biochemistry and Molecular Biology*, Vol. 36, No. 6, pp. 492–504.

Milde, M., R. C. Werthmann, K. von Hayn, and M. Bünemann, 2014, "Dynamics of Adenylate Cyclase Regulation via Heterotrimeric G-Proteins.", *Biochemical Society transactions*, Vol. 42, No. 2, pp. 239–43.

Moore, C. A. C., S. K. Milano, and J. L. Benovic, 2007, "Regulation of Receptor Trafficking by GRKs and Arrestins.", *Annual review of physiology*, Vol. 69, pp. 451–482.

Nikolaev, V. O., M. Bünemann, L. Hein, A. Hannawacker, and M. J. Lohse, 2004, "Novel Single Chain cAMP Sensors for Receptor-Induced Signal Propagation", *Journal of Biological Chemistry*, Vol. 279, No. 36, pp. 37215–37218.

Nikolaev, V. O., and M. J. Lohse, 2006, "Monitoring of cAMP Synthesis and Degradation in Living Cells.", *Physiology (Bethesda, Md.)*, Vol. 21, No. 2, pp. 86–92.

Offermanns, S., 2003, "G-Proteins as Transducers in Transmembrane Signalling", *Progress in Biophysics and Molecular Biology*, Vol. 83, No. 2, pp. 101–130.

Omasits, U., C. H. Ahrens, S. Müller, and B. Wollscheid, 2014, "Protter: Interactive Protein Feature Visualization and Integration with Experimental Proteomic Data", *Bioinformatics*, Vol. 30, No. 6, pp. 884–886.

Palczewski, K., T. Kumasaka, T. Hori, C. A. Behnke, H. Motoshima, B. A. Fox, I. Le Trong, D. C. Teller, T. Okada, … M. Miyano, 2000, "Crystal Structure of Rhodopsin: A G Protein-Coupled Receptor", *Science (New York, NY)*, Vol. 289, No. 5480, pp. 739–745.

Prabhu, Y., and L. Eichinger, 2006, "The Dictyostelium Repertoire of Seven Transmembrane Domain Receptors.", *European journal of cell biology*, Vol. 85, No. 9-10, pp. 937–46.

Purves, D., G. Augustine, D. Fitzpatrick, L. Katz, A.-S. LaMantia, J. McNamara, and M. Williams, 2001, "Neuroscience," *Sunderland (MA): Sinauer Associates.*

Reddy, G. R., H. Subramanian, A. Birk, M. Milde, V. O. Nikolaev, and M. Bünemann, 2015, "Adenylyl Cyclases 5 and 6 Underlie PIP3-Dependent Regulation.", *FASEB journal : official publication of the Federation of American Societies for Experimental Biology*, Vol. 29, No. 8, pp. 3458–3471.

Ritter, S. L., and R. a Hall, 2009, "Fine-Tuning of GPCR Activity by Receptor-Interacting Proteins.", *Nature reviews. Molecular cell biology*, Vol. 10, No. 12, pp. 819–830.

Rovati, G. E., V. Capra, and R. R. Neubig, 2007, "The Highly Conserved DRY Motif of Class A G Protein-Coupled Receptors: Beyond the Ground State.", *Molecular pharmacology*, Vol. 71, No. 4, pp. 959–964.

Ruiz-Velasco, V., and S. R. Ikeda, 2001, "Functional Expression and FRET Analysis of Green Fluorescent Proteins Fused to G-Protein Subunits in Rat Sympathetic Neurons.", *The Journal of physiology*, Vol. 537, No. 3, pp. 679–92.

Runne, C., and S. Chen, 2013, "WD40-Repeat Proteins Control the Flow of Gβγ Signaling for Directional Cell Migration", *Cell adhesion & migration*, Vol. 7, No. 2, pp. 214–218.

Salon, J. A., D. T. Lodowski, and K. Palczewski, 2011, "The Significance of G Protein-Coupled Receptor Crystallography for Drug Discovery.", *Pharmacological reviews*, Vol. 63, No. 4, pp. 901–37.

Seino, S., and T. Shibasaki, 2005, "PKA-Dependent and PKA-Independent Pathways for cAMP-Regulated Exocytosis.", *Physiological reviews*, Vol. 85, No. 4, pp. 1303–1342.

Selvin, P. R., 2000, "The Renaissance of Fluorescence Resonance Energy Transfer", *Nature structural biology*, Vol. 7, No. 9, pp. 730–734.

Siliciano, J. D., and D. a Goodenough, 1988, "Localization of the Tight Junction Protein, ZO-1, Is Modulated by Extracellular Calcium and Cell-Cell Contact in Madin-Darby Canine Kidney Epithelial Cells.", *The Journal of cell biology*, Vol. 107, No. 6 Pt 1, pp. 2389–99.

Spiess, E., F. Bestvater, A. Heckel-Pompey, K. Toth, M. Hacker, G. Stobrawa, T. Feurer, C. Wotzlaw, U. Berchner-Pfannschmidt, and T. Porwol, 2005, "Two-photon Excitation and Emission Spectra of the Green Fluorescent Protein Variants ECFP, EGFP and EYFP", *Journal of microscopy*, Vol. 217, No. 3, pp. 200–204.

Sprang, S. R., Z. Chen, and X. Du, 2007, Structural Basis of Effector Regulation and Signal Termination in Heterotrimeric Galpha Proteins, *Advances in Protein Chemistry*, Vol. 74, pp. 1–65.

Stay, B., and S. S. Tobe, 2007, "The Role of Allatostatins in Juvenile Hormone Synthesis in Insects and Crustaceans.", *Annual review of entomology*, Vol. 52, pp. 277–299.

Stevens, R. C., V. Cherezov, V. Katritch, R. Abagyan, P. Kuhn, H. Rosen, and K. Wüthrich, 2013, "The GPCR Network: A Large-Scale Collaboration to Determine Human GPCR Structure and Function.", *Nature reviews. Drug discovery*, Vol. 12, No. 1, pp. 25–34.

Takeda, S., 2002, "Identification of G Protein-Coupled Receptor Genes from the Human Genome Sequence", *FEBS Letters*, Vol. 520, No. 1-3, pp. 97–101.

Tian, L., S. A. Hires, T. Mao, D. Huber, M. E. Chiappe, S. H. Chalasani, L. Petreanu, J. Akerboom, S. A. McKinney, and E. R. Schreiter, 2009, "Imaging Neural Activity in Worms, Flies and Mice with Improved GCaMP Calcium Indicators", *Nature methods*, Vol. 6, No. 12, pp. 875–881.

Tobe, S. S., and W. G. Bendena, 2006, Allatostatins in the Insects, In *Handbook of Biologically Active Peptides*, pp. 201–206.

Tobin, A. B., 2008, "G-Protein-Coupled Receptor Phosphorylation: Where, When and by Whom.", *British journal of pharmacology*, Vol. 153 Suppl., pp. S167–S176.

Uzman, A., H. Lodish, A. Berk, L. Zipursky, and D. Baltimore, 2000, "Molecular Cell Biology (4th Edition) New York, NY, 2000, ISBN 0-7167-3136-3", *Biochemistry and Molecular Biology Education*, Vol. 29, No.3 pp. 126-128.

Van Wielendaele, P., L. Badisco, and J. Vanden Broeck, 2012, "Neuropeptidergic Regulation of Reproduction in Insects", *General and Comparative Endocrinology*, Vol. 188, No. 1, pp. 23–34.

Venkatakrishnan, A. J., X. Deupi, G. Lebon, C. G. Tate, G. F. Schertler, and M. M. Babu, 2013, "Molecular Signatures of G-Protein-Coupled Receptors.", *Nature*, Vol. 494, No. 7436, pp. 185–94.

Vilardaga, J. P., M. Frank, C. Krasel, C. Dees, R. A. Nissenson, and M. J. Lohse, 2001, "Differential Conformational Requirements for Activation of G Proteins and the Regulatory Proteins Arrestin and G Protein-Coupled Receptor Kinase in the G Protein-Coupled Receptor for Parathyroid Hormone (PTH)/PTH-Related Protein.", *The Journal of biological chemistry*, Vol. 276, No. 36, pp. 33435–33443.

Vilardaga, J.-P., M. Bünemann, C. Krasel, M. Castro, and M. J. Lohse, 2003, "Measurement of the Millisecond Activation Switch of G Protein-Coupled Receptors in Living Cells.", *Nature biotechnology*, Vol. 21, No. 7, pp. 807–812.

Violin, J. D., X.-R. Ren, and R. J. Lefkowitz, 2006, "G-Protein-Coupled Receptor Kinase Specificity for Beta-Arrestin Recruitment to the beta2-Adrenergic Receptor Revealed by Fluorescence Resonance Energy Transfer.", *The Journal of biological chemistry*, Vol. 281, No. 29, pp. 20577–20588.

Wall, M. A., D. E. Coleman, E. Lee, J. A. Iñiguez-Lluhi, B. A. Posner, A. G. Gilman, and S. R. Sprang, 1995, "The Structure of the G Protein Heterotrimer Gi Alpha 1 Beta 1 Gamma 2.", *Cell*, Vol. 83, No. 6, pp. 1047–1058.

Weaver, R. J., and N. Audsley, 2009, "Neuropeptide Regulators of Juvenile Hormone Synthesis: Structures, Functions, Distribution, and Unanswered Questions", *Annals of the New York Academy of Sciences*, Vol. 1163, pp. 316–329.

Wedegaertner, P. B., P. T. Wilson, and H. R. Bourne, 1995, "Lipid modifications of trimeric G proteins", *Journal of Biological Chemistry*, Vol. 270, No. 2, pp. 503–506.

Wess, J., S. Nanavati, Z. Vogel, and R. Maggio, 1993, "Functional Role of Proline and Tryptophan Residues Highly Conserved among G Protein-Coupled Receptors Studied by Mutational Analysis of the m3 Muscarinic Receptor.", *The EMBO journal*, Vol. 12, No. 1, pp. 331–338.

Wheatley, M., and S. R. Hawtin, 1999, "Glycosylation of G-Protein-Coupled Receptors for Hormones Central to Normal Reproductive Functioning: Its Occurrence and Role", *Human Reproduction Update*, Vol. 5, No. 4, pp. 356–364.

Woodhead, A. P., B. Stay, S. L. Seidel, M. A. Khan, and S. S. Tobe, 1989, "Primary Structure of Four Allatostatins: Neuropeptide Inhibitors of Juvenile Hormone Synthesis", *Proceedings of the National Academy of Sciences*, Vol. 86, No. 15, pp. 5997–6001.

Xie, Y., Z. P. Kai, S. S. Tobe, X. Le Deng, Y. Ling, X. Q. Wu, J. Huang, L. Zhang, and X. L. Yang, 2011, "Design, Synthesis and Biological Activity of Peptidomimetic Analogs of Insect Allatostatins", *Peptides*, Vol. 32, No. 3, pp. 581–586.

Xie, Y., L. Zhang, C. Zhang, X. Wu, X. Deng, X. Yang, and S. S. Tobe, 2015, "Synthesis, Biological Activity, and Conformational Study of N-Methylated Allatostatin Analogues Inhibiting Juvenile Hormone Biosynthesis", *Journal of agricultural and food chemistry*, Vol. 63, No. 11, pp. 2870–2876.

Yamanaka, N., S. Yamamoto, D. Žitňan, K. Watanabe, T. Kawada, H. Satake, Y. Kaneko, K. Hiruma, Y. Tanaka, … H. Kataoka, 2008, "Neuropeptide Receptor Transcriptome Reveals Unidentified Neuroendocrine Pathways", *PLoS ONE*, Vol. 3, No. 8, pp. 1–12.

Zandawala, M., and I. Orchard, 2013, "Post-Feeding Physiology in Rhodnius Prolixus: The Possible Role of FGLamide-Related Allatostatins.", *General and comparative endocrinology*, Vol. 194, pp. 311–7.